Organisation of kinetochores in human oocytes

Jessica Patel

Warwick Medical School

University of Warwick

Supervisors:

Geraldine Hartshorne & Andrew McAinsh

Thesis submitted for the degree of Doctor of Philosophy in Medical Sciences

May 2017

Contents

List of Figures

List of Tables

Acknowledgements

I would first like to thank my supervisors Geraldine and Andrew for their excellent guidance and support over the last three and a half years. Without their help and encouragement this PhD would not have been possible. I'm also extremely grateful for the technical help and assistance I had from everyone in the IVF lab at the CRM. Particular thanks to Debbie Taylor for always taking the time to help me and for her support and advice in handling eggs, usually with a big smile on her face! I'd also like to thank Hannah Williams who first showed me how to handle oocytes and her patience in doing so. Also a big thank you to the rest of the CRM staff who were incredibly helpful and patient with my endless requests for oocytes! Thank you to everyone in Andrew's lab, who made me feel welcome and always had good advice and input to give. Particular thanks to Chris for all his work on intra-kinetochore distances, and to Muriel who helped me with all the molecular biology work. I'm also grateful to Eva Hoffmann and Louise Newnham from the University of Sussex for their input into the project and for their technical assistance. I'd also like to thank the people who I shared an office with at CSRL, particularly everyone in the Brosens research group, who made me feel welcome and always showed interest in my work. Thank you too to Jan Brosens, Siobhan Quenby and Andy Blanks for their helpful input and advice during lab meetings. Also thanks to the 12 o'clock lunch club for their entertaining and esoteric lunchtime chat which always provided some welcome relief from work. A big thank you to my partner Pete for keeping me sane during the ups and downs of this PhD. Finally, a very big thank you to the most important people in this work: all the women who donated their oocytes to this project. I'm incredibly grateful for your contribution to this research.

Declarations

This thesis is submitted to the University of Warwick in support of my application for the degree of Doctor of Philosophy. It has been composed by myself and has not been submitted in any previous application for any degree.

The work presented (including data generated and data analysis) was carried out by the author except in the cases outlined below:

- In Methods section 2.1.1, patient consent for donation of oocytes to research was acquired by Geraldine Hartshorne and Debbie Taylor.
- In Methods section 2.2.5, kinetochore tracking using adapted MATLAB code for measurement of intra-kinetochore distances was performed by Christopher Smith.

The work was funded by the Montreal Reproductive and Regenerative Medicine Foundation and a Warwick Collaborative Postgraduate Research Scholarship.

Jessica Patel, May 2017

Publications based on this work

Patel J, Tan SL, Hartshorne GM, McAinsh AD. Unique geometry of sister kinetochores in human oocytes during meiosis I may explain maternal age-associated increases in chromosomal abnormalities. Biol Open. 2015; 5(2): 178-84. doi: 10.1242/bio.016394.

Summary

A large proportion of human pregnancies have the wrong number of chromosomes, known as aneuploidy, with the chances of having an affected pregnancy increasing with maternal age. The majority of these errors can be traced back to the egg (oocyte), which undergoes two meiotic cell divisions to generate a cell with half the number of chromosomes of a somatic cell. The first meiotic division is particularly error-prone and accounts for a significant proportion of aneuploidies in early embryos. This first division is a unique form of cell division because it entails separation of homologous chromosome pairs and co-segregation of identical sister chromatids at anaphase (in mitosis and meiosis II, by contrast, sister chromatids separate at anaphase). The kinetochore is a multiprotein structure that assembles on the centromeres of chromosomes and facilitates chromosome segregation by forming attachments to spindle fibres emanating from one of the spindle poles. For a successful meiosis I division, kinetochores on sister chromatids must act as a single functional unit. In mouse and yeast this is achieved through close physical association of meiotic sister kinetochores; in humans, however, little is known about the arrangement of sisters in oocytes, largely due to the limited availability of human oocytes for research. In this project, I show that in human meiosis I stage oocytes donated to research by women undergoing assisted reproduction, sister kinetochores are not physically fused and are each capable of forming individual attachments to spindle microtubule fibres. I also found a significant increase in the distance between sister kinetochores in patients over 35 years of age, which may indicate a decline in inter-kinetochore cohesion over time. These unique features of sister kinetochore geometry in human oocytes may shed light on why meiosis in humans is susceptible to error with increasing maternal age.

Abbreviations

ART	Assisted reproductive technology
ATP	Adenosine triphosphate
BSA	Bovine serum albumin
CCAN	Constitutive centromere-associated network
CENP	Centromere protein
CGH	Comparative genomic hybridisation
CREST	Calcinosis, Raynaud phenomenon, esophageal dysmotility, sclerodactyly, telangiectasia
DAPI	4',6-diamidino-2-phenylindole
DNA	Deoxyribonucleic acid
EGTA	Ethylene glycol tetraacetic acid
EM	Electron microscopy
FISH	Fluorescence *in situ* hybridisation
FSH	Follicle-stimulating hormone
GFP	Green fluorescent protein
GnRH	Gonadotrophin-releasing hormone
HEPES	4-(2-hydroxyethyl)-1-piperazineethanesulphonic acid
ICSI	Intracytoplasmic sperm injection
IVF	*In vitro* fertilisation
K-fibre	Kinetochore-fibre
LB	Lysogeny (Luria-Bertani) broth
LH	Luteinising hormone
MI	Metaphase I
MII	Metaphase II
min	Minute
mRNA	Messenger ribonucleic acid
MT	Microtubule
NA	Numerical aperture
NBD	Nuclear-binding domain
nm	Nanometre
PB	Polar body
PBS	Phosphate-buffered saline
PCOS	Polycystic ovarian syndrome
PFA	Paraformaldehyde
PGC	Primordial germ cell
PGD	Preimplantation genetic diagnosis
PCR	Polymerase chain reaction
PIPES	Piperazine-1,4-bis(2-ethanesulfonic acid)
PSSC	Premature separation of sister chromatids
RFP	Red fluorescent protein

SC	Synaptonemal complex
SD	Standard deviation
SEM	Standard error of the mean
Sgo	Shugoshin
SMC	Structural maintenance of chromosomes
SNP	Single nucleotide polymorphism
STAG	Stromal antigen protein
µl	Microlitre
µm	Micron/micrometre
UTR	Untranslated region

Chapter 1: Introduction

In humans, the chance of having a pregnancy with the wrong number of chromosomes, a state known as aneuploidy, increases dramatically with maternal age. In women under 25 years of age, around 2% of all clinically recognised pregnancies are trisomic (have an additional chromosome), however this figure rises to 35% for women over 40 (Hassold & Chiu, 1985). Aneuploidy is a leading cause of early miscarriage, as the presence of an extra or a missing chromosome is usually incompatible with normal development. Although some pregnancies with certain chromosomes in incorrect numbers can survive to term, including the sex chromosomes and trisomies 13, 18 and 21, they often result in infants with severe medical problems. With increasing numbers of women choosing to have children at later ages, there has been increased focus on understanding the factors that contribute to this phenomenon.

What we know so far is that the vast majority of aneuploidies in pregnancy are of maternal origin and arise from chromosome segregation errors that occur during the meiotic divisions of the oocyte, in particular the first meiotic division (Hassold *et al.*, 2007). That this first meiotic division is responsible for the majority of aneuploidies is perhaps not surprising given that it has a number of features that differentiate it from a standard equational division that occurs in mitosis and meiosis II. Unlike an equational division in which sister chromatids are separated, the first meiotic division comprises segregation of homologous chromosome pairs (i.e. the maternally- and paternally-inherited copies of each chromosome). For this to happen successfully requires a unique set of chromosomal events to occur, including: (1) resolution of DNA crossovers that physically tether the homologues to one another; (2) protection of centromeric cohesion between sister chromatids so that they remain together during anaphase; and (3) attachment of sister kinetochores to the same, rather than opposing, spindle poles. Failure or mistiming of any of these events can lead to chromosome missegregation at anaphase I. In addition to these events, human

oocyte meiosis I is further complicated by the fact that there is a long gap between initiation of meiosis, which occurs during fetal life, and completion of the first meiotic division, which occurs many years later just before ovulation. In human oocyte meiosis I, we have limited understanding of how kinetochores, multisubunit protein structures that constitute the physical interface between chromosomes and the spindle, form attachments to the same spindle pole. Further understanding of the geometry and architecture of the human meiotic kinetochore during this highly error-prone division is therefore required.

1.1. Meiosis

Meiosis is a specialised form of cell division that involves the generation of haploid gametes from diploid precursor cells, and is a key prerequisite for all sexually reproducing organisms. During meiosis, recombination between maternally- and paternally-inherited chromosomes results in novel combinations of genes that are crucial for the diversity of life. At the chromosomal level, meiosis is fundamentally similar between species and sexes, beginning with doubling of cellular DNA content through DNA replication, followed by two rounds of cell division, generating cells that have half the DNA content of a somatic cell. The first meiotic division is a reductional division in which paired homologous chromosomes (the maternally- and paternally-inherited copy of each chromosome), connected by crossovers formed during meiotic recombination, separate (see **Figure 1.1**). The second meiotic division more closely resembles a mitotic division in which sister chromatids are separated.

1.1.1. From primordial germ cells to oogonia

Although the fundamental features of meiosis are shared, there are a number of aspects of human female meiosis that differentiate it from male meiosis. One key difference is the timing of entry into meiosis. In both males and females, at around 6–8 weeks of development, primordial germ cells migrate to the developing gonads of the embryo, where after several rounds of mitotic

proliferation they differentiate into oogonia (females) or gonocytes (males). In males, gonocytes go on to divide mitotically and differentiate into prespermatogonia which remain mitotically quiescent for several years, only entering meiosis upon reaching puberty many years later. In females, however, oogonia begin to enter meiosis at around 10–11 weeks of gestation, developing into primary oocytes (see **Figure 1.2**). Up to 5 months, it is possible to observe both oogonia and primary oocytes in the fetal ovary, indicating that there is overlap between the period of mitotic proliferation and entry into meiosis. This asynchrony in meiotic entry appears to be linked to spatial features of the ovary, with an anterior-to-posterior gradient of meiotic initiation that arises due to retinoic acid signalling (Suzuki *et al.*, 2015). By the time mitotic proliferation ceases, there are an estimated 10 million oogonia in the fetal ovary (De Felici, 2013).

Dividing oogonia form clusters of cells that are joined by cytoplasmic bridges which arise as a result of incomplete cell division; these clusters are known as germline cysts (De Felici, 2013). During neonatal development, these cysts break down and fragment into smaller cysts, eventually forming a single oocyte surrounded by a layer of pregranulosa cells, also known as a primordial follicle (Lei & Spradling, 2013). During the process of cyst breakdown, a large proportion of cells within the cyst die by apoptosis, with approximately one third surviving (Pepling, 2013). The reasons for this large amount of cell death are not clear, but one theory is that it may ensure that cells destined to become primary oocytes acquire sufficient numbers of mitochondria (Pepling & Spradling, 2001). There are also spatial differences in germ cell cyst breakdown, with cysts in the medulla (inner part) of the ovary entering meiosis first and being the first to form follicles; this has been observed in mammals including mouse, rats and humans (Hirshfield, 1992, Wang *et al.*, 2017). In humans, the first wave of oocytes that enter development do not end up being ovulated because by the time they develop it is too early for them to be rescued by a gonadotrophin surge, so they die as atretic follicles (Mazaud *et al.*, 2002). The reasons for this apparent wastage in the first wave of follicular development are not known.

Figure 1.1

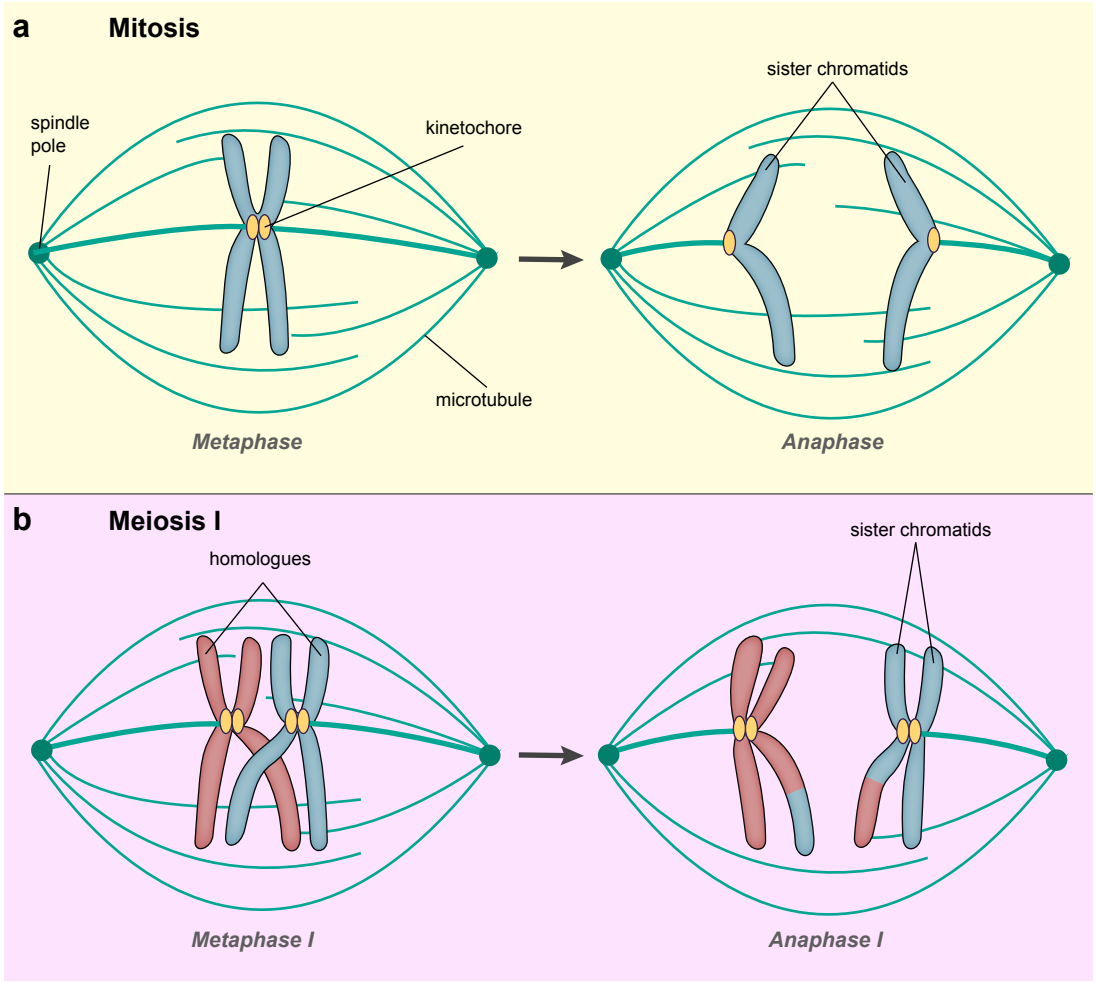

Figure 1.1. Chromosome segregation in mitosis and meiosis I. (a) In mitosis, kinetochores on sister chromatids form attachments to kinetochore-fibres (k-fibres) emanating from opposite spindle poles, resulting in segregation of sister chromatids at anaphase. (b) Meiosis I, on the other hand, entails separation of homologous chromosome pairs (represented here in blue and red), therefore sister kinetochores form attachments to k-fibres from the same spindle pole. This ensures that they co-segregate to the same spindle pole during anaphase I.

Figure 1.2

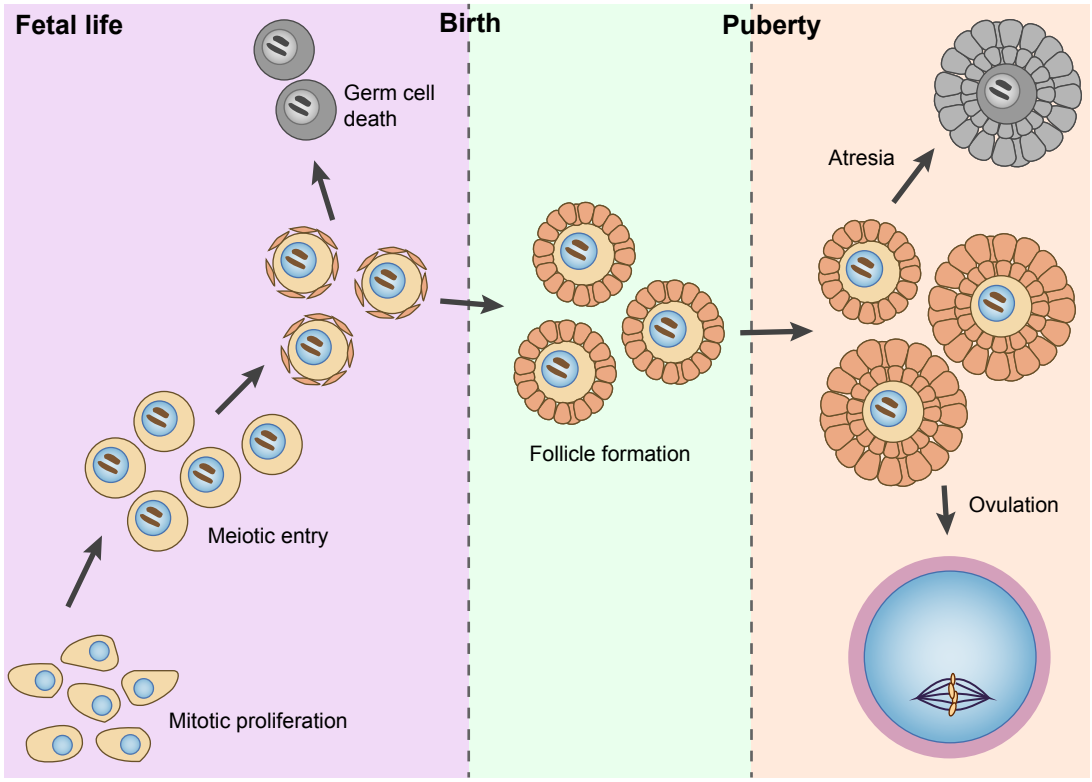

Figure 1.2. Oocyte development from fetal life to ovulation. Oocyte life begins early in fetal development when primordial germ cells divide mitotically to increase their numbers. At 11–13 weeks of gestation, these primordial germ cells begin to enter meiosis, forming primordial follicles which consist of an oocyte surrounded by a single layer of flattened pre-granulosa cells. Most of these primordial follicles remain quiescent or undergo atresia (cell death), but a subset become activated in response to molecular cues, which results in their development and growth into primary, then secondary and finally antral follicles. At puberty, the pulsatile release of follicle-stimulating hormone (FSH) results in the selection of a single dominant follicle, which is ovulated mid-cycle following a surge in luteinising hormone (LH). Follicles that do not receive this stimulation undergo atresia.

1.1.2. Chromosomal events in early meiosis

Entry into meiosis marks several important events at the chromosomal level. Meiosis follows the same stages of cell division as mitosis: prophase, metaphase, anaphase, telophase and cytokinesis. The first prophase in females, however, is a highly extended process, that includes a prolonged arrest that can last from 10–40 years. This stage has classically been divided into five substages, based on the distinct chromosome morphology that can be seen at each stage. During the first stage, leptotene (Greek for 'thin threads'), chromosomes can be visualised as long, thin strands that have begun to condense but have not yet paired with their homologous partners in the cell (see **Figure 1.3**). At this stage, components of the cohesin complex which mediates cohesion between sister chromatids begin to assemble along chromosome arms (Prieto *et al.*, 2004). These elements form a chromosomal scaffold that helps to recruit other essential proteins to the chromosomes during this period (Handel & Schimenti, 2010). Finding and pairing with homologous partners occurs in the next stage of prophase I, zygotene ('paired threads'), a process that depends upon sequence homology alignment (Gerton & Hawley, 2005). Synapsis between homologues is mediated by the synaptonemal complex (SC), a proteinaceous structure that forms a ladder-like assembly between homologous chromosomes. (Page & Hawley, 2004). Synaptonemal complex proteins 2 and 3 (SYCP2 and SYCP3) make up the lateral elements of the structure and assemble along chromosome arms in a cohesin-dependent manner (Prieto *et al.*, 2004). Other SC components, including SYCP1, localise to the central region between chromosomes, forming the rungs of the ladder structure (Handel & Schimenti, 2010). By pachytene ('thick threads'), SC assembly is complete and chromosomes are fully synapsed, enabling DNA crossovers, or chiasmata, to form. At diplotene ('two threads'), the SC disassembles and chromosomes move apart slightly, now connected by chiasmata, where they are held for many years in an extended arrest state.

Assembly of the SC is essential for reciprocal recombination between maternal and paternal copies of each chromosome, which is crucial for keeping homologues together during the long arrest period and for generating

Figure 1.3

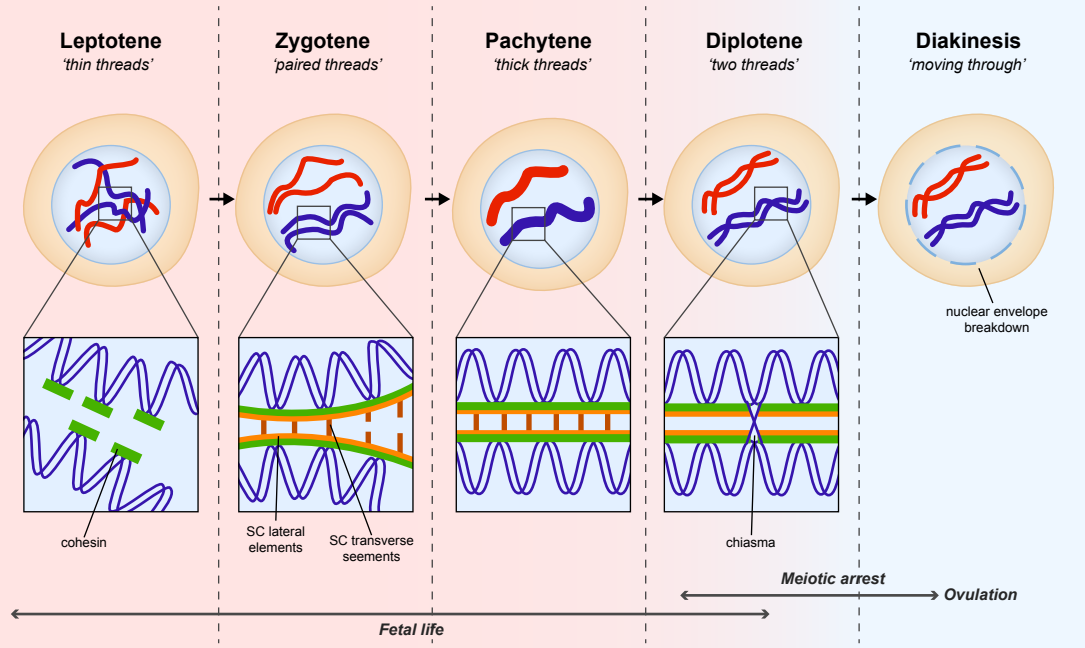

Figure 1.3. Stages of meiotic prophase I. The first meiotic prophase begins with the leptotene (Greek for 'thin threads') stage, in which chromosomes can be visualised as thin strands. Cohesin (green) begins to assemble along chromosome arms, forming a chromosomal scaffold. Leptotene is followed by zygotene ('paired threads'), in which homologous chromosomes begin to pair up and synaptonemal complex (SC) elements begin to assemble along chromosome arms (orange). By pachytene ('thick threads'), chromosomes are completely synapsed and formation of the SC is complete. At diplotene ('two threads') homologues move apart slightly but remain tethered together by chiasmata. They are held in this stage until ovulation, which can occur between 10–40 years later, when they reach diakinesis ('moving through'). At this stage, the nuclear envelope breaks down, chromosomes condense and the first meiotic spindle begins to assemble.

chromosomes with novel combinations of genes. The process of crossover formation has many similarities with homologous repair of DNA double-stranded breaks and shares many of the proteins involved in this mechanism of DNA repair. It begins in leptotene with the formation of Spo11-induced double-stranded breaks in chromosomes (Keeney *et al.*, 1997), which attract the mismatch repair proteins MLH1 and MLH3 that promote crossing-over (Lipkin *et al.*, 2002, Lenzi *et al.*, 2005). Break formation is followed by exonucleolytic resection of the 5' ends of the break which results in two 3' single-stranded overhangs. One of these overhangs invades into the aligned region of its homologous partner, displacing a strand of DNA which forms what is known as a D-loop structure (**Figure 1.4**). This D-loop captures the other 3' end (Hunter & Kleckner, 2001). The ends of the 3' overhangs are then extended by DNA synthesis, using the homologous chromosome partner's DNA as a template, eventually resulting in formation of a double Holliday junction (Schwacha & Kleckner, 1995, Gerton & Hawley, 2005, Handel & Schimenti, 2010). This double Holliday junction forms a physical linkage between homologous chromosomes known as a chiasma. When the SC disassembles during the diplotene stage of meiotic prophase I, chiasmata are responsible for keeping homologues tethered to each other for the duration of the extended arrest period that follows. The resulting chromosome structure is known as a bivalent, which consists of a pair of homologous chromosomes (each comprising a pair of sister chromatids) held together by chiasmata.

1.1.3. Follicular growth during the arrest period

During arrest at diplotene of meiotic prophase I, oocytes are located within primordial follicles, which comprise a meiotically arrested oocyte surrounded by a single layer of somatic pre-granulosa cells which have a flattened appearance (Pepling, 2006). These primordial follicles constitute the total pool of oocytes from which oocytes are then selected for further development. The transition from a primordial follicle to a primary oocyte is known as primordial follicle activation. Over the course of a woman's life, only a small fraction (approximately 1 in 1600) of primordial follicles will be recruited for activation. The rest will remain quiescent within the ovary, or they will undergo atresia (cell

Figure 1.4

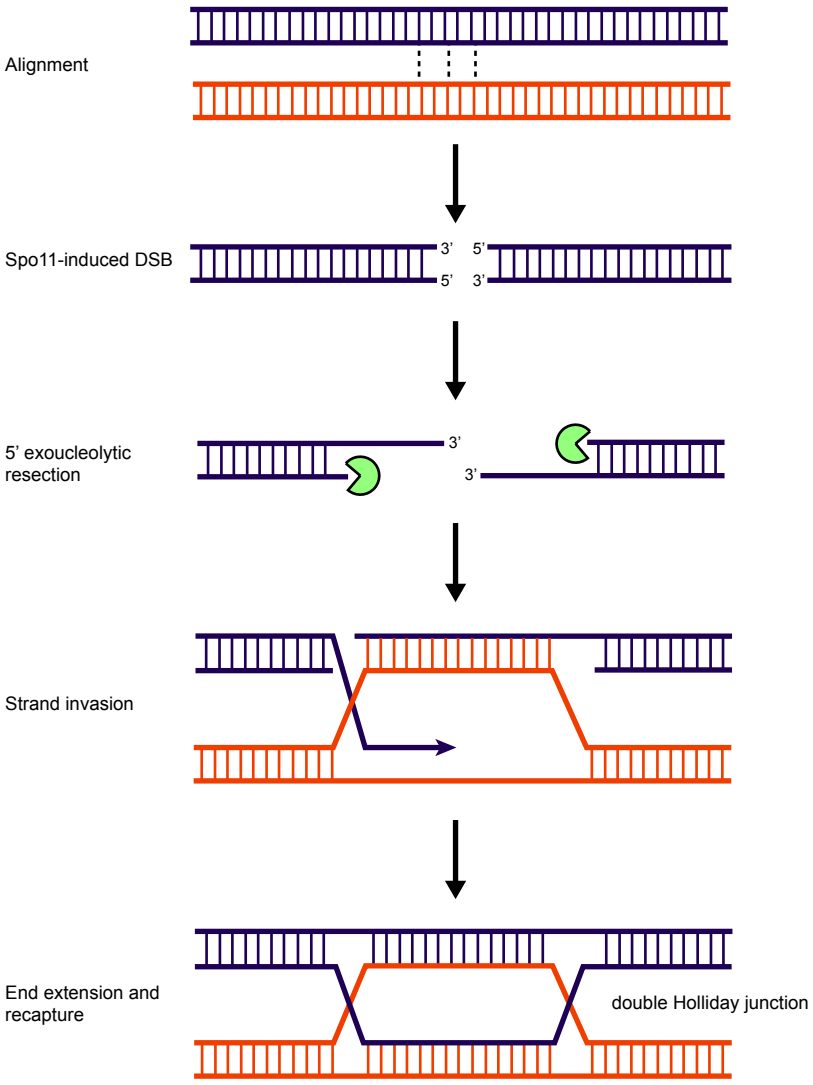

Figure 1.4. The process of crossover formation during meiotic recombination. During leptotene, homologous chromosomes (shown in purple and orange) become aligned. The process of crossover formation begins with the formation of double-stranded breaks (DSBs) in DNA which are introduced by the highly conserved Spo11 protein. An exonuclease (light green) resects DNA in a 3'-5' direction, resulting in two 3' single-stranded overhangs. One of these invades into the homologous partner, displacing a strand of DNA which forms a D-loop structure. The D-loop captures the other 3' ssDNA strand. The strand is extended by DNA synthesis, recapturing the other end of the break and resulting in formation of a double Holliday junction. Adapted from Gerton & Hawley (2005).

death), a process that can occur after activation or directly from quiescence. During fetal life, a vast proportion of follicles undergo atresia, which reduces the total pool of germ cells from 7 million to around 2 million at birth (Pepling, 2013). This process is thought to eliminate cells with DNA damage or other defects, although little is known beyond this. Although some of the molecular signals involved in maintenance of follicular quiescence or follicle activation have been identified, including anti-Mullerian hormone, the tumour suppressor protein PTEN and FOXO3a, all of which are involved in maintenance of quiescence, little is known about the overall cues that determine follicular fate. Over the course of a woman's life, only a very small percentage (<1%) of cells that undergo meiotic initiation make it to ovulation and completion of the first meiotic division, which suggests an overall inefficient process (Adhikari & Liu, 2013). However, this apparent inefficiency may have some purpose that is not currently understood.

The small fraction of follicles that become recruited to grow follow a process of development that begins with growth into primary, then secondary, then antral follicles. The first follicles begin to grow in humans at around 4 months of fetal life, with approximately 1000 follicles per month recruited for growth (Macklon & Fauser, 1999). During the early growth period of the follicle, the pre-granulosa cells of the primordial follicle differentiate and proliferate to form layers around the oocyte. This process is accompanied by an increase in oocyte size, formation of a zona pellucida around the oocyte, and accumulation of mRNA in the ooplasm (Gougeon, 2013). When the oocyte is surrounded by two layers of granulosa cells, it is known as a secondary follicle. Gap junctions between the granulosa cells and the oocyte facilitate cross-communication and signalling which are essential for the oocyte's growth and development (Anderson & Albertini, 1976, Eppig, 2001). Progression from a secondary follicle to an antral follicle is characterised by the formation of a fluid-filled cavity adjacent to the oocyte (the antrum). During this period of early follicular development the oocyte experiences its most rapid growth, increasing from a diameter of 40 μm at the primary follicle stage to 100 μm at the early antral stage (Gougeon, 2013). Throughout this period of follicular growth, the oocyte remains in meiotic prophase I arrest, maintenance of which appears to be achieved through low

concentrations of the cell cycle protein CDK1 (cyclin dependent kinase 1). Oocytes less than 80% of their full size are incapable of undergoing meiotic resumption, which is most likely linked to an inability to build up sufficient CDK1 levels to trigger entry into anaphase (Jones *et al.*, 2013).

1.1.4. Meiotic resumption and fertilisation

In humans, multiple early antral follicles are present during each reproductive cycle, however prior to puberty they do not receive enough stimulation to develop into a fully mature oocyte. At puberty, increased exposure to follicle-stimulating hormone (FSH) and changes in its pulse frequency and amplitude result in the selection of a single dominant follicle, based upon differential sensitivity to FSH among the follicles of a cohort, and mediated by follicular products such as oestradiol and inhibin feeding back to the pituitary gland to regulate gonadotrophin production (Carey & Murray, 2006). Follicles that receive insufficient FSH undergo atresia, a process that is mediated by apoptosis of surrounding granulosa cells (Hsueh & Kawamura, 2013). The selected oocyte develops within its antral cavity, surrounded by cumulus cells which are connected to mural granulosa cells via gap junctions (Carabatsos *et al.*, 2000). A surge in luteinising hormone (LH) from the pituitary gland towards the middle of the menstrual cycle triggers ovulation and meiotic resumption. The transition of the oocyte from prophase I to metaphase I (MI) is characterised by a number of CDK1-mediated events, including chromosome condensation, breakdown of the germinal vesicle (GV; the oocyte nucleus at prophase I arrest) and formation of the first meiotic spindle (Jones *et al.*, 2013). The first live-cell imaging study following human oocytes from GV breakdown to the first meiotic division has shown that the period of spindle assembly lasts for approximately 16 hours (Holubcova *et al.*, 2015), significantly longer than in mouse in which the process takes about 3–5 hours (Schuh & Ellenberg, 2007). Upon completion of the first meiotic division, during which the oocyte releases its first polar body, there is no intervening S-phase and the oocyte assembles the second meiotic spindle. Only oocytes in the metaphase II (MII) stage of meiosis are capable of being fertilised. Completion of the second meiotic division occurs during fertilisation in response to calcium (Ca^{2+}) oscillations, which are triggered when

a spermatozoon has passed through the zona pellucida and fused with the oolemma.

1.1.5. An overview of the IVF/ICSI process

In vitro fertilisation (IVF) treatment is widely used for couples experiencing infertility. The first IVF baby was born in 1978 (Steptoe & Edwards, 1978) following many years of research in animals and studying human eggs and sperm in vitro (Edwards, 1965, Edwards *et al.*, 1969). IVF entails collecting oocytes from women, fertilising them in the laboratory, and returning one or more embryos to the uterus in an attempt to initiate pregnancy. Currently the overall success rate in UK is around 25% per cycle (HFEA, 2016).

Women undergoing IVF first undergo hormonal ovarian stimulation, which involves treatment with exogenous gonadotrophins to promote the growth of multiple follicles *in vivo* and cotreatment with a gonadotrophin-releasing hormone (GnRH) analog to prevent an LH surge (Cheong *et al.*, 2012). This can be done in one of two ways. The first approach involves treatment with a superactive GnRH agonist, which downregulates pituitary GnRH receptors and renders the pituitary gland unresponsive to GnRH, allowing FSH to be administered in controlled doses without risk of an LH surge causing premature ovulation (Griesinger *et al.*, 2006). The second involves use of a GnRH antagonist, which directly interferes with GnRH stimulation by competitively binding to GnRH receptors, thus preventing the LH surge, but not downregulating GnRH receptors at the pituitary and not depleting endogenous FSH or LH (Macklon *et al.*, 2006, Tarlatzis *et al.*, 2006). Both approaches result in multiple growth of follicles in numbers that reflect the number of small antral follicles available at the start of the menstrual cycle in which treatment is provided, which in turn relates to a woman's age. The follicles do not ovulate or undergo atresia because supraphysiological FSH levels are maintained without follicular products triggering an LH surge.

When the growing follicles have reached a diameter of approximately 16–18 mm, as observed by transvaginal ultrasound, the eggs are collected by

aspirating the follicles in the ovary, with the patient under sedation, using an ultrasound-guided transvaginal needle (Barton & Ginsburg, 2012). Upon collection, oocytes are surrounded by granulosa cells comprising the cumulus-oocyte complex. For IVF treatment, collected oocytes are typically incubated for 16–18 hours with prepared sperm from the male partner or donor. In some cases, depending on patient history or sperm quality, intracytoplasmic sperm injection (ICSI) is performed to promote fertilisation, which entails the injection of a single immobilised sperm into the ooplasm. ICSI entails removing the surrounding cumulus cells prior to sperm injection, whereas in IVF the cumulus is not removed until the following day (Maggiulli *et al.*, 2012, Palermo *et al.*, 2012). Following overnight culture, oocytes are assessed under light microscopy for signs of fertilisation. Normal fertilisation is assumed when two pronuclei are visible and the oocyte has extruded the second polar body, thus completing the second meiotic division. The two pronuclei normally contain haploid complements of maternal and paternal DNA. Oocytes that do not fertilise, or which fertilise abnormally, are not usable clinically and are normally discarded. Such oocytes include those which are immature (containing a GV or having failed to produce the first polar body), unfertilised (showing no pronuclei), abnormally fertilised (e.g. containing multiple pronuclei or one pronucleus), may be parthenogenetic or have fused pronuclei, or have failure of one pronucleus to develop. Since these decisions are made solely based upon light microscopic observation and no detailed chromosomal assessment, the categories assigned may not always be correct.

The fertilisation check is the time at which oocytes may become available for research use, provided that patient consent has been previously obtained. For ICSI cycles, immature oocytes may be available earlier, because only MII-stage oocytes are suitable for sperm microinjection. The normally fertilised oocytes are cultured for several days with frequent monitoring until an embryo can be selected for transfer into the patient. Embryo culture to the blastocyst stage, 5-6 days, is applied in order to aid the embryo selection process (Maggiulli *et al.*, 2012).

1.2. Aneuploidy in human oocytes

1.2.1. Early investigations into human aneuploidy

Although the link between Down's syndrome and maternal age was first identified in the 1930s, it was not until the late 1950s that the presence of an additional copy of chromosome 21 was identified as the cause of the syndrome (Jacobs *et al.*, 1959). Following this discovery, karyotyping studies conducted over the next few decades found that in over 60,000 newborns, the incidence aneuploidy was 0.3%. Of these, trisomy 21 was the most common, followed by trisomy of the sex chromosomes and chromosomes 13 and 18, whereas the incidence of aneuploidy in the remaining autosomes was almost non-existent (Hassold *et al.*, 1996). In stillbirths (between 20 weeks gestation and term), the incidence increased to approximately 4%, but the chromosome-specific trends in trisomy remained the same with trisomy 21 again the most commonly identified aneuploidy (reviewed in Nagaoka *et al.*, 2012). However, as this data was only from pregnancies after 20 weeks, with no data from earlier stages of pregnancy, it did not provide a comprehensive picture of aneuploidy in human pregnancy. During the 1970s and 1980s researchers were able to study spontaneous abortions that occurred between 6 weeks and 20 weeks, which found much higher incidences of trisomy of over 35%, with almost all chromosomes involved, but trisomy 16 being the most common (Hassold *et al.*, 1996). These early-stage fetuses also contained trisomies that were rarely observed in newborns or stillbirths, such as sex chromosome monosomy and trisomy of chromosomes 2, 14, 15 and 22 (Hassold *et al.*, 1996). These data provided the first major indication that chromosomal abnormalities were one of the leading causes of miscarriage and congenital birth defects. Using this information, it was possible to derive a minimal estimate of aneuploidy of approximately 5% of all conceptions (Hassold & Hunt, 2001). However, as it was likely that many chromosomally abnormal pregnancies spontaneously abort prior to clinical detection (earlier than 6 weeks gestation), the true incidence was estimated to be much higher.

1.2.2. Aneuploidy in assisted reproduction cycles

The introduction of IVF in the 1980s meant that it became possible for the first time to study human oocytes and human embryos at the earliest stages of development. A number of preimplantation genetic diagnosis (PGD) protocols were developed during this period to enable detection of chromosomal abnormalities in human oocytes and early embryos. Often these involved taking biopsies of the first and/or second polar bodies to work out the chromosomal complement of the oocyte or embryo (reviewed in Nagaoka *et al.*, 2012). Study of these polar bodies began through fluorescence *in situ* hybridisation (FISH), in which a labelled chromosome-specific probe was used to detect individual chromosomes in spreads generated from the cell of interest. A review of over 60 studies using chromosome karyotyping and FISH in MII oocyte chromosome spreads suggested an overall incidence of aneuploidy in human oocytes of 20–30% (Pellestor *et al.*, 2005), which was in agreement with results obtained from spontaneous abortions. However, there was significant variation between studies which was likely to be attributable to technical limitations in the methods used to identify chromosomal abnormalities. In particular, these methods relied on accurate scoring of chromosomes in spreads and the ability to distinguish single chromatids from small chromosomes.

Another method of analysing chromosomal abnormalities that was developed for PGD includes comparative genomic hybridisation (CGH), in which test and control DNA are differentially labelled and then competitively hybridised to normal metaphase chromosomes. The ratio of the control and test DNA samples can be measured along the length of the chromosome, which can give an indication if there is a chromosomal loss or gain. Initial studies using CGH in oocytes and embryos indicated many advantages over FISH because the method enabled all chromosomes to be analysed at once, and thus could detect abnormalities that were likely to have been missed by FISH (Voullaire *et al.*, 2000, Wells *et al.*, 2002, Wilton *et al.*, 2003). However, the time-consuming nature of the procedure meant that it was gradually replaced with array CGH (aCGH), in which DNA is hybridised to probes on microarrays, and single nucleotide polymorphism (SNP) arrays, which enable detection of crossover

location and parental origin of aneuploidy. The use of these methods in PGD revealed an incidence of aneuploidy in pregnancy of between 10–40% (Fragouli *et al.*, 2008, Fragouli *et al.*, 2011, Treff *et al.*, 2011), figures which are in keeping with initial cytogenetic studies into human aneuploidy from natural conceptions. Moreover, they also found that there was overrepresentation of small/acrocentric chromosomes, including 13, 18 and 21, and the sex chromosomes (Nagaoka *et al.*, 2012).

1.2.3. Endocrine origins of missegregation

A caveat of the work from oocytes derived from assisted reproductive technology (ART) cycles is that they are not representative of the normal population: they are from a population of infertile women, the oocytes come from hyperstimulated ovaries, and moreover the oocytes studied are those that have failed in IVF. A particular concern is the effect of ovarian hyperstimulation on aneuploidy. Most of the oocytes on which our estimations of aneuploidy incidence are based came from cycles of IVF in which patients were exposed to an ovarian stimulation regimen involving treatment with exogenous FSH. FSH binds to its receptors which are exclusively found on granulosa cells (O'Shaughnessy *et al.*, 1996) which communicate bidirectionally with the oocyte to regulate follicular development and oocyte maturation (Eppig, 2001). There have therefore been concerns that exposure of oocytes to supraphysiological levels of gonadotrophins in ART may result in disturbances to oocyte growth which may increase chances of chromosomal abnormalities or errors in meiosis (Hodges *et al.*, 2002). Moreover, FSH levels in women rise with age (Klein *et al.*, 1996); therefore, there are concerns that rising FSH levels may contribute to the increased levels of aneuploidy seen in older women.

A number of studies in mouse have investigated whether there are changes in oocyte chromosomal abnormalities as a result of stimulation with gonadotrophins. Early studies reported differing effects on non-disjunction in oocytes from stimulated versus unstimulated cycles (reviewed in Santos *et al.*, 2010); however, a more recent study by Roberts *et al*. found that mouse oocytes exposed to high levels of FSH during *in vitro* maturation were more likely to

undergo aneuploidy at the first meiotic division compared with oocytes treated with lower doses of FSH. Moreover, they found that high FSH levels altered chromosome congression, with oocytes treated to high doses more likely to have chromosomes scattered across the spindle (Roberts *et al.*, 2005). This is in keeping with studies from older women who have been shown to have oocytes with abnormal spindle morphology (Battaglia *et al.*, 1996).

In humans, high rates of mosaicism have been reported in embryos from IVF cycles, which has also led to concerns that ovarian stimulation protocols may result in an increase in aneuploidy (Munne *et al.*, 1997). Mosaicism generally arises from mitotic, rather than meiotic, segregation errors, leading to genetically distinct cell lineages within an individual. To test whether FSH can contribute to increased aneuploidy, Baart *et al.* utilised FISH to study chromosomes in blastomeres obtained from a high-dose FSH protocol versus those obtained from a low-dose FSH protocol. They found that embryos obtained from the high-dose protocol were more likely to have aneuploidy, which often arose from mitotic segregation errors, leading to mosaicism (Baart *et al.*, 2007). This study supports the increasing call for milder ovarian stimulation in IVF cycles, which does not appear to increase the rates of chromosomal abnormalities in embryos (Labarta *et al.*, 2012).

1.2.4. The origins of aneuploidy

Given the high incidence of aneuploidy in human eggs, the next step was to pinpoint the stage at which these errors were prone to arising. This was not always straightforward because it soon emerged that different chromosomes are associated with different patterns of missegregation. For instance, some of the most common trisomies, including 13, 21 and 22 are more likely to arise in meiosis I than meiosis II (Yoon *et al.*, 1996, Hall *et al.*, 2007, Hall *et al.*, 2007). On the other hand, trisomy 18, one of the few trisomies that is compatible with live birth, is more likely to originate at the second meiotic division (Fisher *et al.*, 1995). Trisomy of chromosome 16 almost always arises during maternal meiosis I (Hassold *et al.*, 2007), whereas the additional X chromosome in 47,XXY has an equal probability of arising paternally or maternally (MacDonald

et al., 1994). These differences are believed to arise as a result of differences in chromosome architecture. In particular, small acrocentric chromosomes, including 13, 14, 15, 21 and 22, appear to be particularly prone to non-disjunction, which may arise as a result of achiasmate short chromosome arms. They are also more likely to have crossovers that are either pericentromeric or telomeric, which can increase the chance of non-disjunction, as discussed in further detail below. For the majority of these acrocentric chromosomes, non-disjunction occurs in maternal meiosis I (Zaragoza *et al.*, 1994). Indeed, despite these chromosome-specific trends, when taking all chromosomes into account, a number of studies found that errors in meiosis I are more prevalent overall than errors in meiosis II (Verlinsky *et al.*, 2001, Hassold *et al.*, 2007, Kuliev *et al.*, 2011). Given the long gap between initiation and completion of the first meiotic division, this is perhaps not surprising.

Although this thesis focuses on meiotic aneuploidy, it is also important to mention that there is also a high incidence of mitotic aneuploidy that arises during the mitotic divisions of the embryo, often leading to mosaicism (Handyside, 1996). As discussed above, it is possible that ovarian stimulation protocols contribute to this chromosomal instability. Estimates of mosaicism in human embryos derived from IVF vary from 30% to as high as 90%. This variability is partly due to fixation techniques such as FISH, variations in clinical settings and differing criteria for mosaicism (reviewed in Munne & Wells, 2017). Levels of mosaicism for trisomy 21 are estimated to be between 1.3–5% of all conceptuses; however, because the phenotype of mosaicism can be mild in comparison to having full trisomy 21, it is possible that undetected cases exist (Papavassiliou *et al.*, 2015). There is also some evidence of a link between maternal age and embryonic mosaicism (Munne *et al.*, 2002), however this relationship is debatable and it appears that embryos across all maternal ages are prone to a certain level of chromosomal instability (Munne & Wells, 2017).

1.2.5. Mechanisms of missegregation in meiosis I

During the first meiotic division, there are a number of different mechanisms through which aneuploidy can arise. This includes: (1) non-disjunction, which

involves missegregation of an entire chromosome, (2) premature separation of sister chromatids and (3) reverse segregation (see **Figure 1.5**). Non-disjunction was initially identified as the main mechanism of aneuploidy, because prior to IVF, early studies focused on chromosomes that led to viable offspring, many of which were more likely to undergo non-disjunction. This includes the error-prone chromosomes 13, 18 and 21 (Hassold *et al.*, 2007). There are two different types of non-disjunction: true non-disjunction, in which both homologues segregate together, and achiasmate non-disjunction, in which homologues that have not recombined travel independently to the same spindle pole (Hassold & Hunt, 2001). However, when it became possible to analyse leftover oocytes from IVF treatment, researchers began to identify the presence of single chromatids (half-chromosomes) in MII oocyte spreads, suggesting that non-disjunction was not the main mechanism of aneuploidy in meiosis (Angell, 1991, Angell, 1997). It soon emerged that premature separation of sister chromatids is a more frequent mechanism by which aneuploidy arises in the first meiotic division (Pellestor *et al.*, 2002, Gabriel *et al.*, 2011). Premature separation can occur when the connections between sister chromatids are lost, resulting in gain or loss of a single chromatid.

A limitation of the cytogenetics approaches that have been used to identify whole chromosomes and single chromatids in IVF-derived MII oocytes is that they cannot pinpoint the precise origin of extra-chromosomal material. Ottolini et al. genotyped over 4 million SNPs (single nucleotide polymorphisms) in human oocytes and their corresponding first and second polar bodies, which enabled precise mapping of crossover locations. Using this approach, they were able to identify another type of missegregation at the first meiotic division of human oocytes that involves balanced predivision of sister chromatids, or reverse segregation. This occurs when a bivalent is converted into two univalents (a pair of sister chromatids) which separate at MI, generating an MII product that contains two non-sister chromatids (see **Figure 1.5d**). Although this is a balanced division, it can predispose to aneuploidy at the second meiotic division if the non-sister chromatids (which are not connected at the centromeres) segregate randomly (Ottolini *et al.*, 2015). Direct visualisation of this phenomenon has also been observed in live-cell imaging of mouse oocytes

Figure 1.5

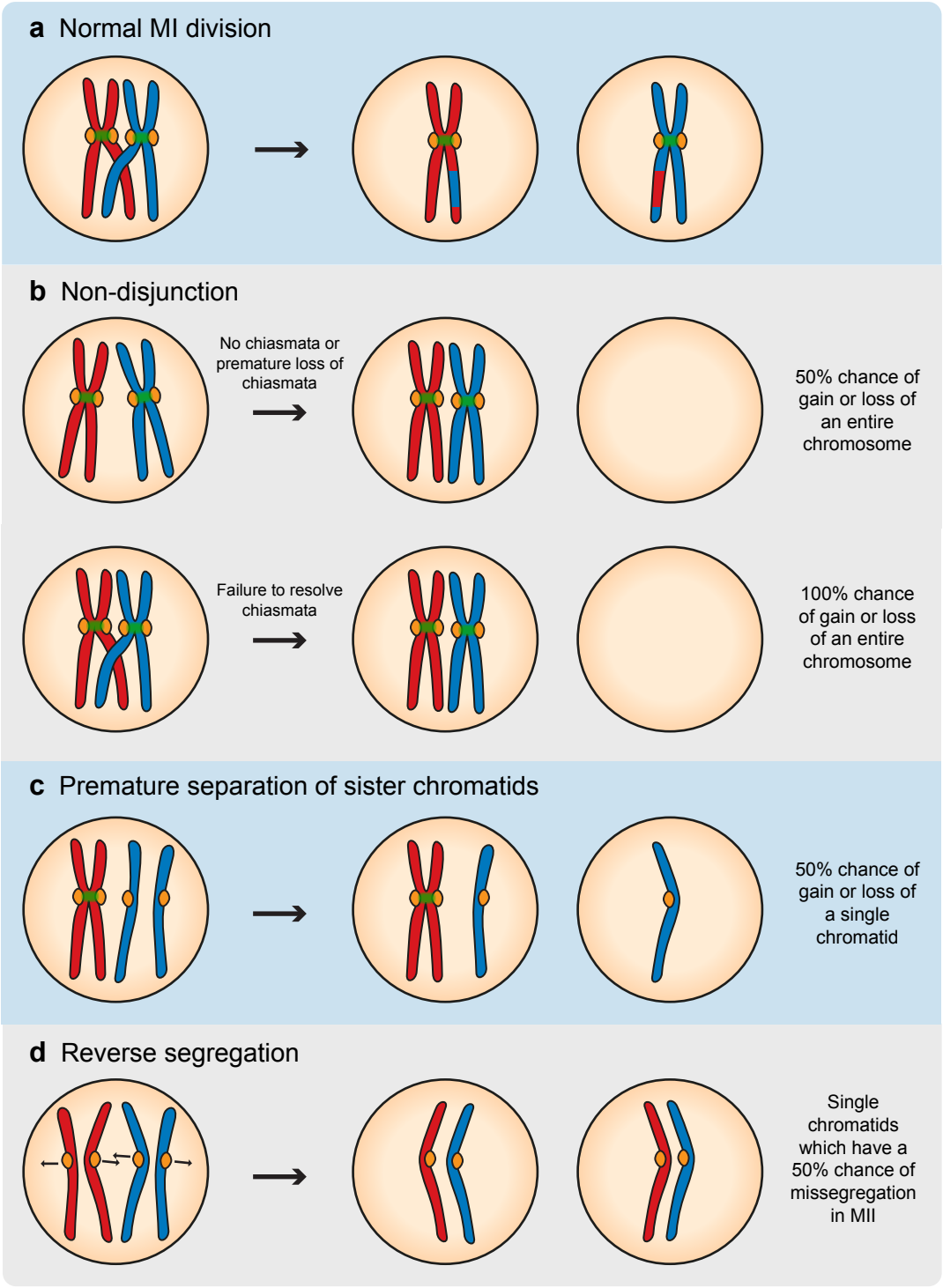

Figure 1.5. Mechanisms through which aneuploidy can arise at the first meiotic division. Homologous chromosome pairs represented in red and blue, kinetochores in orange and centromeric cohesin in green.

as they undergo the first meiotic division, in which predivision of sister chromatids accounted for 80% of the errors observed (Sakakibara *et al.*, 2015). Although reverse segregation in oocytes has been reported in just two studies so far, the data from these studies suggest that it is a frequent occurrence in MI.

These different mechanisms of aneuploidy arise from the unique series of events that needs to occur during MI for a successful first meiotic division. This includes: resolution of chiasmata formed during the recombination process, maintenance of centromeric cohesion, and attachment of sister kinetochores to microtubules emanating from the same spindle pole. These features of MI will be examined in turn.

1.3. Meiotic recombination and aneuploidy

During meiosis I, homologous chromosomes are tethered together by chiasmata formed during recombination. These connections are important because they ensure that homologues remain together during the long arrest period of the oocyte. A number of early studies into maternal-origin human trisomies mapped the inheritance of polymorphic alleles to identify crossover locations in the additional chromosome. Study of these trisomies, including trisomies 15, 16, 18, 21, Klinefelter (47,XXY) and 47,XXX, identified a clear link between reduced recombination in the oocyte and aneuploidy (Lamb *et al.*, 2005). In many cases, the non-disjoined chromosome was achiasmate, meaning that it had not engaged in the recombination process. This absence of a physical connection between homologous chromosomes can result in their random segregation at the first meiotic division, which can lead to aneuploidy in 50% of cases if both homologues segregate to the same pole (see **Figure 1.5b**). Small, acrocentric chromosomes in particular, such as chromosome 21, often do not have a crossover on the short arm, which may increase their chances of non-disjunction (Hassold *et al.*, 2007). Further research into recombination involved the genome-wide mapping of recombination foci in fetal oocytes by immunostaining with antibodies against MLH1 (mutL homologue 1), a DNA mismatch repair protein which localises to sites of recombination in pachytene.

This approach revealed a high level of heterogeneity in the number of MLH1 foci in fetal oocytes, and frequent observation of achiasmate chromosomes and chromosome arms (Tease *et al.*, 2002, Lenzi *et al.*, 2005).

In addition to the number of crossovers, the placement of crossovers also appears to affect chances of missegregation in MI. Mapping of crossover locations in chromosome 21 in cases of trisomy revealed that crossovers that were positioned too near or too far from centromeres were more likely to lead to non-disjunction (Lamb *et al.*, 2005) (Lamb 1996). This was corroborated by studies in trisomy 16 (Hassold *et al.*, 1995). One mechanism that has been proposed to explain this is terminalisation or 'slippage' of chiasmata, in which crossovers gradually move towards the end of the chromosome where they eventually 'fall off'. Maintenance of chiasmata during the long arrest period depends on cohesin, based on data from yeast, Drosophila and mouse (Buonomo *et al.*, 2000, Bickel *et al.*, 2002, Hodges *et al.*, 2005), leading to the possibility that cohesin loss can cause slippage. Hodges et al. found evidence for terminalisation in a mouse model deficient for the SMC1β subunit of cohesin. By imaging chromosomes as they underwent the transition from diakinesis (the last substage of prophase I) to MI, they were able to visualise chiasmata in postnatal oocytes. They found that in mice deficient for SMC1β crossovers were located further towards the chromosome ends (Hodges *et al.*, 2005). Cohesin along chromosome arms may prevent slippage by acting as a physical barrier to chiasmata movement along the chromosomes (Jessberger, 2012).

Since chiasmata are formed in fetal life, the connection between recombination and maternal age-related non-disjunction is not clear. One theory that has been proposed to explain this is the production-line hypothesis, which states that the first oocytes to enter meiosis in fetal life are the first to be ovulated, and that oocytes formed earlier have more recombination foci than ones that form later (Henderson & Edwards, 1968). Later oocytes, therefore, are more prone to having achiasmate chromosomes which can lead to non-disjunction. Although studies in rodents in which germ cells were radiolabelled support the idea that oocytes are ovulated in the order in which they were formed (Polani & Crolla, 1991, Hirshfield, 1992), a comparison of the numbers of recombination foci

between early and late human fetal oocytes found no difference in the number of crossover sites (Rowsey *et al.*, 2014). Moreover, studies looking at the relationship between recombination rates and maternal age have been inconclusive, with some reporting a decrease in recombination in older women (Hussin *et al.*, 2011, Bleazard *et al.*, 2013), while others have reported no difference or an increase (Kong *et al.*, 2004).

A hypothesis that is more commonly cited is the 'two-hit' model of aneuploidy (Lamb *et al.*, 1996), in which vulnerable crossover configurations constitute the first hit and the second hit is an age-related component.

1.4. The role of cohesin during meiosis I

Although non-disjunction is frequently observed amongst particular chromosomes, when considering all chromosomes, premature separation of sister chromatids is the most common mechanism of aneuploidy. This, in addition to the protracted arrest period of the oocyte in which cohesin needs to be maintained, has led to a focus on cohesin as the basis for maternal age-related aneuploidy (Jessberger, 2012). Loss of this centromeric cohesin in meiosis I can lead to premature separation of sisters and hence missegregation of individual sister chromatids.

1.4.1. Structure of the cohesin complex and its association with DNA

Cohesin belongs to the structural maintenance of chromosomes (SMC) family of proteins; the other main member of this family is condensin which confers structural rigidity upon chromosomes (Uhlmann, 2016). SMC complexes were first identified in a mutant form of *Saccharomyces cerevisiae* that was unable to maintain an artificial centromeric mini-chromosome. The gene responsible, called SMC1 (stability of mini-chromosomes), was found to encode an essential 141 kDa protein that had sequence similarity to genes in both prokaryotes and eukaryotes indicating it was highly conserved (Larionov *et al.*, 1985, Strunnikov *et al.*, 1993). Although SMC1 appeared to play a role in accurate chromosome

segregation, its physiological role was not known until later genetic screens in *S. cerevisiae* identified mutants that were able to separate sister chromatids at mitosis in the absence of APC/C activation. Of the six genes responsible for this phenotype, four were identified as being part of a core cohesin complex, SMC1, SMC3, SCC1 (sister chromatid cohesion) and SCC3, while the remaining two, SCC2 and ECO1, were required for cohesin establishment and association with chromosomes respectively (Michaelis *et al.*, 1997, Toth *et al.*, 1999). This core cohesin complex was found to be highly conserved, from bacteria to eukaryotes (reviewed in Wood *et al.*, 2010).

The core cohesin complex consists of four subunits: two SMC subunits, an α-kleisin subunit and a stromal antigen (STAG) protein. SMCs are large polypeptides, made up of between 1000–1300 amino acids. They have globular domains at their N- and C- termini which respectively contain the Walker A and Walker B nucleotide-binding motifs which are found on almost all nucleotide-binding proteins (Hirano, 2006). Crystal structure analysis of bacterial and yeast SMCs, combined with biochemical and electron microscopy analysis, found that the SMC subunits each fold up to form rod-shaped structures which comprise globular domains at either end that are linked by a 45 nm antiparallel coiled-coil (see **Figure 1.6a**). This distance is equivalent to approximately 150 bp of DNA (Hirano, 2006), and is larger than the width of a chromatin fibre which is approximately 30 nm (Li & Zhu, 2015). When the structure folds up, it unites the ATP-binding Walker A motif on the N-terminus with the Walker B motif on the C-terminus to form a functional ATPase (Haering *et al.*, 2002). The other globular domain forms the 'hinge' domain of the protein; measurement of the hinge angle by EM has found it to be approximately 88 degrees (Anderson *et al.*, 2002). The hinge domains of Smc1 and Smc3 interact with each other, forming a V-shaped Smc1/3 heterodimer (Haering *et al.*, 2002). The nuclear-binding domains (NBDs) of SMC proteins interact with another family of proteins known as kleisins. There are four major classes of kleisins (α, β, γ, and δ), of which α-kleisins are present in all eukaryotes and are essential for cohesin function (Nasmyth & Haering, 2005). In eukaryotes, The NBDs of Smc1 and Smc3 bind the N and C terminus of the α-kleisin SCC1 respectively, forming a

tripartite ring structure. The kleisin component then recruits Scc3 (or STAG3 in humans) and completes the complex (**Figure 1.6a**).

Given the molecular architecture of the cohesin complex, it has been proposed that cohesin mediates sister chromatid cohesion by trapping DNA duplexes within its ring structure. Support for a topological link between cohesin rings and DNA comes from the fact that cleavage of Scc1 or the Smc3 coiled-coil results in its disassociation of the complex from DNA (Gruber *et al.*, 2003). In addition, the SMC heterodimer is highly flexible, with a range of conformations observed in the bacterial forms of the protein under electron microscopy (Melby *et al.*, 1998). Opening and closing of the ring is controlled by ATP binding at the NBD domains: ATP binding causes the NBDs of the SMC subunits to associate with each other, thus closing the ring, and ATP hydrolysis results in disassociation (Shintomi & Hirano, 2007). In this way, the SMC heterodimer is though to act as a gate for DNA that can open and close in a highly regulated fashion. Two different models for the cohesin ring structure have been proposed: the strong ring model, in which two DNA duplexes are captured within the coiled-coil region of the SMC complex (Haering *et al.*, 2002), and the weak ring model, in which two cohesin rings each capture a single DNA duplex and are linked together in some way, forming a handcuff-like structure (see **Figure 1.6b-c**). There is little evidence that multimeric forms of cohesin exist, suggesting that the strong ring model is a more likely possibility (Nasmyth & Haering, 2009).

1.4.2. Cohesin localisation

In *S. pombe* and *S. cerevisiae*, cohesin has been shown to localise to regions of heterochromatin, which appears to be specifically required for cohesin recruitment (Bernard *et al.*, 2001, Chang *et al.*, 2005). Heterochromatin is highly dense, transcriptionally silent DNA, characterised by methylation of lysine 9 on histone H3 (H3K9me), and is found at centromeres and telomeres throughout the cell cycle. Other regions of the genome also remodel DNA into heterochromatin in response to cellular signals or gene activity, where it is known as facultative heterochromatin (Grewal & Jia, 2007). The pericentromere, the region surrounding the centromere, is where cohesin is

Figure 1.6

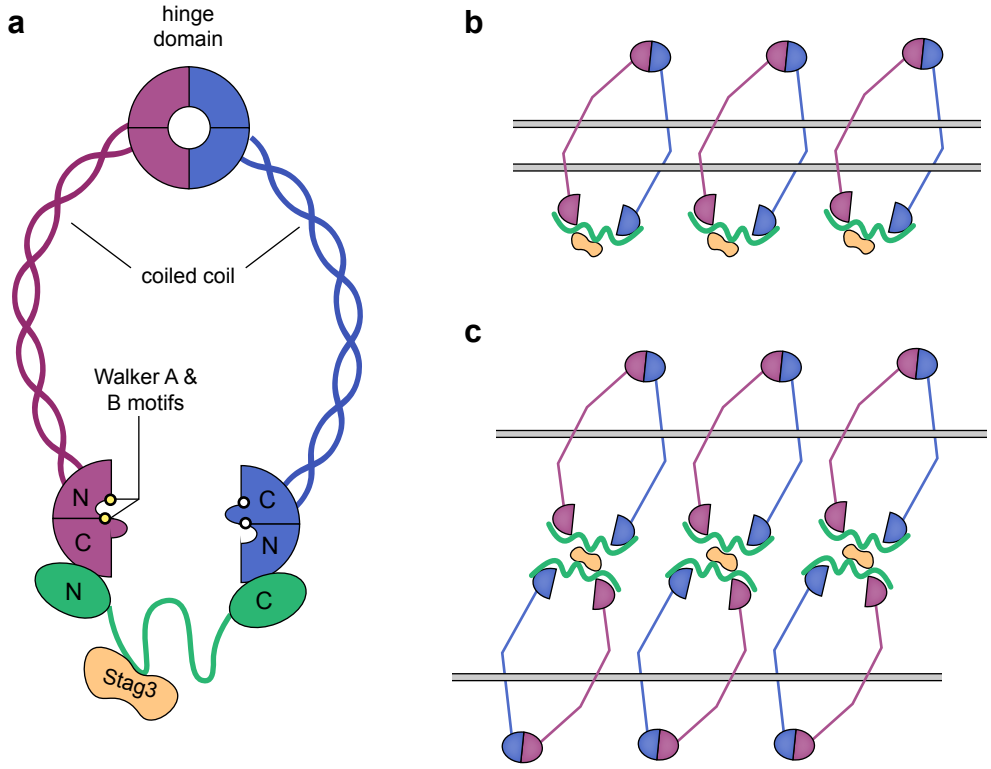

Figure 1.6. Structure of meiotic cohesin. (a) Structure of the cohesin complex. Meiotic cohesin is made up of two structural maintenance of chromosomes (SMC) family proteins, shown here in blue and purple, each of which fold up to form a structure that contains two globular domains connected by a 45 bp coiled-coil. The two SMC subunits form a V-shaped complex with a hinge domain at one end and an ATP-binding domain at the other end containing the Walker A and B motifs. Rec8 (green) binds to this region and closes the ring. It also recruits the final cohesin component, Stag3. (b) Strong ring model of cohesin in which two sister chromatids (grey) are trapped within the ring structure. (c) Weak ring model, in which linked cohesin rings each trap a single sister chromatid. Shown here is just one of the proposed models for a weak ring structure. Adapted from Hirano (2006) and Nasmyth & Haering (2009).

most concentrated. Centromeres are regions of heterochromatin characterised by the presence of a histone 3 variant, centromeric protein A (CENP-A), and enriched in cohesins, condensins and topoisomerase II (Bloom, 2014). In addition to acting as a site for kinetochore formation, the heterochromatic architecture of the centromere also dictates the geometry and function of kinetochore and the spindle (Verdaasdonk & Bloom, 2011). In budding yeast, which have short 125 bp 'point' centromeres that form attachments to a single microtubule, cohesin is enriched by about threefold in the 30–50 Kb region surrounding the centromere (Weber *et al.*, 2004, Bloom, 2014). Cohesin appears to play an important role in maintaining chromatin architecture at the centromeres, as a reduction in centromeric cohesin in budding yeast causes increased centromere stretching and increased chromosome missegregation (Eckert *et al.*, 2007). Unlike yeast, mammals have larger and more complex regional centromeres composed of highly repetitive DNA sequences. In humans, they can be up to 5 Mb and contain anywhere between 1–4 Mb of 171-bp α-satellite repeats (Verdaasdonk & Bloom, 2011). The repetitive sequences of mammalian centromeres preclude genome-wide mapping based approaches to measure centromeric cohesin levels, but immunofluorescent staining has shown that cohesin is also enriched in centromeric regions in human mitotic cells (Hoque & Ishikawa, 2001).

In addition to the centromeric localisation of cohesin, genome-wide mapping of cohesin in yeast has also shown that the position of cohesin on chromosomes changes with transcriptional activity, with cohesins enriched at 3' ends of genes and in the intergenic regions of genes that are transcribed in converging directions (Lengronne *et al.*, 2004). In mammals, on the other hand, cohesin along chromosome arms appears to be equally distributed between genic and intergenic regions, with its positioning dependent on the underlying DNA sequence; in particular, it is enriched at binding sites for the DNA-binding protein CTCF (Parelho *et al.*, 2008). The average spacing distance between cohesin molecules in mammalian chromosomes has been measured to be 22.2 Kb, although its positioning along chromosomes is irregular (Parelho *et al.*, 2008).

1.4.3. Differences between mitotic and meiotic cohesin

There are some differences between mitotic and meiotic cohesin, which reflect the different roles that cohesin plays in each of these divisions; namely, that in meiosis, cohesin is protected at centromeres during the first meiotic division. In mitosis, the human cohesin complex is made up of SMC1α, SMC3, the α-kleisin RAD21 and STAG1/2. In meiosis, SMC1α, RAD21 and STAG1/2 are replaced respectively with the meiosis-specific components SMC1β, REC8 and STAG3 (Nasmyth & Haering, 2009). The meiotic structure of cohesin is similar to that of mitotic cohesin: the SMC subunits form a V-shaped structure that is bridged by the α-kleisin Rec8 to form a ring (Revenkova *et al.*, 2004, Nasmyth & Haering, 2009, Jessberger, 2012), and STAG3 associates with Rec8 and completes the complex (Revenkova & Jessberger, 2005). Although the molecular structure of the complex is the same, the different cohesin components have meiosis-specific roles. For instance, the meiosis-specific α-kleisin Rec8 appears to be essential for the reductional division in meiosis I, because deletion of the Rec8 gene in *S. pombe* causes sister chromatids to separate at meiosis I (Watanabe & Nurse, 1999). STAG3, the meiotic equivalent of STAG 1/2, is involved in sister chromatid arm cohesion as it comprises the axial/lateral elements of the synaptonemal complex (Pezzi *et al.*, 2000, Prieto *et al.*, 2001). Loss of STAG3 in mice results in sterility due to failure of homologous chromosomes to synapse as a result of incomplete assembly of synaptonemal complex axial elements (Winters *et al.*, 2014).

1.4.4. Mechanisms of cohesin dissociation from chromosomes

In vertebrates, cohesin is removed from chromosome arms by two separate pathways, which are characterised by different temporal regulation and mechanisms. The first removal pathway occurs between prophase and prometaphase, and removes most arm cohesin in a process that is dependent on a chromosome-associated protein known as Wapl (Gandhi *et al.*, 2006, Kueng *et al.*, 2006). The second mechanism of cohesin removal is via proteolytic cleavage of the kleisin subunit of cohesin by a protein called separase (Buonomo *et al.*, 2000, Hauf *et al.*, 2001, Kitajima *et al.*, 2003).

At centromeres, cohesin is protected from removal by the prophase pathway by a protein called shugoshin 1 (Sgo1) which acts together with protein phosphatase 2A (PP2A) to protect cohesin (Watanabe & Kitajima, 2005, Nasmyth & Haering, 2009). Purified Sgo complex can dephosphorylate of cohesin *in vitro* suggesting that the mechanism of cohesin protection is likely to involve dephosphorylation (Kitajima *et al.*, 2006). In mouse oocytes, Sgo2 is required for centromeric Rec8 protection: loss of Sgo results in centromeric cohesin removal during meiosis I, indicating its role as a meiosis-specific coordinator of centromeric protection (Lee *et al.*, 2008, Llano *et al.*, 2008).

1.4.5. Is there turnover of cohesin during meiotic prophase I arrest?

In mammalian meiosis, including humans and mice, cohesin is loaded onto chromosome arms early in first meiotic prophase, which occurs during fetal life (Garcia-Cruz *et al.*, 2010, Kuleszewicz *et al.*, 2013). The first meiotic division is completed shortly before ovulation, so cohesin is required to keep chromosomes together for several months in mice and many years in humans. This raises the question of whether there is turnover of cohesin subunits during the long period of prophase arrest.

Work in mouse oocytes has indicated that there is no cohesin turnover during the arrest period. In the first of these studies, the SMC1β gene was inactivated in mice shortly after birth using Cre-mediated recombination, preventing synthesis of new cohesin transcripts. The treated mice retained full fertility, and chiasmata position and number in their oocytes appeared normal, which indicates that expression of cohesin is not required during prophase I arrest in mouse (Revenkova *et al.*, 2010). This does not, however, exclude the possibility that new cohesin is synthesised from pre-existing mRNA or is reloaded onto chromosomes from existing pools of protein in the cell. A further study by Tachibana-Konwalski et al. created mice with a cleavable form of the Rec8 protein by incorporating a TEV site into the protein. This enabled cohesin inactivation in oocytes after birth through TEV protease treatment. As might be expected, Rec8 cleavage resulted in conversion of bivalents to univalents and

then to single chromatids. Activation of a transgene, driven by a *Zp3* (zona pellucida 3) promoter which is only activated during oocyte growth, encoding non-cleavable Rec8 did not prevent the conversion of bivalents into chromatids, indicating that newly-synthesised Rec8 was not loaded onto chromosomes during the period of oocyte growth (Tachibana-Konwalski *et al.*, 2010). However, as the transgene was only expressed during oocyte growth there is still the possibility that turnover occurs later in development. Building on this work, a further study used tamoxifen-induced activation of a transgene for non-cleavable Rec8 in the same mouse model, enabling the researchers to test whether there was cohesin reloading over a period of months. As in the earlier study, protease treatment resulted in bivalent conversion to chromatids, despite activation of the transgene over a period of 2 or 4 months (Burkhardt *et al.*, 2016). Hence, results from mouse oocytes indicate that there is no cohesin turnover during the prophase arrest period of the oocyte.

1.4.6. The relationship between cohesin levels and age

Given the apparent lack of cohesin turnover, the next important question to ask is whether there is a deterioration in cohesin levels over time. A study conducted in a naturally-ageing mouse strain treated MI-stage oocytes with monastrol, a kinesin-5 inhibitor (Mayer *et al.*, 1999), to create monopolar spindles, then generated chromosome spreads from these eggs. Treatment with kinesin-5 minimises the pulling forces generated on sister kinetochores by microtubules, meaning any inter-kinetochore distance reflects the amount of centromeric cohesin. They found that the distance between sister chromatid kinetochores increases with age, indicating a decline in cohesin; importantly, this distance was found to be increased in aneuploid eggs (Chiang *et al.*, 2010). Another study stained Rec8 in mouse oocyte spreads and showed that Rec8 abundance was reduced in spreads from older mice (Lister *et al.*, 2010). Using the same approach, the researchers also identified a concomitant decline in levels of Sgo2, which protects Rec8 from cleavage by separase (Lee *et al.*, 2008). An age-dependent decline in Sgo2 could therefore also contribute to the maternal age effect. Another study measured Rec8, STAG3 and SMC1b levels in senescence-accelerated mice that have been used in aging studies, and found

that levels were markedly reduced in oocytes from these strains (Liu & Keefe, 2008), There is therefore evidence from mouse that cohesin declines with age and is a likely contributor to aneuploidy in older oocytes.

Given the difficulty of obtaining human oocytes for research purposes, relatively few studies on cohesin decline have been conducted in humans. Duncan et al. measured inter-kinetochore distances in 18 MII oocytes from 6 women aged between 16 and 37 years who had their ovaries removed for medical indications, with the aim of identifying whether there was a decline in cohesin with age. The oocytes were isolated and matured in vitro, then treated with monastrol, an inhibitor of the Eg5 kinesin, to generate monopolar spindles, which limits the effect of pulling forces from spindle kinetochore-fibres which can alter inter-kinetochore distance. After fixation and immunostaining of kinetochores using CREST antisera, they measured inter-kinetochore distance and found that it was greater in the oocytes from older patients, suggesting a decline in centromeric cohesin (Duncan *et al.*, 2012). However, as most of the women in the study had cancer the possibility that the oocytes had undergone chromosomal deterioration or molecular damage cannot be ruled out. Furthermore, the study only includes women up to the age of 37 years, which means they had no women in their late 30s/early 40s when the aneuploidy risk becomes significant. Another study in humans used immunofluorescence to measure the relative intensities of Rec8 and Smc1β levels in oocytes in adult ovarian tissue sections from eight women with ovarian tumours. They showed that cohesin formed thread-like patterns (comparable to fetal oocytes) and identified a decline in levels of Rec8 and Smc1β between older and younger women (Tsutsumi *et al.*, 2014). However, the study quantified cohesin in thin tissue sections, which does not give a full picture of cohesin in individual oocytes. Moreover, as the material for this work came from women with ovarian tumours, this raises concerns about sample quality.

Therefore, there are indications that cohesin declines with age in humans, however as the research performed so far has been on samples obtained from women with cancer or ovarian tumours, the data from human studies should be treated with caution. Given the limited amount of research conducted on

cohesin in human samples, further work is needed to determine whether cohesin decline contributes to aneuploidy in humans.

1.5. Kinetochores in the first meiotic division

During the first meiotic division, protection of centromeric cohesin is important for keeping sister chromatids together, but it may also help to ensure that kinetochores on sister chromatids form attachments to the same spindle pole. Kinetochores are multiprotein assemblies that constitute the physical interface between the chromosome and the spindle. As well as acting as a mechanical link between chromosomes and spindle microtubule fibres, they are also a signalling platform for spindle checkpoint proteins that control entry into anaphase (Musacchio & Salmon, 2007). Accurate chromosome segregation, in both mitosis and meiosis, depends on the formation of stable kinetochore-microtubule attachments and correction of any erroneous attachments.

1.5.1. Kinetochore structure and function

Kinetochores are disk-shaped structures, consisting of three distinct layers when examined by electron microscopy (Jokelainen, 1967; Comings and Okada, 1971): the inner plate, outer plate and fibrous corona (Chan *et al.*, 2005). Kinetochores assemble on centromeres, regions of specialised DNA, characterised by the presence of the histone 3 variant CENP-A which assembles into specialised nucleosomes (Sullivan & Karpen, 2004). Although centromeres vary in size between species, from the point centromeres of *S. cerevisiae* to the large regional centromeres found in mammals, the CENP-A protein is highly conserved, and loss of it is lethal in every organism studied to date (McKinley & Cheeseman, 2016). The timing of CENP-A incorporation into centromeric nucleosomes varies between species, but in humans it occurs between anaphase and G1 of the cell cycle. The geometry of centromeric chromatin is thought be such that the CENP-A containing nucleosomes are exposed to the spindle poles, whilst H3 nucleosomes are found within the inner chromatid region (Sullivan & Karpen, 2004, Verdaasdonk & Bloom, 2011,

Schalch & Steiner, 2017). This gives rise to the mitotic ‘back-to-back’ arrangement of sister kinetochores which can facilitate amphitelic attachment in mitosis. Inner centromeric components and kinetochores are interlinked, as we shall see.

The kinetochore inner plate consists of a number of components that make up the constitutive centromere-associated network (CCAN), which provides structural integrity and acts as a platform for subsequent loading of outer kinetochore proteins (Suzuki *et al.*, 2014). CENP-A is an important component of the CCAN, already discussed. Of the other components that constitute the CCAN, CENP-C and CENP-T, interact with the highly-conserved KMN network of outer kinetochore components that forms attachments to microtubules (Foley & Kapoor, 2013). The KMN network consists of three complexes, Knl1, Mis12 and Ndc80, and forms the interface between centromeric DNA and microtubule attachment. Specifically, the four-subunit Ndc80 complex (made up of hNdc80/Hec1, Nuf2, Spc24 and Spc25) forms attachments to microtubule plus-ends, which are strengthened by Knl1. Phosphorylation of Ndc80/Hec1 by Aurora B kinase regulates attachment status (Cheeseman *et al.*, 2006). The Mis12 component of KMN links the complex with CENP-C. These connections enable inner kinetochore stretching to link with stabilisation of microtubule attachments. The outermost region of the kinetochore, the fibrous corona, comprises components of the kinetochore that are more transiently linked to the kinetochore and include spindle assembly checkpoint and motor proteins. This includes the microtubule plus-end-directed motor protein CENP-E, which is essential during mitosis for transporting misaligned chromosomes towards the cell equator and for stabilising kinetochore-microtubule attachments (Kapoor *et al.*, 2006, Gudimchuk *et al.*, 2013).

In mitosis, during the process of chromosome alignment at the metaphase plate, inter-kinetochore distance is not fixed, and the linkages between sisters stretch in response to chromosome oscillations, a behaviour referred to as ‘breathing’ (Skibbens *et al.*, 1993). Oscillations are linked to chromosome congression, as a reduction in oscillation speed results in a thinner metaphase plate, indicating that chromosomes have become aligned (Jaqaman *et al.*, 2010). Oscillations

appear to depend on the stiffness of the mechanical linkages between sister kinetochores which are mediated by cohesin (Nasmyth, 2002) and condensin (Ono *et al.*, 2004, Oliveira *et al.*, 2005, Hirano, 2012). Condensin subunit depletion, resulting in a less stiff linkage, increases oscillation speed and periodicity, whilst increased stiffness, achieved through separase depletion, had the opposite effect (Jaqaman *et al.*, 2010). These results indicate that centromeric stiffness play a role in regulating chromosome oscillations and hence chromosome congression at the metaphase plate.

In addition to inter-kinetochore distance, intra-kinetochore distances during mitosis are also not fixed. The relative positions of certain components that make up the inner plate, outer plate and fibrous corona change during metaphase when chromosomes are aligning. This stretching is thought to be important for satisfying the spindle assembly checkpoint, particularly as loss of stretch results in checkpoint activation (Maresca & Salmon, 2009). The degree of stretch and identification of compliant regions can be determined by measuring the distances between different inner and outer components. For instance, using two-colour immunofluorescence in fixed HeLa cells in metaphase, Wan et al. measured the distance between antibody-tagged kinetochore proteins to an accuracy of <5 nm. Using this approach, it was possible to build up a nanoscale map of kinetochore architecture, which revealed that most compliancy is within the inner region of the kinetochore that interacts with centromeric chromatin (Wan *et al.*, 2009). Further work by Suzuki et al. used this method to investigate the architecture of the CCAN. They found that depletion of CCAN components resulted in hyperstretching of the inner kinetochore, which in turn led to decreased Ndc80/Hec1 phosphorylation, indicating that inner kinetochore stretch is closely linked to regulation of kinetochore-microtubule attachments (Suzuki *et al.*, 2014).

1.5.2. Kinetochore-microtubule attachment stability in MI

Studies looking at kinetochore architecture have so far been limited to mitosis, in which sister kinetochores form attachments to microtubule kinetochore-fibres (k-fibres) from opposite spindle poles. During the first meiotic division, however,

the opposite is true: sisters form attachments to k-fibres from the same spindle pole. There is evidence that formation of k-fibre attachments in oocytes during MI is impaired. Immunofluorescence analysis of mouse oocytes, fixed at various timepoints after nuclear envelope breakdown, found that they are prone to forming incorrect attachments, such as merotelic attachments (in which kinetochores are attached to microtubule fibres from both poles). Like in mitosis, correction of these attachments is dependent on the activity of Aurora B kinase (Kitajima *et al.*, 2011). There are also indications that formation of stable attachments is related to age. Shomper et al. compared kinetochore-microtubule attachments in fixed oocytes from young and aged mice, and found that oocytes from older mice have a higher proportion of incorrect attachments than those from younger mice (Shomper *et al.*, 2014). This propensity to form incorrect attachments also appears to apply to human oocytes. Live-cell imaging in human oocytes after GV breakdown found that the prolonged spindle assembly period of ~16 hours was accompanied by a high proportion of erroneous kinetochore-microtubule attachments (Holubcova *et al.*, 2015). It is not clear why attachment is so error-prone in MI, but one possibility may be the altered sister kinetochore geometry that enables sisters to attach to k-fibres from the same pole.

1.5.3. Kinetochore geometry during the first meiotic division

The first meiotic division represents a unique situation for sister kinetochores because sister chromatids must segregate together, so the mitotic back-to-back arrangement is no longer appropriate. Electron microscopy in mouse spermatocytes has provided support for a ‘side-by-side’ arrangement of sister kinetochores in meiosis I bivalents (Parra *et al.*, 2004), a configuration that would enable co-segregation of sister chromatids. This altered arrangement has implications for the geometry and internal architecture of the meiotic kinetochore (**Figure 1.7**). I examine here what is known about sister kinetochore geometry during MI.

Most studies have indicated that fusion of sisters is the main mechanism of ensuring co-segregation of sisters in MI. A functional genomics screen in

Figure 1.7

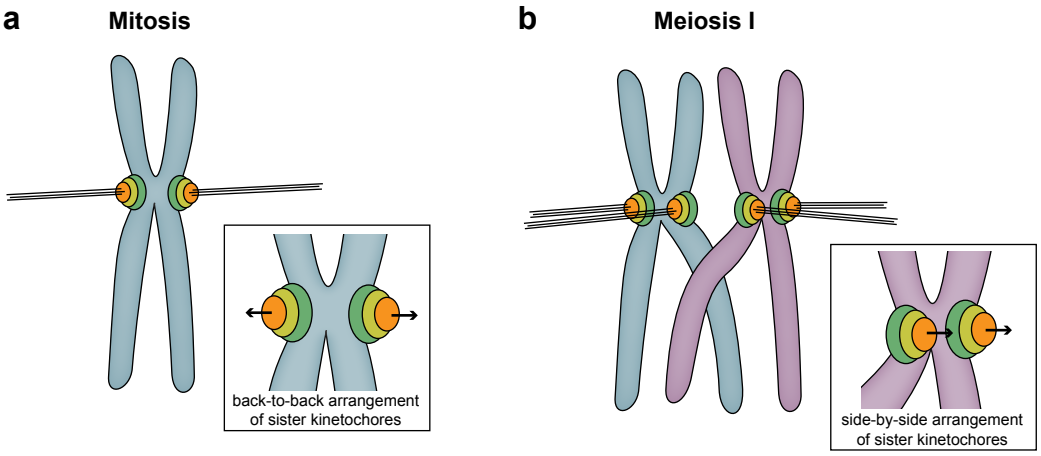

Figure 1.7. Kinetochore orientation in mitosis and meiosis I. (a) In mitosis, kinetochores are in a back-to-back arrangement, with the outer regions of each kinetochore (orange) facing opposite spindle poles. (b) In meiosis I, however, sister kinetochores are in a side-by-side arrangement with their outer regions facing the same spindle pole. In both cases, the inner plate of the kinetochore (green) faces inwards towards the centromeric chromatin.

budding yeast identified the kinetochore-localised Mam1 protein as being crucial for homologue segregation in MI by promoting attachment of sister kinetochores to microtubules from the same spindle pole (Toth *et al.*, 2000). Further work identified three other proteins, Csm1, Lrs4 and Hrr25, that act in complex with Mam1 to ensure homologue separation (Rabitsch *et al.*, 2003, Petronczki *et al.*, 2006). Collectively, these proteins are known as the monopolin complex as they are required for sister kinetochore monopolar attachment (attachment to one spindle pole). It is likely that monopolin induces a physical linkage between sister kinetochores, because expressing monopolin components in mitotic yeast cells results in mono-orientation of sister kinetochores (Monje-Casas *et al.*, 2007). Crystal structure analysis revealed that monopolin forms a V-shaped complex that may enable it to directly crosslink sisters (Corbett *et al.*, 2010).

An alternative model for sister kinetochore arrangement in MI is one in which one sister is selectively inactivated or 'shut off'. Electron micrographs of kinetochore-microtubule attachments in budding yeast MI cells revealed that fused sister kinetochores form a single kinetochore-fibre attachment, like in mitosis (Winey *et al.*, 2005). This may indicate that sisters fused by monopolin behave as a single functional unit; however an alternative explanation for this could be selective inactivation of a kinetochore within the pair. To address whether kinetochore inactivation occurs in yeast, Sarangapani *et al.* isolated fused sister kinetochores from MI yeast cells and found that, compared to their mitotic counterparts, they have more microtubule-binding elements and form stronger attachments, indicating that both sister kinetochores contribute to k-fibre attachment formation (Sarangapani *et al.*, 2014). It therefore appears that in yeast, fused kinetochores act as a co-functional unit to ensure homologue segregation in MI.

There does not appear to be conservation of mono-orientation between different yeast species, as orthologues of monopolin have not been identified in other species. In fission yeast, homologue segregation is instead promoted in a cohesin-dependent manner by the kinetochore protein Moa1 (Yokobayashi & Watanabe, 2005). Moa1 does not share homology with any of the proteins

required for mono-orientation in budding yeast, indicating significant divergence in the proteins involved in monopolar attachment. Moa1 is recruited to the centromere by the inner kinetochore protein Cnp3 (Tanaka *et al.*, 2009), a homologue of CCAN component CENP-C, where it induces sister kinetochore mono-orientation through direct interaction with Rec8. In the absence of centromeric Rec8, Moa1 is unable to establish mono-orientation, indicating that cohesin is an essential component in fission yeast mono-orientation (Yokobayashi & Watanabe, 2005). Although cohesin is not needed in budding yeast for mono-orientation, another complex containing components of the SMC (structural maintenance of chromosomes) family, condensin, is important; without it, there is an increase in the numbers of bi-oriented sister kinetochores during MI and a decrease in Mam1 association with kinetochores (Brito *et al.*, 2010).

In mouse, a yeast two-hybrid screen for CENP-C interactors during meiosis in testis samples identified Meikin, which localises to kinetochores during MI in mouse spermatozoa and oocytes. In Meikin-deficient mouse oocytes, sister kinetochores in MI appear as two spots under light microscopy, rather than a single spot, indicating loss of fusion. Like in fission yeast, there appears to be a role for Rec8 in mouse MI, because in Meikin-deficient oocytes, the cohesin complex component Rec8 is lost at the centromere in metaphase II chromosomes (Kim *et al.*, 2015). A separate study in mouse oocytes found that selective cleavage of Rec8 at the centromeres resulted in sister kinetochore splitting, supporting its role in mono-orientation (Tachibana-Konwalski *et al.*, 2013).

An alternative model of sister kinetochore arrangement in MI comes from plants. In maize MI, the inner kinetochore is separated, but the outer kinetochore components Mis12 and Ndc80 (part of the KMN complex) form a bridge structure linking the two sister kinetochores, which can be visualised using immunofluorescence microscopy. As the outer plate is involved in formation of stable k-fibre attachments, this model would enable sisters to form a single k-fibre attachment between them to ensure co-segregation. Depletion of Mis12 causes breaking of the bridge structure and random attachment of sister

kinetochores, resulting in subsequent failure to complete anaphase (Li & Dawe, 2009).

Thus, there are a number of mechanisms in which sister kinetochores can be arranged to achieve the first meiotic division. All of the mechanisms described involve some form of physical association between the two sisters, whether it is linkage by a regulator such as monopolin or Meikin, or direct linkage of kinetochore components as in plants. Although a homologue of Meikin exists in humans, its presence in human oocytes has not been observed, and the geometry of the human oocyte kinetochore remains uncharacterised.

1.6. Aim of this project

An understanding of meiotic kinetochore arrangement in human oocytes may help us to understand why the first meiotic division is highly error-prone. To characterise the geometry and organisation of kinetochores in the first meiotic division of human oocytes, I aimed to fix intact human MI oocytes and study their chromosomes and kinetochores at high-resolution using spinning-disk confocal microscopy. Immunofluorescence will be used to visualise chromosomes and kinetochores in these oocytes, using different markers of kinetochore proteins to build up a picture of internal kinetochore architecture. The advantage of fixing oocytes intact is that this will enable study of kinetochore arrangement within bivalents *in situ*, as previous approaches that have used chromosome spreading result in loss of spatial information of kinetochore arrangement. A particular area of focus in my research into the human female meiotic kinetochore will be to determine whether there are any age-associated changes in organisation. I aim to follow up meiotic kinetochore characterisation with establishing a live-cell imaging platform for studying kinetochore dynamics during the first meiotic division.

Chapter 2: Materials and Methods

2.1. Human oocytes

2.1.1. Donation of oocytes to research

Oocytes used in this study were donated by patients undergoing *in vitro* fertilisation (IVF) or intracytoplasmic sperm injection (ICSI) at the Centre for Reproductive Medicine, University Hospitals Coventry & Warwickshire. **Table 2.1** gives details of the oocytes and patients used in the study. Informed consent for donation of oocytes to research was obtained from all patients whose oocytes were used. Approval for this research was granted by the NHS Research Ethics Committee and the Human Fertilisation and Embryology Authority (HFEA; research licence RO155). See **Appendix C** for copies of HFEA licences and documentation pertaining to acquisition of patient consent. All oocytes donated to research were unsuitable for use in the donating patient's treatment and would otherwise have been discarded. Unsuitable oocytes obtained from IVF patients were those that had been incubated with sperm overnight, but showed no indications of having been fertilised. From ICSI patients, unsuitable oocytes were those that had been assessed as being at germinal vesicle (GV) or metaphase I (MI) stage, by light microscopy prior to sperm microinjection. The decision as to which oocytes were suitable for research use, checking of consent, and witnessing of their removal from the clinical pathway, was undertaken by clinical embryologists. For purposes of selection for research use, oocytes were presumed to be in metaphase I (MI) if neither a germinal vesicle (GV) nucleus nor polar bodies were visible by light microscopy. This initial clinical assessment was further informed by detailed analysis of chromosomes in the course of the research.

2.1.2. Ovarian stimulation

All women who received IVF/ICSI treatment first underwent a period of ovarian stimulation through one of two protocols, administered under the guidance of medical personnel. In the ‘long’ protocol, a gonadotrophin-releasing hormone (GnRH) agonist was administered to achieve pituitary suppression, which was then followed by a period of exogenous FSH administration. In the antagonist (or short) protocol, a GnRH antagonist was administered which competitively binds to FSH receptors, thus requiring a shorter period of treatment and generally lower doses of FSH. For the patients included in the study, daily gonadotrophin doses varied from 150–450 i.u. (**Table 2.1**). There did not appear to be a relationship between the total FSH dose received by women and the proportion of distinct kinetochore pairs or inter-kinetochore distance (**Figure 2.1**).

2.1.3. Whole oocyte fixation

Fixation and staining of human oocytes was performed using an adapted version of a previously published protocol (Riris *et al.*, 2013). Upon allocation to research, oocytes were washed briefly in PHEM buffer (60 mM PIPES, 25 mM HEPES, 10 mM EGTA, 4 mM MgSO4.7H2O; pH 6.9) with 0.25% Triton X-100 at 37°C to stabilise microtubules and permeabilise the cell membrane. They were then fixed in 3.7% paraformaldehyde in PHEM for 30 min at room temperature. Following fixation, oocytes were placed in PBB (0.5% BSA in PBS) for 5 min, then permeabilised with 0.25% Triton X-100 in PBS for 15 min. To prevent non-specific antibody binding they were then transferred to a blocking solution (3% BSA in PBS with 0.05% Tween-20) where they were stored at 4°C overnight. For cold shock treatment, oocytes were placed in ice-cold media for 2 min upon receipt, then fixation was performed as described. All fixation steps were performed in 4-well IVF plates (Nunc).

Table 2.1.

Patient no.	Age	Pre-treatment parity	Reason for treatment	Treatment	Stimulation protocol	Days of stimulation	Daily dose (i.u.)	Total dose (i.u.)	Gonadotrophin	Total oocytes collected	2PN rate	Outcome of treatment cycle
1*	27.7	0+0	Same-sex female couple	IVF	antagonist	8	150	1200	Menopur	10	7	Neg
2*	28.6	0+0	Male factor infertility	IVF	long	14	150	2100	Menopur	10	8	1FH
3	39.0	0+0	Unexplained infertility	ICSI	long	11	450	4950	Gonal-F	12	2	Neg
4	39.0	0+0	Unexplained infertility	IVF	long	11	225	2475	Menopur	16	10	Neg
5	28.1	0+0	Polycystic ovarian disease	IVF	antagonist	11	150	1650	Menopur	11	6	1FH
6*	29.1	0+1	Azoospermia	IVF	long	11	225	2475	Menopur	7	4	1FH
7	38.4	0+0	Unexplained infertility	IVF	long	13	225	2925	Menopur	14	7	1FH
8	40.7	0+3	Recurrent miscarriage / unexplained subfertility	IVF	long	13	450	5850	Menopur	15	7	2FH
9	32.4	0+0	Uterine factor	ICSI	antagonist	12	450	5400	Menopur	10	2	1FH
10	38.3	0+0	Unexplained infertility	ICSI	long	14	225	3150	Menopur	4	2	1FH
11*	34.9	0+0	Male factor infertility	IVF	long	14	300	4200	Menopur	9	6	1FH
12	30.2	0+0	Polycystic ovarian syndrome	IVF	antagonist	12	150	1800	Menopur	12	8	Neg
13	39.8	1+1	Endometriosis, bicornate uterus	IVF	long	11	225	2475	Menopur	21	12	Neg
14	35.1	0+0	Polycystic ovarian syndrome	IVF	antagonist	8	150	1200	Menopur	8	2	Neg
15	26.2	0+0	Endometriosis	IVF	long	14	150	2100	Menopur (75) + Bemfola (75)	13	10	1FH
16	35.3	0+0	Unexplained infertility	ICSI	antagonist	8	450	3600	Menopur	3	1	Neg
17	34.7	0+1	Severe endometriosis; left tube blockage	IVF	long	11	225	2475	Menopur (150) + Bemfola (75)	30	23	1FH
18*	33.8	0+0	Male factor infertility	ICSI	long	11	150	1650	Menopur (75) + Bemfola (75)	9	2	1FH
19	39.1	1+1	Cardiomyopathy†	ICSI	long	11	225	2475	Menopur (150) + Bemfola (75)	8	5	Neg
20	32.1	0+1	Polycystic ovarian syndrome	IVF	antagonist	9	150	1350	Menopur	14	11	1FH

Table 2.1. Details of the women donating oocytes to this study, including reasons for assisted reproductive treatment, stimulation data and outcomes. Patients 2, 5, 6, 7, 9, 10, 11, 12, 14 and 16 have demonstrated fertility by becoming pregnant either as a result of treatment or previously. Patients underwent one of two stimulation protocols, described in more detail in the Materials and Methods section. Briefly, the 'long' protocol involves pituitary suppression with GnRH agonists over several weeks to prevent a surge in luteinising hormone (LH). The 'antagonist' protocol involves treatment with gonadotrophin-releasing hormone (GnRH) antagonists which competitively bind to pituitary GnRH receptors, resulting in rapid inhibition of gonadotrophin release. This avoids the long down-regulation period involved in the long protocol and is often used in women where there is a risk of ovarian hyperstimulation syndrome. Asterisks indicate women with no known fertility issues, whose partner's infertility or absence of a male partner may explain the couple's infertility. Parity data is shown as parity (number of births >24 weeks) + gravidity (number of pregnancies). FH: fetal heart visible on ultrasound scan. IVF: *in vitro* fertilisation. ICSI: intracytoplasmic sperm injection. Neg: no pregnancy. †Patient was undergoing IVF for surrogacy, due to cardiomyopathy.

Figure 2.1

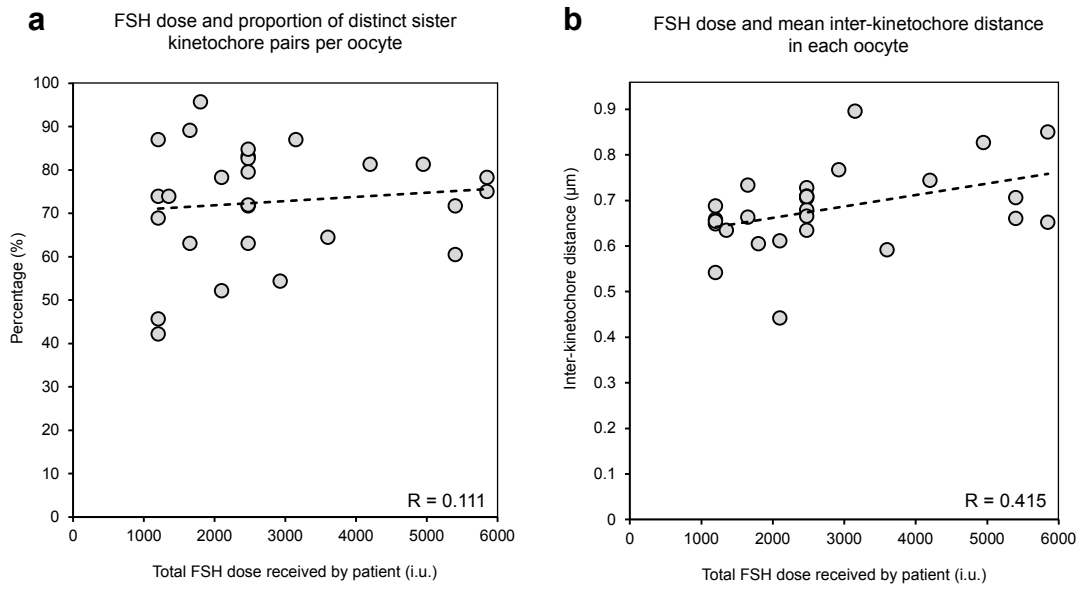

Figure 2.1. Examination of the effect of total follicle-stimulating hormone (FSH) dose on the results reported in this thesis. Women included in this study received daily exogenous FSH in varying doses for between 8–14 days prior to oocyte collection. (a) There does not appear to be a correlation between FSH dose and the proportion of distinct sister kinetochore pairs (sister kinetochores that appear as two distinct foci under high-resolution immunofluorescent imaging) per oocyte. Pearson's R = 0.111. (b) There is weak correlation between FSH dose and inter-kinetochore distance. Pearson's R = 0.415.

2.1.4. Immunofluorescence of fixed human oocytes

Fixed oocytes were incubated at 37°C for 1 hr in 20 µl droplets of blocking solution containing primary antibodies at the relevant dilution (see **Table 2.2**). The droplets were placed in 4-well IVF dishes and were overlaid with sterile mineral oil (Sigma) to prevent evaporation of the blocking solution. Oocytes from different patients were processed separately. Oocytes from the same patient were stained in batches only if they were to be stained with the same combination of primary antibodies. Incubation with primary antibodies was followed by a 15 min wash at room temperature in PBB with 0.05% Tween-20. This was followed by 1 hr incubation with secondary antibodies at 37°C, followed by a final wash. Oocytes were mounted in a 5 µl droplet of ProLong® Gold Antifade Mountant with DAPI (Invitrogen) mixed 1:1 with blocking solution in 35 mm dishes with No. 0 coverglass bottoms (MatTek). After transferral into mountant, oocytes were left overnight where they settled naturally towards the base of the dish. After mounting, oocytes were stored at 4ºC.

2.1.5. Oocytes included in the study

In total, 216 oocytes from 81 patients underwent fixation, immunofluorescence and high-resolution imaging, as described above. Of these, 119 (from 58 patients) were classified as 'immature' by embryologists upon donation (i.e. GV or MI stage). Although the aim of this research was to study MI oocytes, GV stage oocytes were also fixed because there was the possibility that they would have advanced to MI by the time of fixation. Upon high-resolution imaging, only a small fraction of the oocytes classified as immature (27/119, from 20 patients) were found to be in MI and therefore were suitable for analysis of kinetochores at the first meiotic division. Oocytes were excluded if they contained a GV (n = 12), had advanced to MII (n = 37), were in telophase (n = 2) or contained abnormalities that made them unsuitable for analysis (n = 41). Common abnormalities included: presence of multiple spindles, abnormal chromosome appearance, chromosomes scattered throughout oocyte cytoplasm. See **Figure 2.2** for examples of oocytes that were excluded. In addition, 97 MII stage

Table 2.2.

Antibody	Type	Dilution	Source
CREST antisera	1º	1:50	Antibodies Incorporated
Rabbit CENP-E	1º	1:200	Meraldi et al. (2004)
Mouse monoclonal a-tubulin	1º	1:200	Sigma (T6074)
Mouse monoclonal against Hec1-9G3	1º	1:50	Abcam (ab3613)
Mouse monoclonal Bub1	1º	1:50	Meraldi et al. (2004)
Anti-mouse Alexa Fluor 488®	2º	1:200	Stratech
Anti-mouse Alexa Fluor 594®	2º	1:200	Stratech
Anti-mouse Alexa Fluor 647®	2º	1:200	Stratech
Anti-human Alexa Fluor 488®	2º	1:200	Stratech
Anti-human Alexa Fluor 594®	2º	1:200	Stratech
Anti-human Alexa Fluor 647®	2º	1:200	Stratech
Anti-rabbit Alexa Fluor 488®	2º	1:200	Stratech
Anti-rabbit Alexa Fluor 594®	2º	1:200	Stratech
Anti-rabbit Alexa Fluor 647®	2º	1:200	Stratech

Table 2.2. Primary and secondary antibodies used in MI and MII oocytes.

Figure 2.2

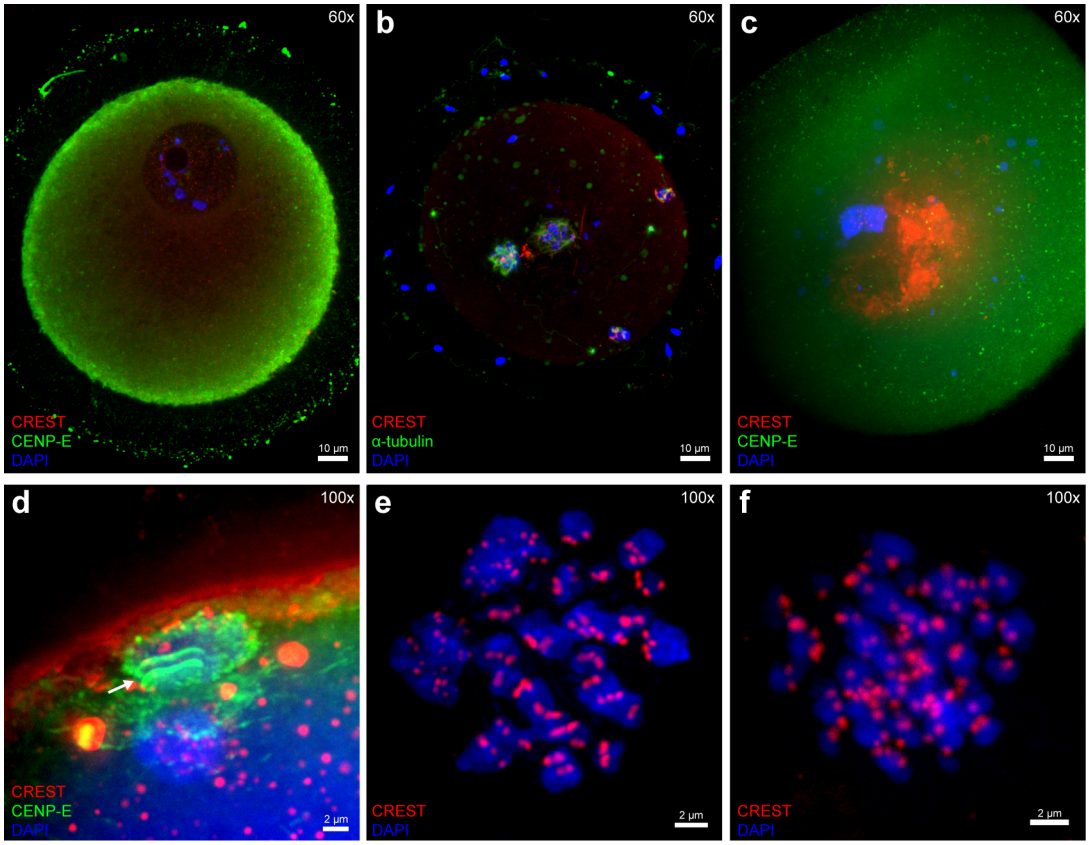

Figure 2.2. Examples of oocytes excluded from final analysis. (a) GV stage oocyte. Circular GV structure containing oocyte chromosomes can be visualised within oocyte. (b) Oocyte with multiple spindles. (c) Oocyte of unclear stage; there is neither GV nor polar body, indicating it is in metaphase I, but the chromosomes are clumped closely together with no obvious bivalent structures. (d) Telophase stage oocyte: CENP-E (green) can be seen localising to the midbody (marked with arrow) of the spindle. DAPI staining forms two patches on either side of the midbody, one of which is destined for the polar body, the other to remain in the oocyte. (e) MI oocyte with abnormalities. Although there are 23 bivalents present in this oocyte, each associated with four kinetochores, there are two additional DNA structures present towards the upper left region of the image, each of which contain 22 kinetochores. (f) Oocyte of unclear stage; there is no polar body indicating this is in MI, supported by the fact that there are approximately 92 kinetochores, however chromosomes do not appear to be in bivalent structures and instead the oocyte appears to contain mostly univalents associated with two kinetochores each.

oocytes were fixed and stained. These were used for testing alternative antibodies and for analysis of intra-kinetochore distances.

2.1.6. Antibody testing

Because CREST stains multiple inner kinetochore and centromere proteins, I wanted to use an inner-kinetochore specific antibody to mark the inner kinetochore. Multiple anti-CENP-A antibodies, as well as antibodies against CENP-H and CENP-C, all of which are markers specific to the inner kinetochore, were tested (details of antibodies are given in **Table 2.3**). These antibodies were tested on MII oocytes, which were more readily available (as unfertilised oocytes), than oocytes in MI, and were fixed and stained in the same way as MI, as described above. Three different concentrations were tested for each antibody: 1:10, 1:20 and 1:50. None of these antibodies were successful in staining the inner kinetochore in oocytes, with most demonstrating no specificity for the kinetochore (for examples, see **Figure 2.3**).

2.2. Imaging and image analysis

2.2.1. Imaging

All imaging was performed on an UltraView spinning-disk confocal microscope controlled by Volocity software (Perkin Elmer). Oocytes were imaged under the 488, 561, 640 and 405 wavelengths. Laser power was set to 5% for the 405, 488 and 640 wavelengths, and an image exposure time of 50 ms was used. For the 561 wavelength, laser power was set to 2% and an exposure time of 30 ms was used. Image stacks were collected using a 100x NA1.4 oil objective. Approximately 250 z-slices were taken over the spindle region of each oocyte separated by 50 nm (covering a total z-distance of 12.5 µm). To obtain images of the entire oocyte, a 60x NA1.4 oil objective was used, with around 100 z-slices taken, covering a z-distance of 100 µm. MII oocyte images were acquired using the same settings, but with z-spacing of 100 nm.

Table 2.3.

Antibody	Source
Anti-CENP-A (mouse monoclonal)	Abcam (ab13939)
Anti-CENP-A (mouse monoclonal)	Enzo Life Sciences (ADI-KAM-CC006-E)
Anti-CENP-A (mouse monoclonal)	Thermo Pierce (PIEAMA120832)
Anti-CENP-A (rabbit polyclonal)	Cell Signaling Technology (2186)
Anti-CENP-C (rabbit polyclonal)	Abcam (ab33034)
Anti-CENP-H (mouse monoclonal)	Abcam (ab77207)
Anti-Rec8 (mouse polyclonal)	Garcia-Cruz et al. (2010)

Table 2.3. List of all primary antibodies tested in MI/MII oocytes. These antibodies were tested at concentrations of 1:10 to 1:20 and 1:50, but none were successful when used in oocytes.

Figure 2.3

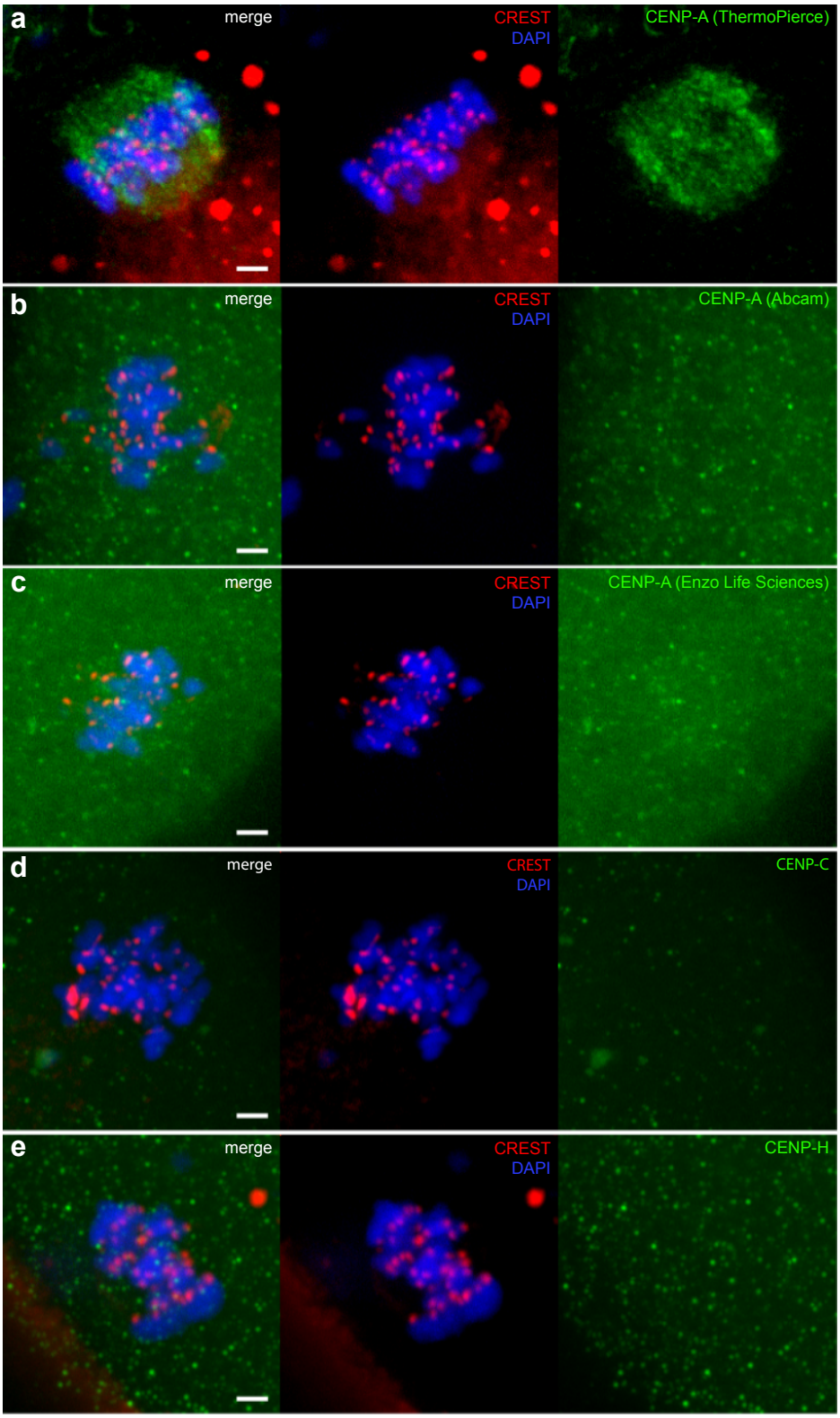

Figure 2.3. Antibody testing in metaphase II oocytes. (a–e) MII stage oocytes immunostained with CREST antisera, DAPI and an antibody against either CENP-A, CENP-C or CENP-H (all in a 1:50 dilution). Antibody details are given in **Table 2.3**. In (a), CENP-A stains the general spindle area, but does not show any specificity for kinetochores. The other antibodies did not show any specificity. Scale bars = 2 μm.

2.2.2. Image deconvolution

To improve the quality of the images and reduce the effects of out-of-focus blurring introduced by the limited aperture of the objective, images were deconvolved prior to analysis. Image stacks were deconvolved in Huygens X11 software (Scientific Volume Imaging B.V.) which generates a theoretical point-spread function (PSF) from the imaging parameters for each channel. Parameters input into the software for each channel included: excitation and emission wavelengths, numerical aperture (NA) of lens, sampling intervals, mounting medium and thickness of coverslip. The software generates a PSF from this data, which it uses to deconvolve the images.

2.2.3. Classification of kinetochores pairs in meiosis I

All image analysis was performed on image stacks acquired using the 100x objective and deconvolved as described above. Kinetochores were classified in Fiji software and in Imaris (Bitplane). To begin with, all kinetochores or kinetochore pairs were manually marked in Fiji and each point saved as a 'region of interest' (ROI). Image stacks centred about each ROI were then produced. These were 2 x 2 µm and incorporated 20 z-sections (10 sections above and 10 below each point). Using the stacks, it was possible to identify distinct sister kinetochore pairs (a pair made up of two distinct CREST foci) and single CREST foci that could represent a single kinetochore or a pair of overlapping kinetochores. Some of these single spots had an elongated appearance (see **Figure 3.5a** for representative images), indicating that they represented more than one kinetochore pair. A decision tree for kinetochore classification is shown in **Figure 2.4**.

To be able to determine whether single spots represented overlapping sister kinetochore pairs or single kinetochores, image stacks of oocyte kinetochores (CREST) and chromosomes (DAPI) were reconstructed in 3D in Imaris (Bitplane) to identify bivalents and thus deduce whether CREST foci associated with that bivalent corresponded to a single kinetochore or a pair of kinetochores.

Bivalents could be identified by counting the total number of discrete chromosomal structures within a cell and then assessing their relative sizes. For instance, if an oocyte contained 23 discrete structures, it was likely that each structure represented a bivalent (as there are 23 bivalents in a normal MI oocyte). In some cases, more than 23 structures were identified within a cell: usually 24, with 22 larger structures and 2 smaller ones. In these cases, the larger ones were deemed to represent bivalents and the smaller ones univalents (see **Figure 3.15c**). Bivalents could also be identified by assessing the CREST signal associated with each; in many cases, the larger structures were associated with at least one distinct kinetochore pair, providing reassurance that they were indeed bivalents.

If foci could not be reliably classified, for instance due to overlapping chromosomes or kinetochore signal, they were classified as unclear. This gave rise to the following final four categories:

- **Distinct pair:** A pair of sister kinetochores that appear as two separate spots.
- **Overlapping pair:** A pair of sister kinetochores comprising a single spot.
- **Unpaired:** A single kinetochore with no clearly identifiable partner, or far away enough from its partner to no longer be considered as part of a side-by-side sister kinetochore pair (>1.2 µm).
- **Unclear:** Cannot be reliably classified as a pair or single kinetochore, usually due to unclear or overlapping DAPI or CREST signals.

2.2.4. Measurement of inter-kinetochore distances

Inter-kinetochore distances were measured using both CREST and CENP-E to mark individual kinetochores. Inter-kinetochore distance was measured using the FindFoci plugin in ImageJ, which identifies regions of peak intensity in 3D image stacks (Herbert, Carr, & Hoffmann, 2014). Peaks were identified in 2 x 2 µm image stacks incorporating 40 z-sections that were centred about manually marked kinetochore pairs. The Pythagorean formula was used to calculate inter-

Figure 2.4

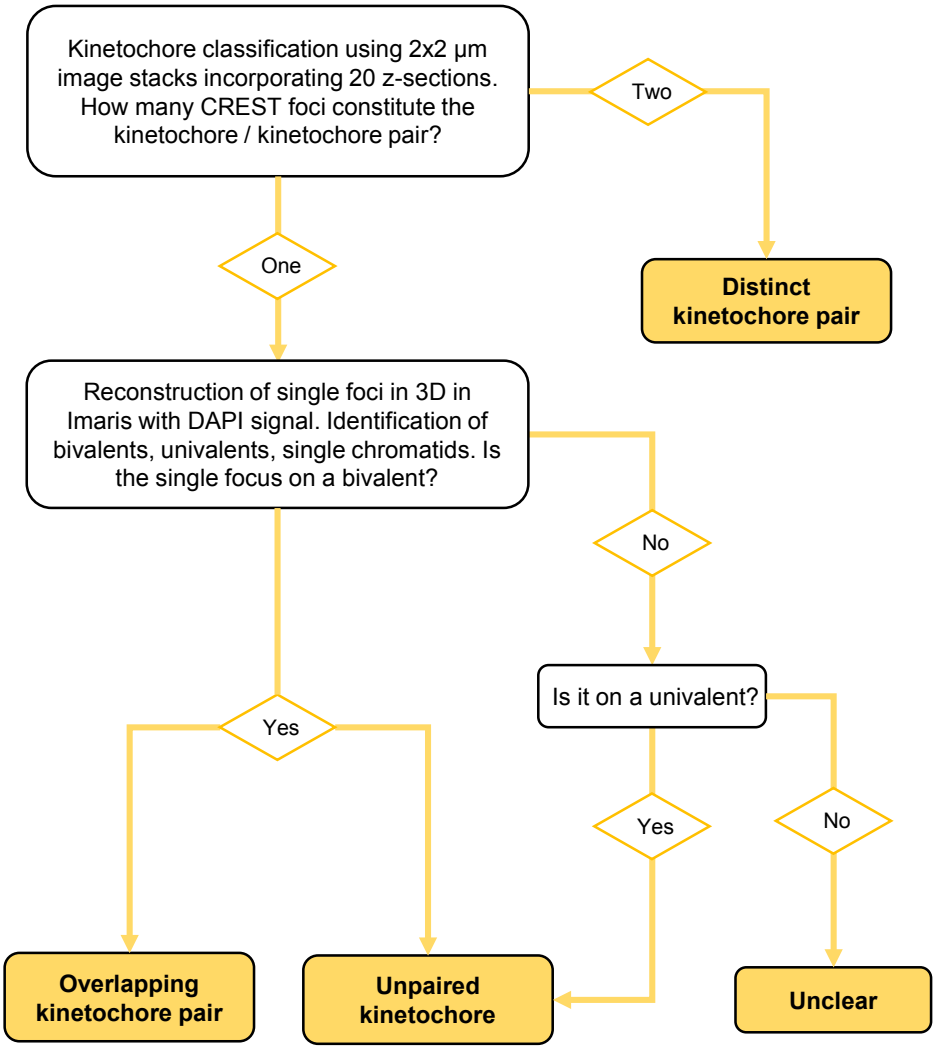

Figure 2.4. Decision tree for classification of kinetochores in metaphase I stage human oocytes. Kinetochore classification was initially performed using high-resolution 2 x 2 µm image stacks (incorporating 20 z-sections) centred about marked CREST foci. Using the stacks, it was possible to identifiy and categorise distinct sister kinetochore pairs which consist of a pair of sister kinetochores represented by two distinct CREST foci. To determine whether single spots (one CREST focus) represented overlapping kinetochore pairs or single kinetochores, image stacks of oocyte kinetochores (CREST) and chromosomes (DAPI) were reconstructed in 3D in Imaris. This enabled identification of bivalents and univalents, and hence enabled the CREST foci associated with each to be classified. Foci associated with regions of chromatin that could not be reliably identified as a bivalent or univalent were classified as unclear. In total, there were four classes of kinetochore: Distinct pairs, Overlapping pairs, Unpaired and Unclear.

kinetochore distance in 3D, using the x, y and z coordinates of each peak. Statistical analysis of inter-kinetochore measurements was performed in Microsoft Excel and R.

2.2.5. Measurement of intra-kinetochore distances

Measurement of intra-kinetochore distances was performed by Christopher Smith. For accurate measurement of intra-kinetochore distance it was first necessary to calculate the chromatic shift between different wavelengths. Chromatic shift corrections were calculated in MII oocytes stained with CREST antisera or anti-CENP-E antibody. Primary antibodies were detected using two secondary antibodies to enable calculation of chromatic shift for each fluorescent marker. Alexa Fluor 488® and Alexa 647® were localised to CREST, while Alexa 561® and Alexa 647® were localised to CENP-E. Distances between the two wavelengths of markers were calculated in 3D in MATLAB using Gaussian mixture-model fitting to identify the sub-pixel location of the centre of each spot (Armond *et al.*, 2016). The median distance between the two wavelengths of the markers was used as the chromatic shift correction value for those wavelengths. In order to measure intra-kinetochore distances, Gaussian mixture-model fitting was used to locate the centre of 3D fluorescent spots stained with different kinetochore markers, including CREST, Bub1 and CENP-E. Intra-kinetochore distances above 300 nm were excluded because these were likely to represent distances between two neighbouring spots rather than the same spot. Intra-kinetochore distances were calculated in 2D, given the high degree of variability in the z-axis. Median values (± standard deviation) of distance distributions were given (rather than mean values) to minimise the effect of any extreme values at the upper ends of the distribution, which in this case were more likely to represent signal from neighbouring spots rather than the same spot.

2.2.6. Statistical analysis

Statistical analysis was performed in R or Microsoft Excel 2016. Pearson's R correlation coefficient was calculated to measure correlation. A student's *t*-test

was used to compare means for small sample sizes. A single-factor analysis of variance (ANOVA) was used to test whether the variations in the mean between the different age groups of women were significant (see **Table 3.1**). Following the ANOVA test, a post-hoc Tukey honest significant difference (HSD) test was used for pairwise comparison of age groups. Where box-and-whisker plots were used to represent data, the boxes represent the interquartile range, with the lower whiskers extending to the farthest point within 1.5 times the lower quartile, and the upper whiskers to the farthest point within 1.5 times the upper quartile.

Chapter 3: Results

3.1. Introduction

The first meiotic division in human females is highly error-prone, for reasons that have not been fully elucidated. During metaphase I (MI), sister kinetochores need to attach to microtubule fibres emanating from the same spindle pole, as opposed to mitosis and meiosis II in which sisters attach to opposite spindle poles. In yeast and mouse, this is achieved through close physical association of sister kinetochores, mediated by the monopolin complex and Meikin respectively. In humans, however, the mechanism for sister kinetochore co-orientation is not known. Because human oocytes undergo a protracted spindle assembly period in which a high proportion of erroneous attachments form (Holubcova et al., 2015), it has been suggested that altered meiotic kinetochore geometry may be a factor that contributes towards this. Characterisation of human meiotic kinetochore organisation has not yet been achieved. In this chapter, I present the results of my investigations into kinetochore organisation in MI-stage human oocytes.

3.2. Kinetochore geometry & architecture in meiosis I

3.2.1. Sister kinetochores are not fused during meiosis I

To investigate the organisation of meiotic kinetochores in females, I examined sister kinetochore pairs in MI-stage oocytes obtained from women undergoing assisted reproduction (IVF or ICSI) following hormonal ovarian stimulation. Patient details, including indications for undergoing assisted reproduction, are given in **Table 2.1**. Common reasons for undergoing treatment included polycystic ovarian syndrome (n = 4) and endometriosis (n = 3), however unexplained infertility (n = 6) was the most common reason. Oocytes presented in this chapter are those that had assembled the first meiotic spindle, but had

not yet undergone the first meiotic division; this was confirmed by the absence of a polar body (**Figure 3.1**). To avoid any changes to kinetochore geometry and to be able to examine meiotic chromosomes and kinetochores *in situ*, oocytes were fixed intact in 3.7% paraformaldehyde (PFA). In total, 27 MI stage oocytes were included in the final analysis (**Figure 3.2**). These 27 oocytes came from 20 patients (details in **Table 2.1**).

To image kinetochores in human oocytes we fixed the cells and stained them with CREST antisera (to mark the centromere and inner kinetochore) and DAPI (to mark chromosomes). CREST is derived from the serum of CREST (calcinosis, Raynaud's phenomenon, esophageal motility abnormalities, sclerodactyly and telangiectasia) patients and contains anticentromeric antibodies (Fritzler & Kinsella, 1980). 3D image stacks (250 sections, spaced 50 nm apart) were captured using an Ultraview spinning disk confocal microscope (see Methods for details) and images were deconvolved using Huygens software. Kinetochores, marked with CREST antisera, were analysed in these image stacks using Fiji software. The use of closely-spaced z-sections (taken every 50 nm) enabled acquisition of detailed information on oocyte chromosomes and kinetochores and their 3D arrangement (**Figure 3.3a**). In MI oocytes, the majority of kinetochores appeared to be in pairs made up of two distinct CREST foci (**Figure 3.3b**). In an MI oocyte in which all kinetochores were fused, I would have expected to see 46 CREST foci per oocyte (two foci per bivalent). However, the number of CREST foci within these oocytes was considerably higher than 46, and it was often possible to identify individual bivalents associated with four CREST foci, which indicated that sister kinetochores were not fused in MI (**Figure 3.3c-d**). However, in addition to these paired structures composed of two foci, there were also many structures consisting of a single CREST focus which may have represented a fused pair of sister kinetochores. To be able to determine whether these single foci represented a single kinetochore or a pair of kinetochores I used surface rendering in Imaris software to reconstruct the oocyte chromosomes and kinetochores in 3D. This enabled clear visualisation of individual bivalents and the kinetochores associated with each (**Figure 3.4**), enabling me to determine whether a single spot corresponded to a kinetochore pair.

Figure 3.1

MI stage human oocyte, 60x (z-projection)

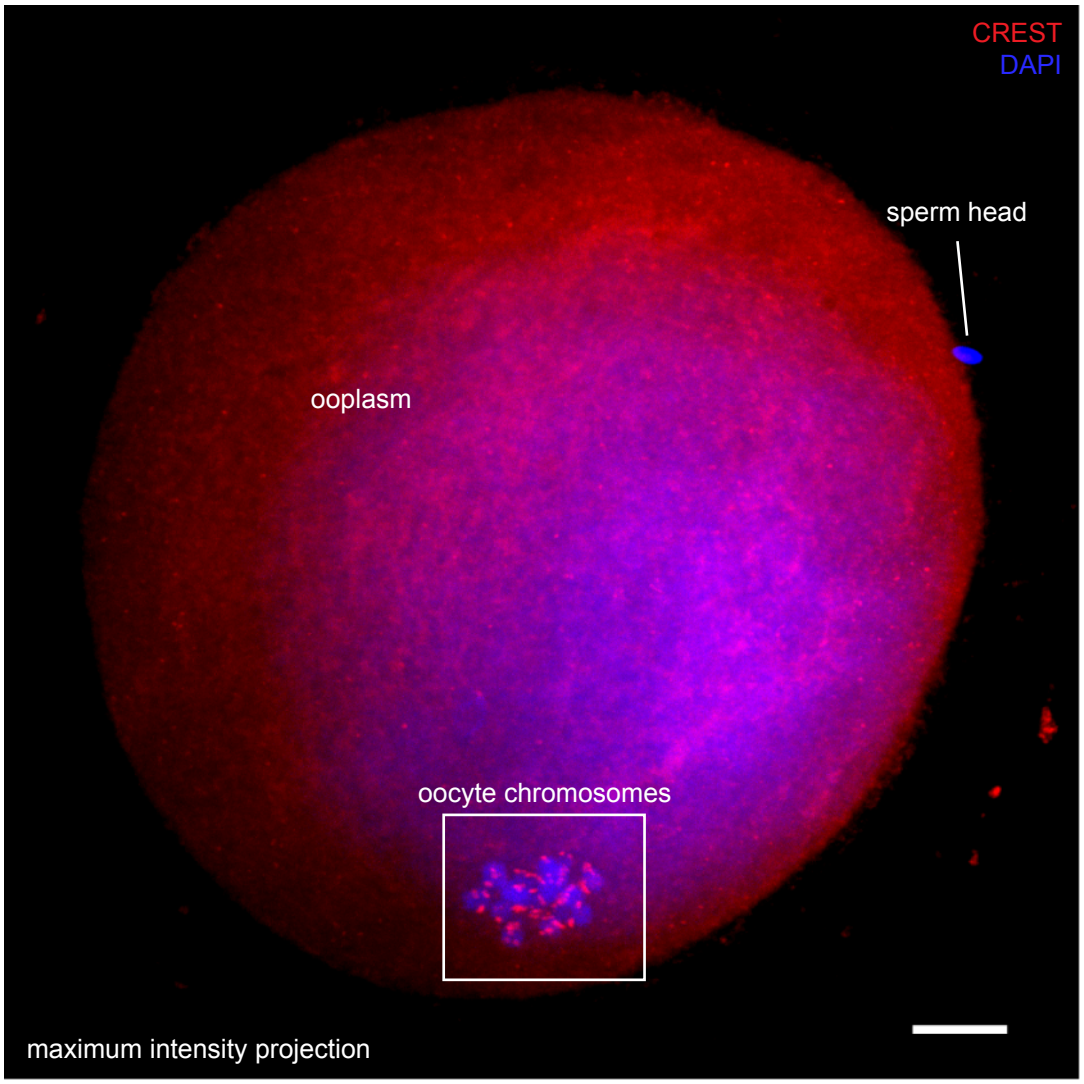

Figure 3.1. 60x maximum intensity projection of an metaphase I stage human oocyte. Chromosomes are stained with DAPI (blue) and kinetochores with CREST antisera (red). Image was formed from 80 z-slices, taken every 1 µm, and acquired on a spinning-disk confocal microscope. The absence of a polar body indicates that this oocyte has not yet undergone the first meiotic division. As this oocyte was acquired from an IVF cycle, it has been incubated overnight with a sperm preparation, hence the chromosomes from a spermatozoon can be seen towards the top right edge of the oocyte. Scale bar = 10 µm.

Figure 3.2a

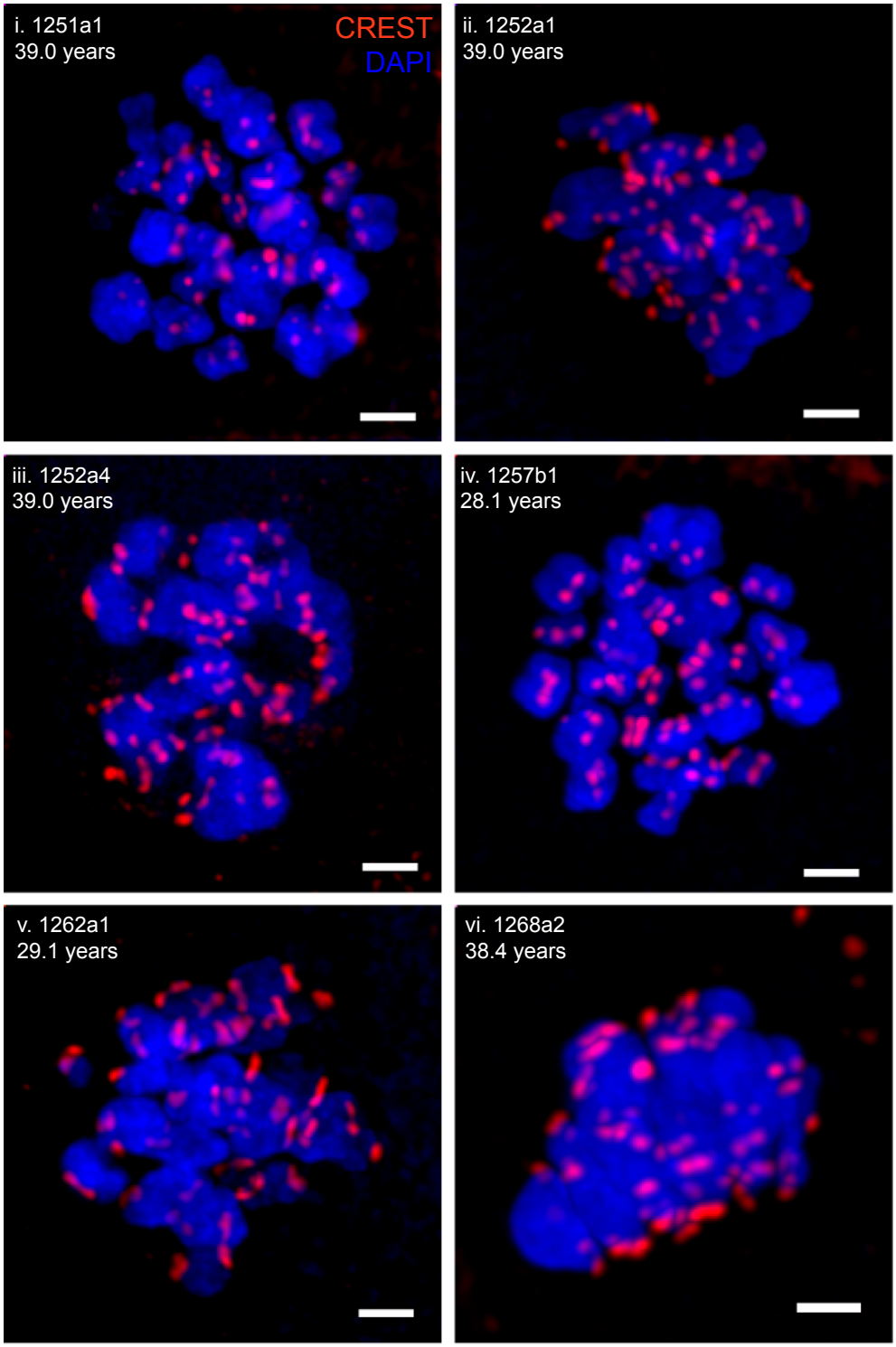
i. 1251a1
39.0 years
CREST
DAPI
ii. 1252a1
39.0 years
iii. 1252a4
39.0 years
iv. 1257b1
28.1 years
v. 1262a1
29.1 years
vi. 1268a2
38.4 years

Figure 3.2b

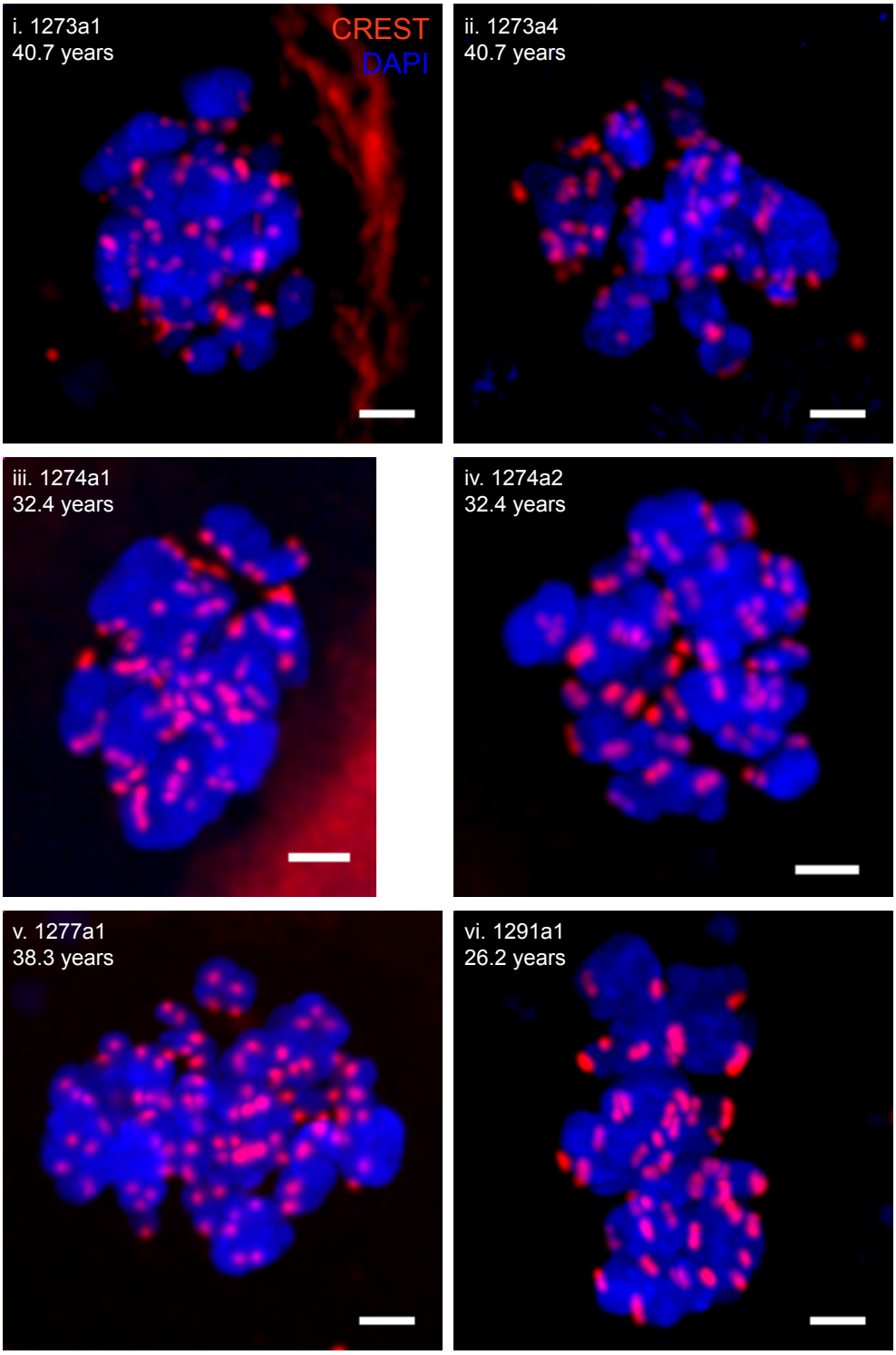
i. 1273a1
40.7 years
CREST
DAPI
ii. 1273a4
40.7 years
iii. 1274a1
32.4 years
iv. 1274a2
32.4 years
v. 1277a1
38.3 years
vi. 1291a1
26.2 years

Figure 3.2c

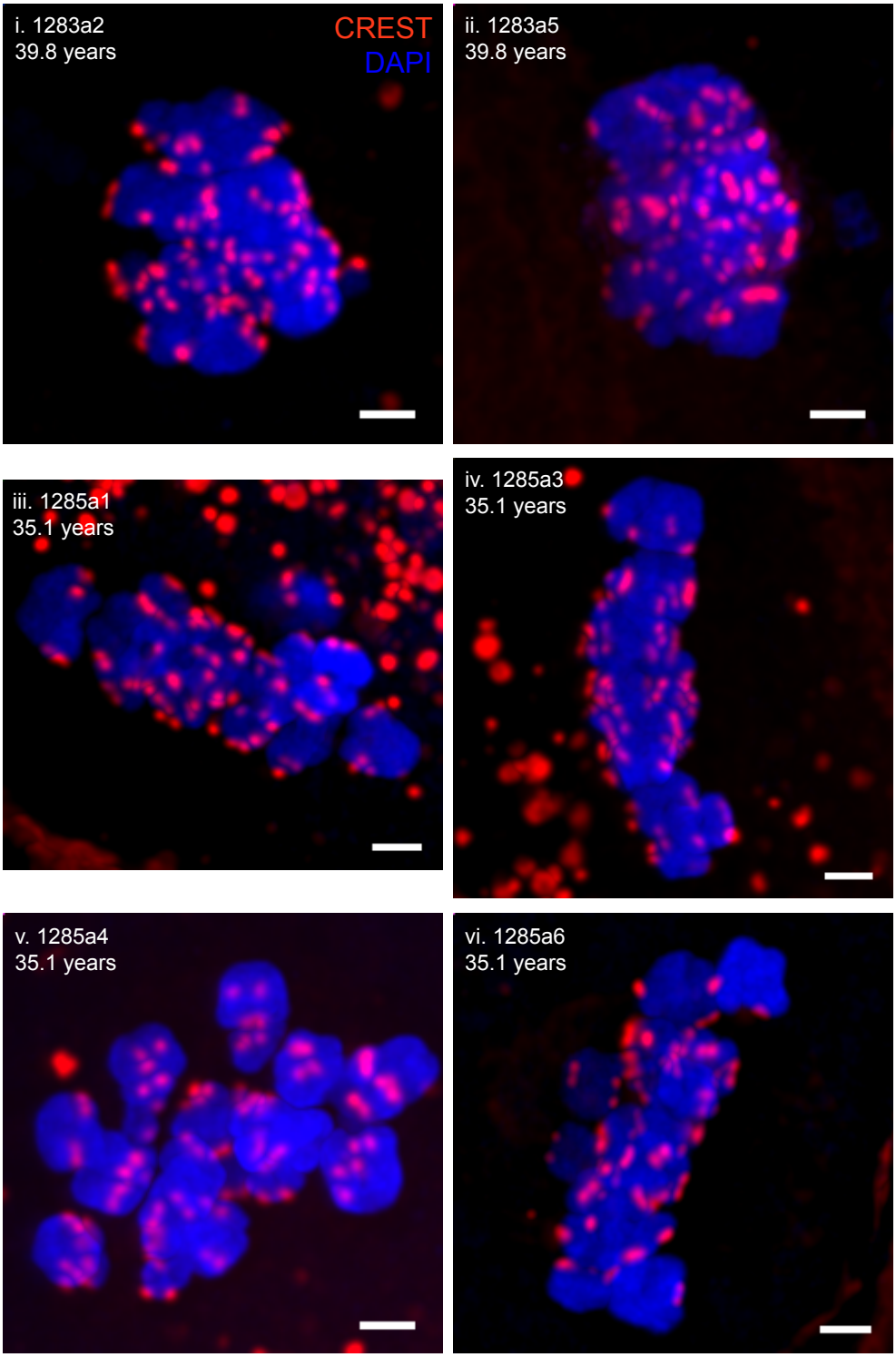
i. 1283a2
39.8 years
CREST
DAPI
ii. 1283a5
39.8 years
iii. 1285a1
35.1 years
iv. 1285a3
35.1 years
v. 1285a4
35.1 years
vi. 1285a6
35.1 years

Figure 3.2d

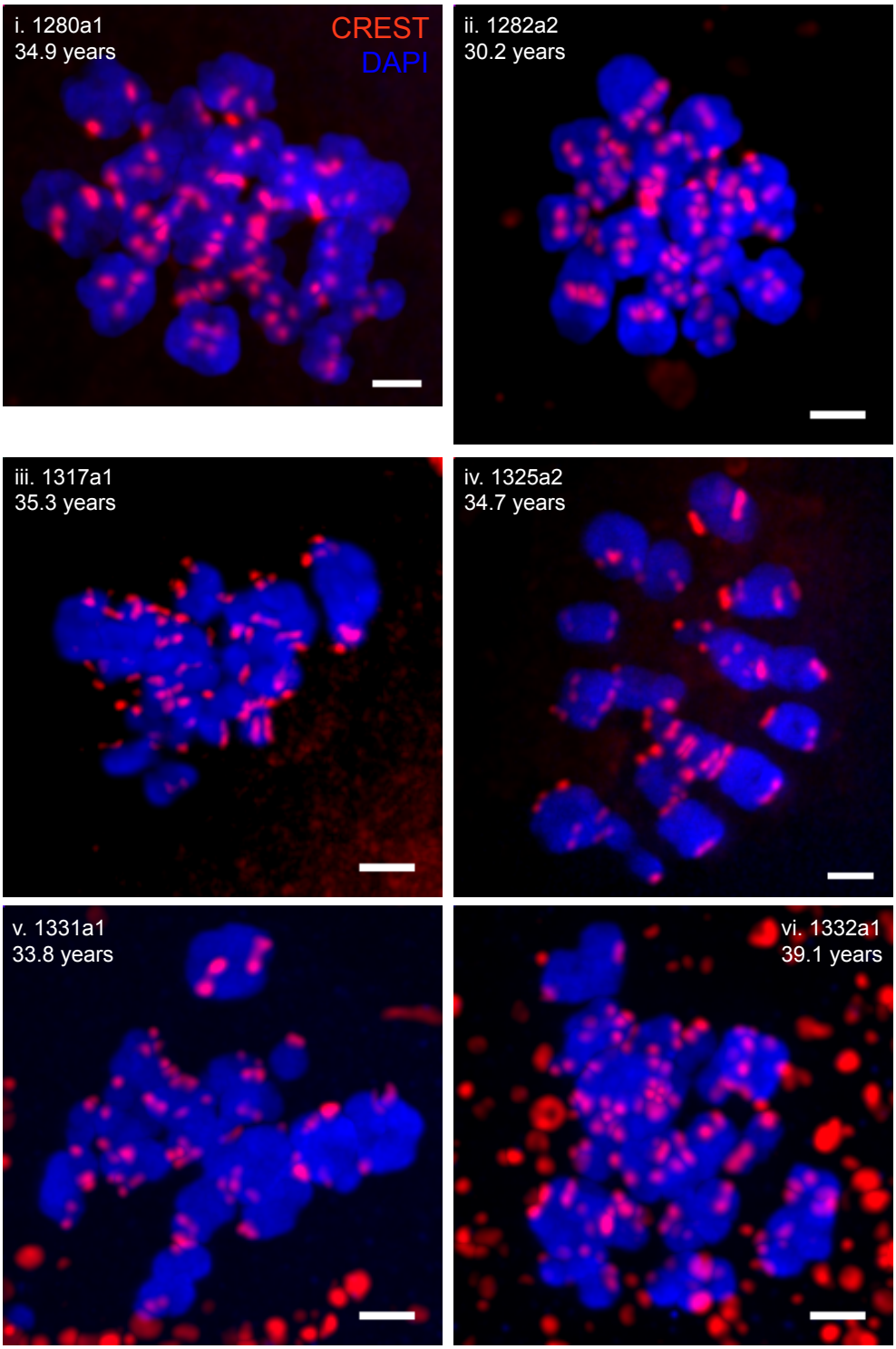
i. 1280a1
34.9 years
CREST
DAPI
ii. 1282a2
30.2 years
iii. 1317a1
35.3 years
iv. 1325a2
34.7 years
v. 1331a1
33.8 years
vi. 1332a1
39.1 years

Figure 3.2e

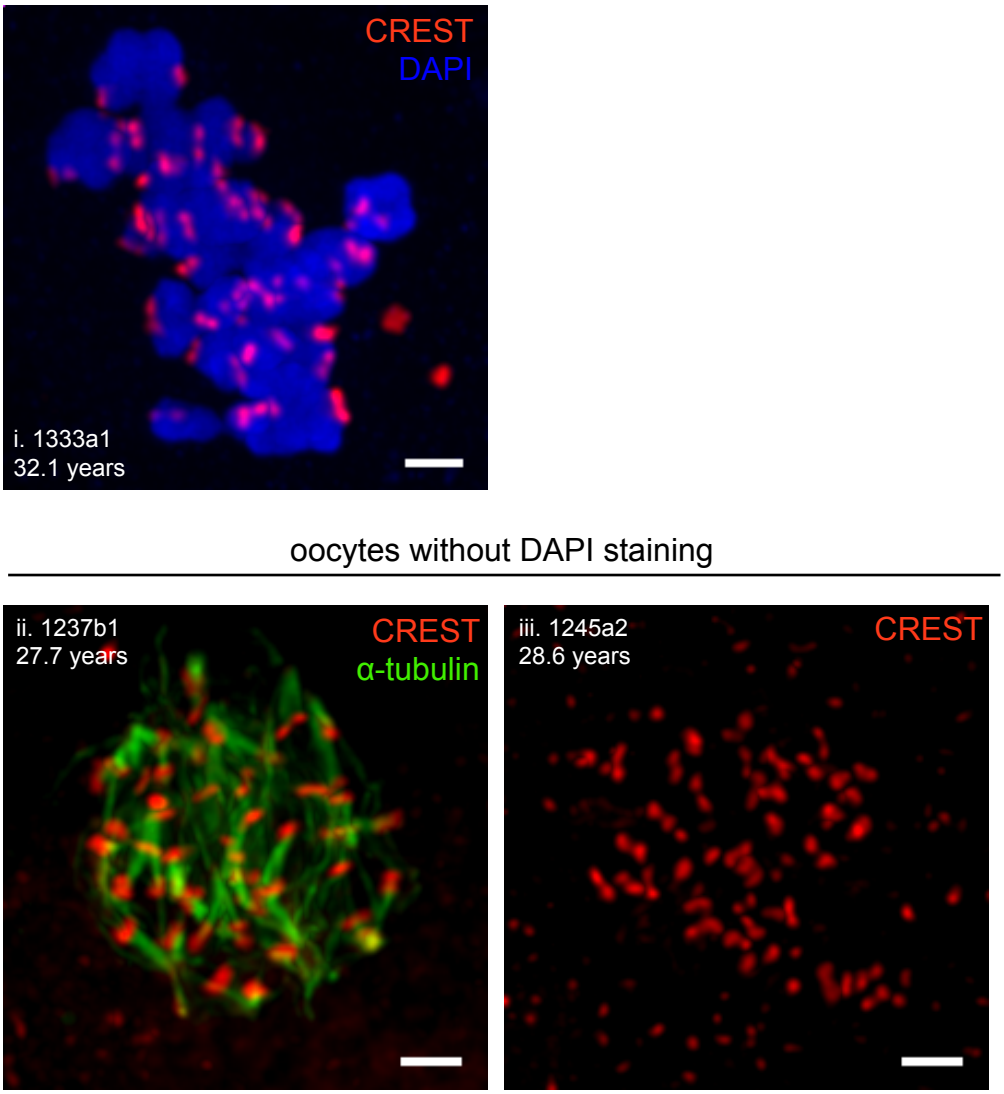

Figure 3.2. (a–e) Maximal projection images of all metaphase I oocytes for which kinetochore pairs were analysed (n = 27 in total). For each oocyte, its unique oocyte identification code and the age of the donating patient are given. For the final two oocytes shown, I was unable to acquire clear DAPI channel images, therefore these are shown without. Note that for some oocytes (1331a1, 1332a1, 1285a4, 1285a1, 1285a3) there is 'granular' CREST staining which is present throughout the entire oocyte cytoplasm. Despite this staining pattern, CREST is still highly specific to the kinetochores, as can be seen in the images, therefore these oocytes have been included in the final analysis.

Figure 3.3

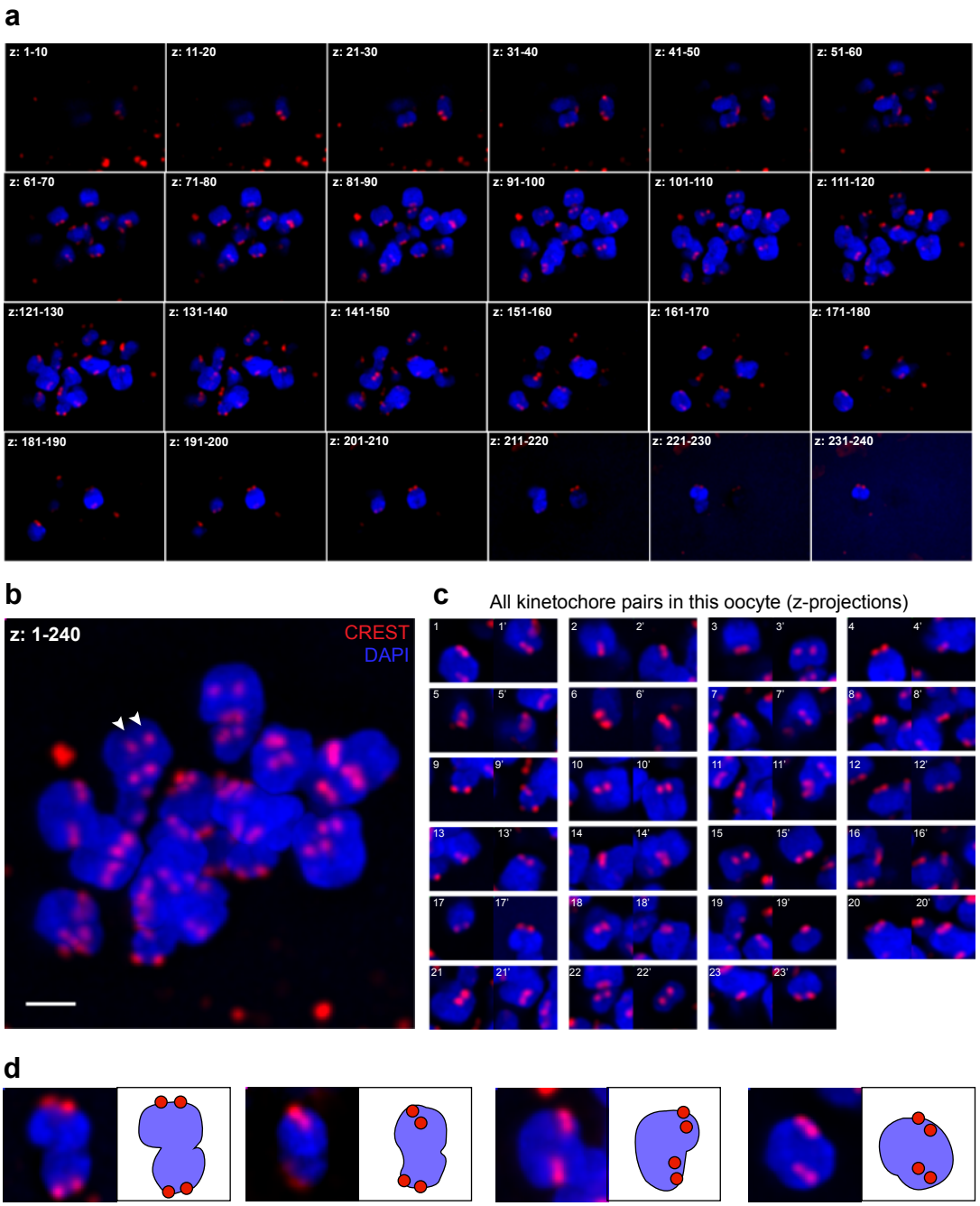

Figure 3.3. Kinetochores in image stacks of metaphase I stage human oocytes. (a) A montage of z-projections of the chromosomes from a metaphase I oocyte, with each image incorporating information from 10 z-slices. Each z-section is spaced 50 nm apart, therefore each image covers a z-distance of approximately 500 nm. (b) Left panel shows a 100x close-up of the chromosomes and kinetochores in this oocyte. (c) Z-projection images incorporating 20 x 50 nm z-slices centred about a manually marked kinetochore pair (centre of panel). Sister kinetochore pairs on homologous chromosomes are shown alongside each other. Panels are 4 x 4 μm. (d) Individual bivalents from this oocyte, each associated with 4 kinetochores. Panels are 4 x 4 μm.

Figure 3.4

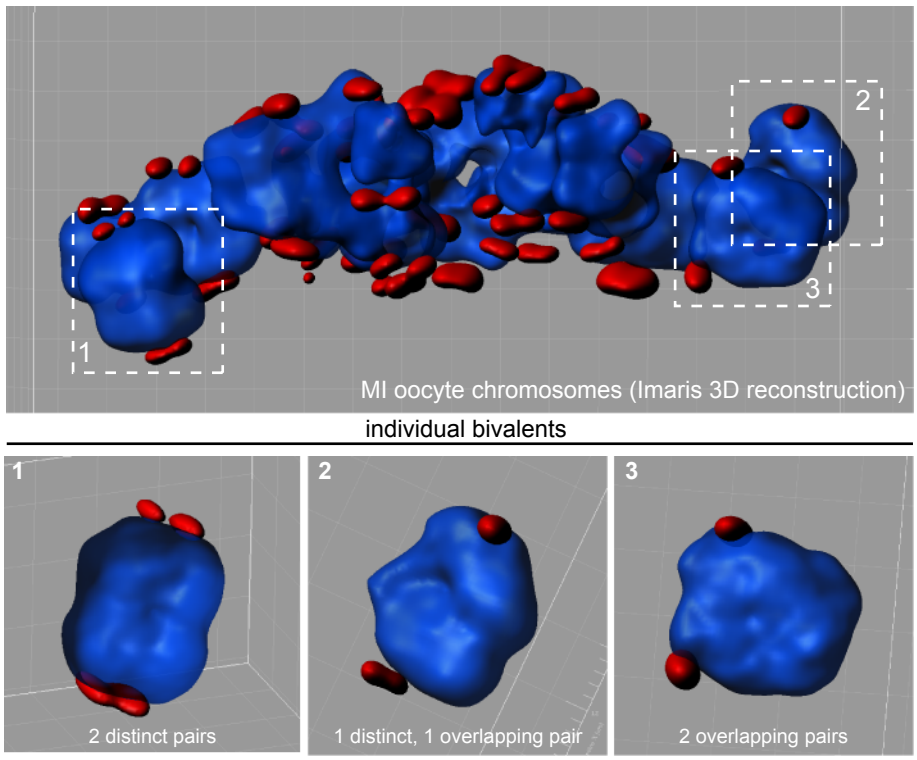

Figure 3.4. 3D reconstruction of oocyte chromosomes. Reconstruction of chromosomes and (blue) and kinetochores (red) in Imaris (Bitplane) from a high-resolution stack acquired using spinning-disk confocal microscopy. The maximal projection image of this oocyte is shown in Figure 3.2c(iv). Upper panel shows the entire set of chromosomes from this oocyte and lower panels show individual bivalents and the kinetochore pairs associated with each.

Using a combination of 3D image stacks centred about kinetochore pairs and 3D reconstruction in Imaris, kinetochores in the 3D image stacks were classified on the basis of whether they appeared as part of a 'distinct' pair (made up of two distinct CREST spots) or 'overlapping' pairs (appearing as a single spot). For examples, see **Figure 3.5a**. In total, it was possible to classify the majority of kinetochores in all 27 oocytes, however a small proportion (1.1%) could not be reliably classified due to overlapping DAPI and/or CREST staining. The majority (72.1%) of kinetochores were identified as being within a distinct pair, with an average of 33 (range: 19–44) distinct pairs per oocyte (**Figure 3.5b**). The remaining 22.9% of sister kinetochore pairs were classified as 'overlapping', with an average of 10 (range: 0–22) overlapping pairs per oocyte. A small proportion (3.8%) of foci were classified as 'single' kinetochores if they had no clearly identifiable partner or if they had come far apart enough from their partner (>1.2 µm) to be considered as a single kinetochore. The 'single' kinetochores were often found on univalents (bivalents that have come apart), and are examined in greater detail in section **3.3.3**. There were no differences in oocytes from women with no known fertility issues, i.e. couples with male factor infertility (marked with asterisks in **Figure 3.5c**; see also **Table 2.1**), indicating that these observations are unlikely to result from infertility factors. In addition, there was no correlation between the total dose of FSH received by patients and the proportion of separated sister kinetochores (Pearson's R = 0.111; **Methods Figure 2.1**). Together, these results indicated that sister kinetochores in MI were routinely separated in human MI oocytes.

To quantify the degree of separation, I measured the inter-kinetochore distance between distinct sister pairs. Distances were measured in 3D using the peak intensity of the CREST signal, detected in Fiji using the FindFoci plugin (Herbert *et al.*, 2014), to mark individual kinetochores. The average degree of separation between sister kinetochores in MI was 0.69 ± 0.20 µm (mean ± SD; n = 818 pairs from 27 oocytes). Based on this information, I concluded that the inner plates of sister kinetochore pairs in MI human oocytes can be separated. This is in stark contrast to what is known about mouse MI oocytes in which sister kinetochores are fused together by Meikin (Kim *et al.*, 2015), suggesting that in

Figure 3.5

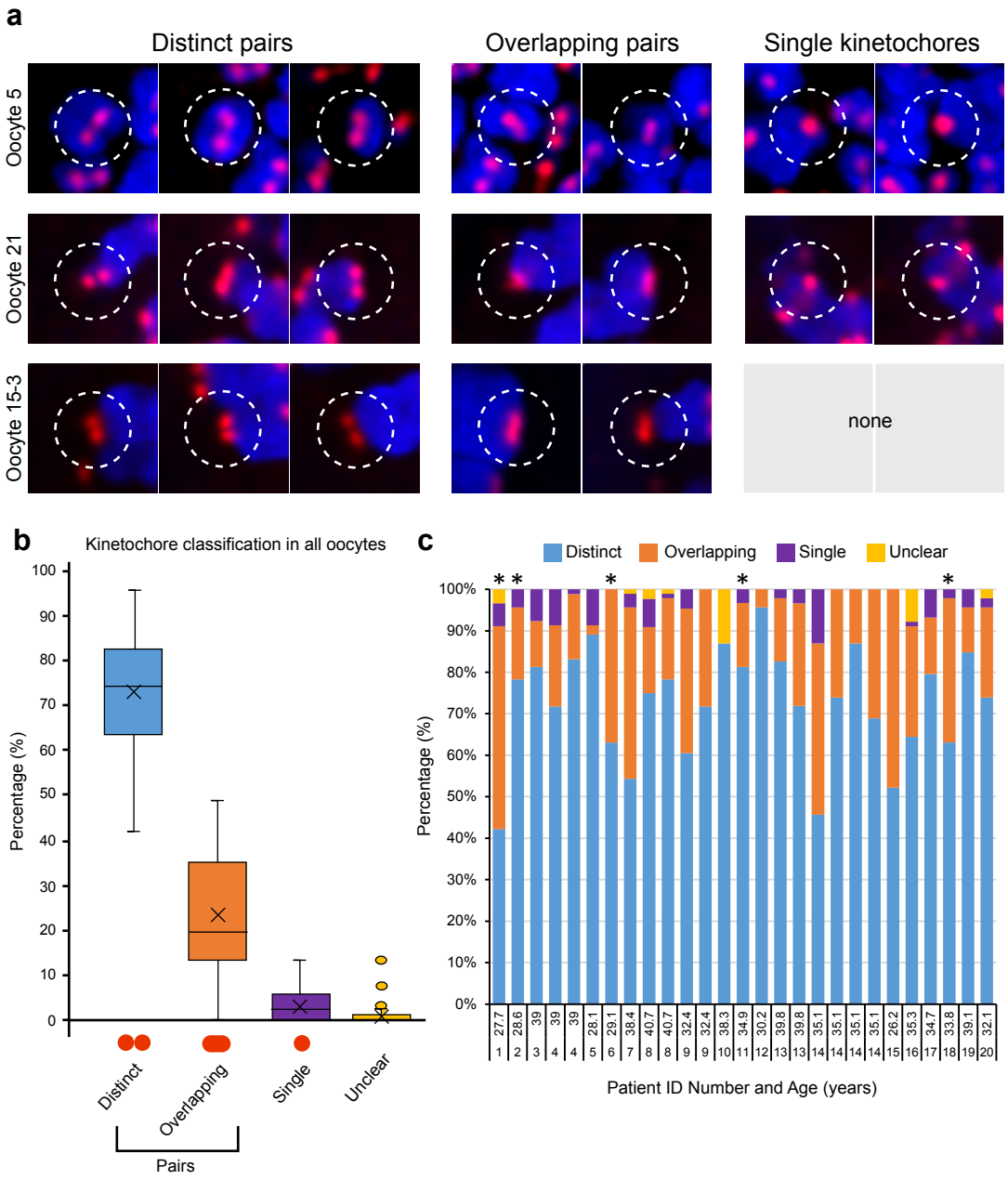

Figure 3.5. Kinetochore classification in metaphase I oocytes. (a) Examples of kinetochore classification images taken from 3 different oocytes. Images are 4 x 4 µm maximal projections incorporating 10 z-sections taken above and below a manually-marked kinetochore/kinetochore pair (20 z-sections total). To verify that 'single' kinetochores were true singles and not overlapping pairs, they were examined in Imaris. (b) Box-and-whisker plot showing mean percentage of each class of kinetochore/kinetochore pair for each oocyte, classified according to whether kinetochores were within distinct or overlapping pairs (*n* = 2456 kinetochores from 27 oocytes). For a small number of kinetochores, sister kinetochores were so far apart (>1.2 µm) that they were classified as 'unpaired'. A small number of foci could not be reliably identified as being either single kinetochores or overlapping pairs, usually due to overlapping CREST or DAPI fluorescence from neighbouring bivalents, and these were classified as 'unclear'. (c) Proportion of distinct and overlapping pairs for each individual oocyte. Asterisks indicate oocytes from women with no known fertility issues.

human MI oocytes there may be a different method of establishing sister kinetochore association.

3.2.2. The inner, outer and corona regions of each kinetochore are distinct

Having established that the inner plates of the kinetochore were separated in human MI, I next sought to determine whether the entire kinetochore structure (from the inner to outer regions) was separated. As CREST antisera stains only the inner kinetochore and centromere, it does not provide information on whether the outer regions of the kinetochore (the outer plate and fibrous corona) are separated. In maize, for instance, the inner plate of the kinetochore is separated in MI but the outer plate, the region responsible for attachment to microtubules, forms a 'bridge' structure that can be visualised under immunofluorescence microscopy (Li & Dawe, 2009). It was therefore a possibility that this arrangement also applied in human oocytes. To test this, the outer regions of the kinetochores of human MI oocytes were labelled using antibodies against Hec1 (to mark the outer plate) and CENP-E (fibrous corona) (Wan *et al.*, 2009, Earnshaw, 2015); see **Figure 3.6a**. Because the Hec1-9G3 antibody showed high levels of background staining and only weakly stained kinetochores in a few oocytes, an additional outer plate marker, Bub1, which is located in a similar position within the kinetochore to Hec1, was tested (Wan *et al.*, 2009). This antibody demonstrated a more consistent staining pattern (**Figure 3.6b**). Comparing these outer kinetochore markers with that of the inner kinetochore (marked by CREST) showed that the staining patterns of outer plate and fibrous corona kinetochore markers resembled those of the inner kinetochore, indicating that the entire kinetochore structure is separated in MI.

The degree of separation was compared in oocytes that had both CENP-E and CREST staining (n = 24 oocytes) to test whether the outer kinetochore was separated to a similar degree as the inner kinetochore. There was a strong correlation between CREST and CENP-E measurements that had been made for the same kinetochore pairs (R = 0.80; **Figure 3.7a**), indicating that the entire inner and outer plate are separated to a similar degree. However, using CREST as a marker, the overall mean (± SD) inter-kinetochore distance was 0.69 ± 0.21

Figure 3.6

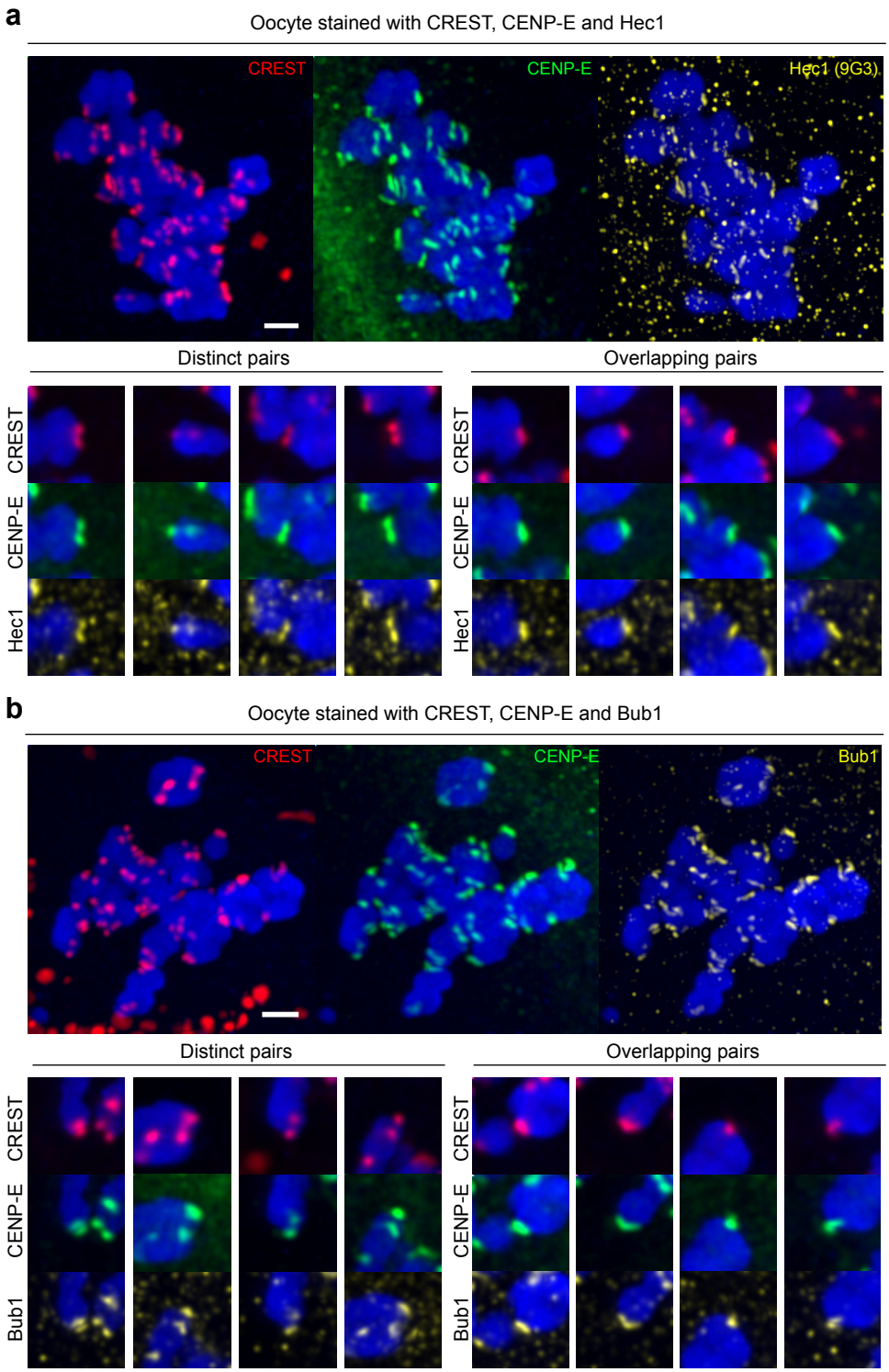

Figure 3.6. The entire kinetochore is separated in the majority of metaphase I oocytes. (a-b) Oocytes stained with markers for the kinetochore inner plate (CREST), outer plate (Hec1 or Bub1) and fibrous corona (CENP-E). The pattern of staining for individual kinetochore pairs does not differ between markers, which shows that, in distinct kinetochore pairs, the entire kinetochore is separated.

μm for all pairs (similar to the average across all 27 oocytes) and for CENP-E it was slightly increased to 0.75 ± 0.23 μm. **Figure 3.7b**), which may indicate that the outer region of the kinetochore is separated to a greater degree than the inner plate. However, using a *t*-test to compare the two means, the difference between the groups was not significant ($p = 0.2969$), indicating that this is a minimal effect. Together, these data show that the entire kinetochore structure is separated in MI.

3.2.3. Kinetochore architecture in metaphase of meiosis I

In mitosis, the inner architecture of the kinetochore changes depending on kinetochore attachment status. Stretching of centromeric chromatin between mitotic sister kinetochores is needed to stabilise bipolar attachment (Lampson & Cheeseman, 2011) and can impose conformational changes within the kinetochore (Wan *et al.*, 2009). In meiosis, however, because sister chromatids segregate together, a 'side-by-side' arrangement of sister kinetochores is adopted, with the outer plates of both sisters oriented towards the same spindle pole and inner plates facing the centromeres. By fixing whole intact oocytes, it was also possible to visualise the side-by-side arrangement of sister kinetochores, and show that the inner kinetochore (CREST) is located towards the centromeric chromatin, with the outermost region of the kinetochore (CENP-E) facing outwards towards the spindle (**Figure 3.8**).

To test whether this side-by-side arrangement of sisters alters the internal architecture of the kinetochore, the intra-kinetochore distance between markers of the kinetochore inner plate/centromere (CREST), outer plate (Bub1) and fibrous corona (CENP-E) was measured in both MI and MII oocytes. To do this, a modified version of kinetochore-tracking software developed in MATLAB (Armond *et al.*, 2016) was used to identify individual kinetochores in different channels, with each channel corresponding to a different marker. The software fits a 3D Gaussian to the fluorescent spots in different channels to find the sub-pixel spot centre coordinates, which are then manually filtered for quality. The distance between the spot centres in different channels gives the intra-kinetochore distance in 3D. The distances were chromatic shift-corrected using

Figure 3.7

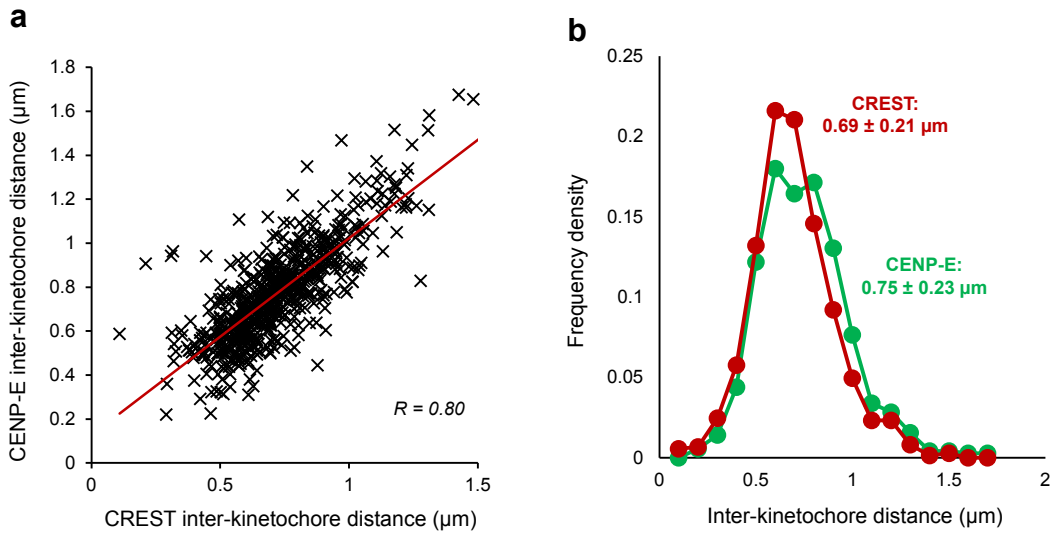

Figure 3.7. Comparison of inter-kinetochore distance as measured using CREST and CENP-E. (a) Strong correlation between measurements for kinetochore pairs for which distance was measured using both CREST and CENP-E as markers showing that the outer kinetochore separates to the same degree as the inner kinetochore. (b) Frequency density chart comparing CREST and CENP-E inter-kinetochore distances. CENP-E gives a slightly higher mean inter-kinetochore distance than CREST, however using a comparison of two means *t*-test, the difference between the two groups is not significant (p = 0.2969).

Figure 3.8

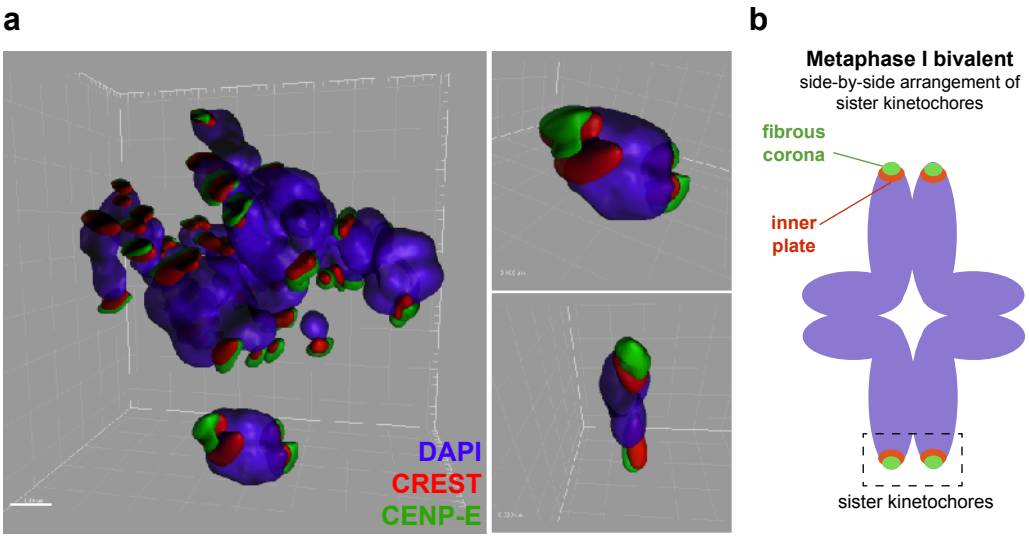

Figure 3.8. Relative arrangement of inner and outer kinetochore components in metaphase I oocytes. (a) 3D reconstruction of MI oocyte chromosomes in Imaris (Bitplane) from an oocyte stained with CREST antisera (red), anti-CENP-E antibody (green) and DAPI (blue). Right panel: individual bivalents shown in closer detail, in which the relative positions of CREST and CENP-E staining can be clearly visualised. (b) Schematic of a bivalent in MI, showing side-by-side arrangement of sister kinetochores. The inner plate of the kinetochore (here shown in red) is oriented towards the centromeric chromatin.

chromatic shift values calculated from MII oocytes stained with a single primary antibody (CREST or anti-CENP-E) detected by two secondary antibodies with different fluorescent tags.

In MI, the distance between CREST and CENP-E was measured as 151 ± 60 nm (median ± SD; n = 162 kinetochores), with a smaller distance of 129 ± 36 nm (n = 32) measured between CREST and Bub1 (**Figure 3.9**). Thus, CENP-E is located approximately 22 nm outside of Bub1, consistent with measurements of the same proteins on human mitotic kinetochores (Wan *et al.*, 2009). In MII, the distance between CREST and CENP-E was measured as 156 ± 54 nm (median ± SD; n = 176 kinetochores). The software was not able to detect enough spots for the CREST to Bub1 distance to be measured, but CENP-E to Bub1 was measured as 36 ± 27 nm (median ± SD; n = 17 kinetochores). Common to both MI and MII measurements was a longer distance between the kinetochore inner plate (represented by CREST) and outer plate / fibrous corona (represented by Bub1 and CENP-E respectively) than in mitosis, suggesting that the kinetochore is further stretched in meiosis.

One limitation of this experiment is that my marker for the inner plate, CREST, stains the centromere and multiple inner kinetochore markers (including CENPs A, B and C) (Earnshaw, 2015). Moreover, we cannot use CREST in mitotic cells as it locates throughout the centromere making tracking spots impossible. As a result, it is difficult to make comparisons between meiosis and mitosis. To solve this, I attempted to stain kinetochores in oocytes with a different marker that was specific to the inner plate, such as CENP-A, CENP-C or CENP-H. However, none of the inner plate antibodies tested demonstrated any specificity for the inner kinetochore when used in MII oocytes (see **Figure 2.1**).

3.2.4. Sister kinetochores in meiosis I form dual k-fibre attachments

Because the outer plates of sister kinetochores were separated in MI, I next studied how they form attachments to spindle microtubules. Understanding this is important, because in MI sisters need to attach to the same, rather than opposing, spindle poles. If sisters are separated, this raises questions about

Figure 3.9

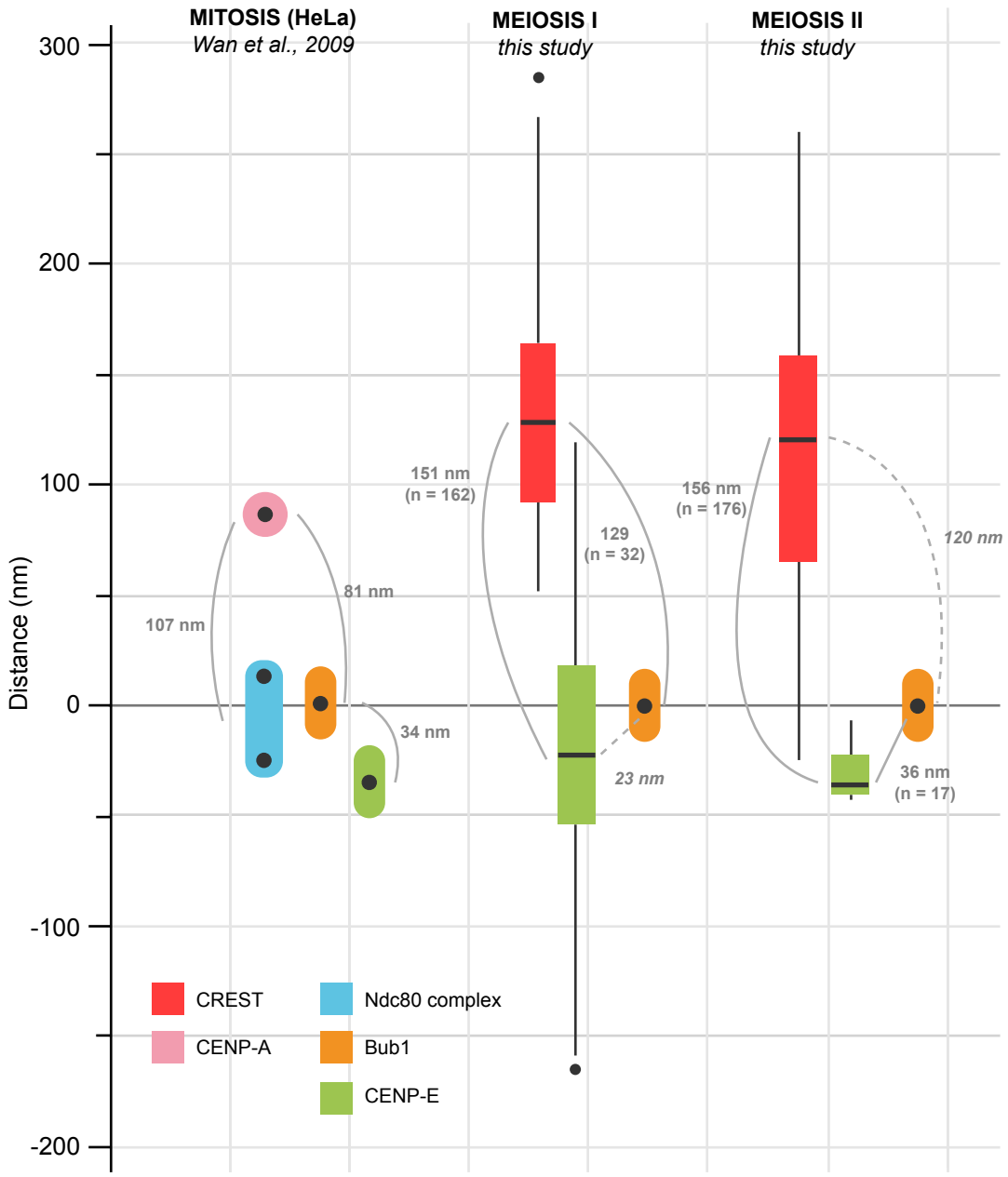

Figure 3.9. Map of kinetochore architecture in meiosis I and II stage oocytes, with mitotic kinetochore architecture shown for comparison. As Bub1 staining was common to all, measurements are given relative to Bub1. For meiosis, CREST and CENP-E are shown as box-and-whisker plots to show the spead of data. The positioning of the medians of the plots are given relative to Bub1 (designated as 0). In meiosis I, the red box-and-whisker plot represents the CREST-Bub1 distance, and the green represents the CREST-CENP-E distance. In meiosis II, the red represents the CREST-CENP-E distance and the green the CENP-E-Bub1 distance. Grey solid lines represent measured distances, with *n* representing the number of kinetochores. Dotted lines represent inferred distances. A caveat of these measurements is that we were unable to stain CENP-A (or another inner kinetochore-specific marker) in oocytes, which makes it difficult to assess whether the extended length of the kinetochore inner plate in meiosis is of significance.

how they form attachments to the same spindle pole. A possible model for meiotic sister kinetochore attachment is one in which only one 'active' sister forms attachments to microtubules, and the other sister is inactivated. Alternatively, both sisters may remain 'active' and capable of binding to spindle microtubules. To test this, I examined kinetochore-microtubule attachments in oocytes subjected to cold-shock treatment and then stained with antibodies against α-tubulin and kinetochores. Cold treatment causes most microtubules to depolymerize, however microtubules attached to the outer kinetochore plate, specifically to Hec1/Ndc80, are resistant to this effect (Miller *et al.*, 2008). This makes it easier to visualise end-on attachments within the meiotic spindle. In a small number of cases (n = 5 sister kinetochore pairs from three oocytes), I observed pairs in which one kinetochore was attached to a k-fibre but its sister was not. However, more frequently, I noted the presence of kinetochore pairs with dual k-fibre attachments (n = 20), in which each sister within the pair was attached to a distinct k-fibre (**Figure 3.10**). These attachments were observed in both distinct (18/20) and overlapping (2/20) kinetochore pairs, thereby showing that homologous chromosomes can connect to the meiotic spindle via two independent attachment sites. This surprising result may make the process of bi-orientation challenging in MI compared to MII (or mitosis).

3.3. The effect of maternal age

3.3.1. Introduction

The relationship between maternal age and aneuploidy in oocytes is well established (Hunt & Hassold, 2008). Many studies investigating maternal age-related aneuploidy have focused on cohesin (Jessberger, 2012), because of the role that it plays in keeping sister chromatids together during the long arrest period of the oocyte. Loss of cohesin, particularly at the centromeres, could impact on sister kinetochore organisation and architecture in MI. Given that the oocytes I studied had originated from women of various ages, I sought to identify whether there were any changes in MI sister kinetochore geometry with age that could reflect a decline in cohesin.

Figure 3.10

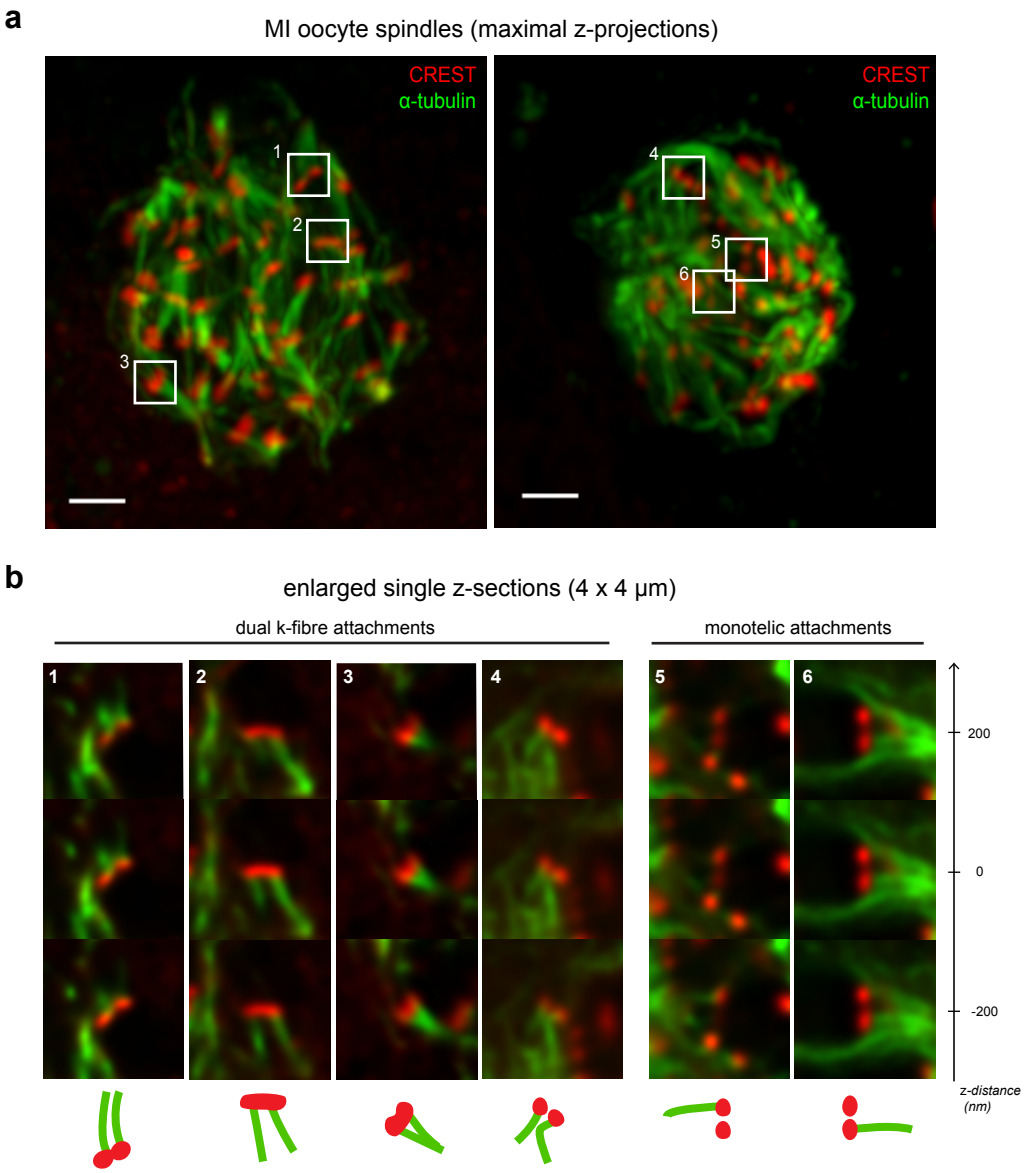

Figure 3.10. Sister kinetochore pairs in metaphase I engage with independent kinetochore-fibres. (a) Maximal projections of two MI human oocyte spindles stained for microtubules (green, alpha-tubulin) and kinetochores (red, CREST) after cold-shock treatment. (b) Enlarged z-sections of kinetochore pairs from 3.10a with dual and monotelic attachments as indicated. Scale bar = 2 µm.

3.3.2. Sister kinetochores are further apart with increasing maternal age

As kinetochores are connected by centromeric chromatin, the distance between them can act as a proxy for the status of cohesin. To investigate whether there were signs of cohesin decline in older oocytes, I first analysed whether the proportion of distinct kinetochore pairs within each oocyte increased with age, which would reflect the coming apart of sister kinetochores. I found that there was not a significant relationship (Pearson's correlation coefficient, R = 0.283) between age and proportion of distinct pairs in this sample (**Figure 3.11a**), although in the two youngest patients (ages 26.2 and 27.7) a smaller proportion of kinetochore pairs were classified as 'distinct' (52.2% and 42.2% respectively, compared to 72.6% for all oocytes). When comparing kinetochore classifications by age group, the differences remained negligible between the 'under 33' and 'mid-30s' age groups (69.8% and 70.4% respectively), with a slight increase to 77.0% for the 'over 38' age group (**Figure 3.11b**). Together, this data does not indicate that there is a relationship between female age and separated sister kinetochores.

Although the proportions of separated sister kinetochores did not increase with age, I noticed that in oocytes from older women, sister kinetochore pairs appeared to be further apart than in oocytes from younger patients (**Figure 3.12**). I therefore examined inter-kinetochore distance measurements in the context of age. Using CREST as a kinetochore marker, I found that there was a gradual increase in inter-kinetochore distance with age (n = 27 oocytes; Pearson's correlation coefficient, R = 0.645; **Figure 3.13a**). As the majority of aneuploidies in human embryos arise when a woman is in her mid to late thirties (Hassold & Hunt, 2001), I compared oocytes from women under 33 years of age (age range: 26.2–32.4 years) with oocytes from women in their mid-30s (age range: 33.8–35.5 years) and those over 38 years of age (age range: 38.4–40.7 years). These specific ages were selected because they ensured a clear distinction in age between each of the groups. Using a single-factor ANOVA, there was a significant difference in inter-kinetochore distance between age groups for both CREST ($p = 0.00265$) and CENP-E ($p = 0.00225$). For CREST,

Figure 3.11

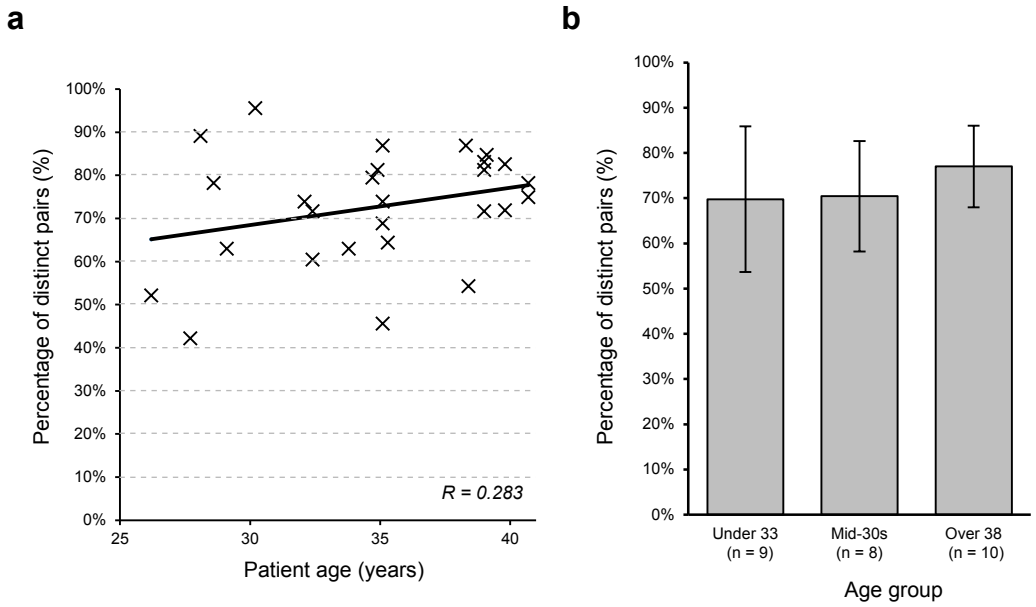

Figure 3.11. No relationship between the proportion of distinct pairs and patient age. (a) Percentage of distinct pairs within each oocyte. Each cross represents a single oocyte. Pearson's correlation coefficient, R = 0.283. (b) A comparison of the average proportion of distinct kinetochore pairs by age group. All patients in the 'mid-30s' group were aged between 33.8–35.5 years. The cut-offs for each age group were selected because they ensured a clear gap between the oldest members of the younger age groups and the youngest members of the next age group up.

Figure 3.12

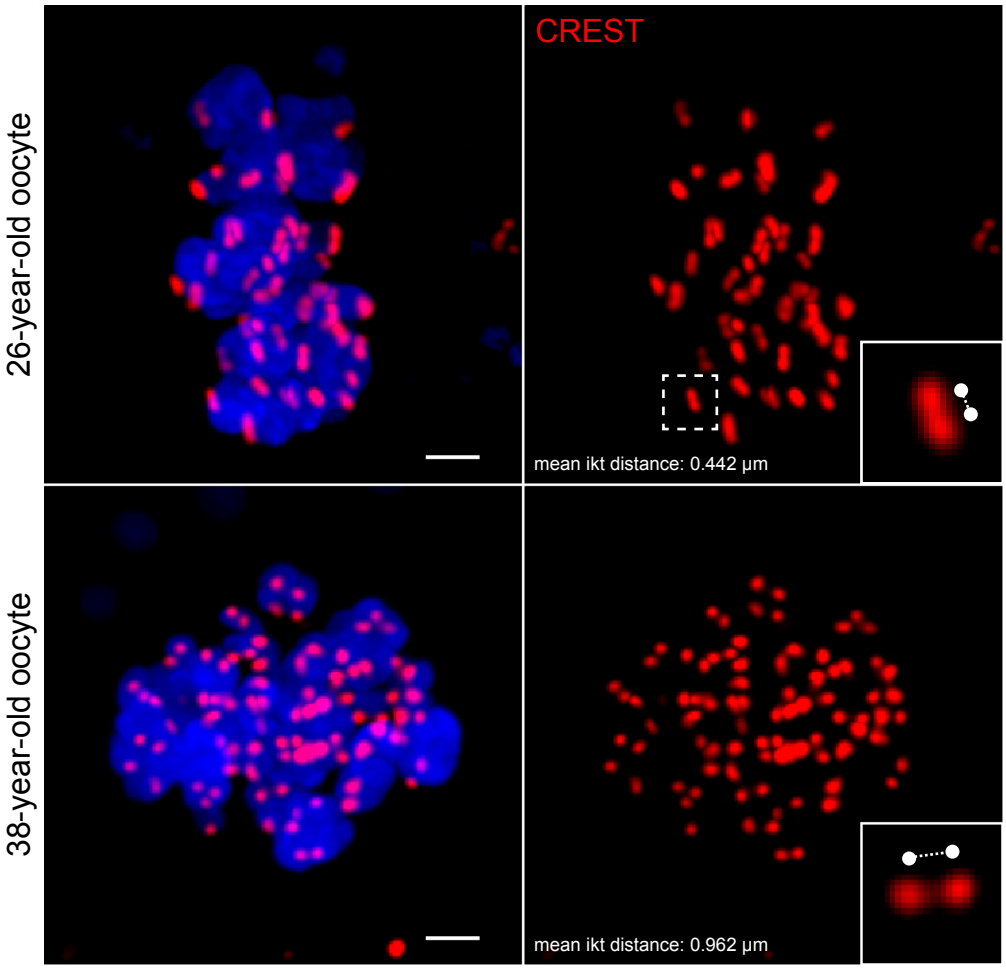

Figure 3.12. Sister kinetochores in older oocytes are further apart. Upper panels show maximal projection images of an oocyte from a 26-year-old woman compared with one in the lower panels from a 38-year-old woman. Scale bar = 2 µm.

Figure 3.13

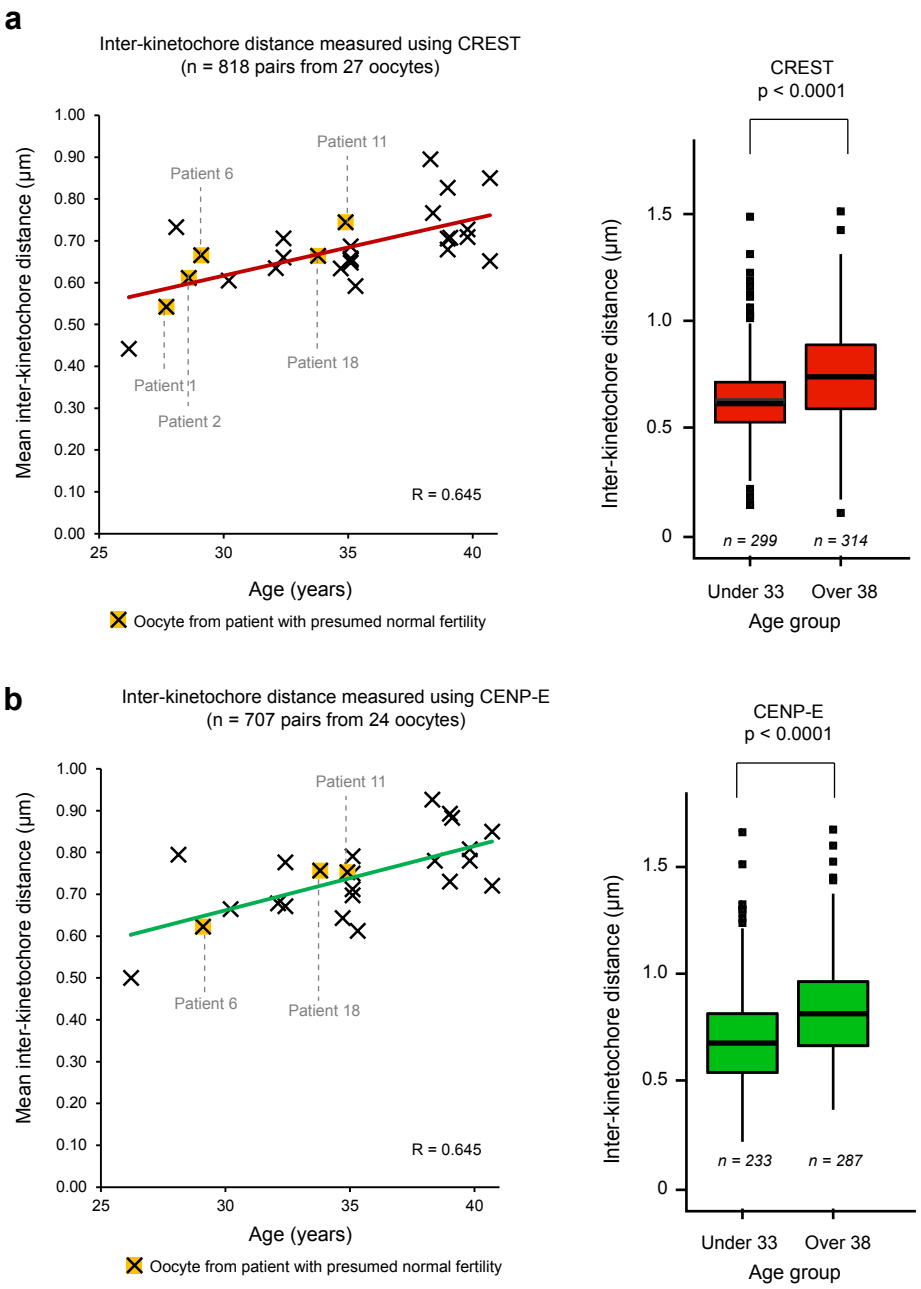

Figure 3.13. Inter-kinetochore distance between sister kinetochores in meiosis I increases with maternal age. (a) Increasing inter-kinetochore distance with female age using (a) CREST to mark the kinetochore. Patients with no known fertility problems (n = 5) are highlighted in yellow. Box plot shows comparison of inter-kinetochore distance between women under 33 years of age with women over 38 ($p<0.0001$, unpaired t-test). (b) The same measurements using CENP-E as a marker for the kinetochore. Patients numbers correspond to those shown in Table 2.1. R = linear correlation coefficient. Boxplots represent interquartile range (IQR); whiskers extend to most extreme value within 1.5*IQR.

post-hoc comparisons using the Tukey HSD test with a 0.05 level of significance showed that the difference between the Under 33 and Mid-30s group was not significant. However, there were significant differences between the Under 33 and Over 38 group ($p<0.05$), going from 0.63 ± 0.18 µm in the younger group to 0.76 ± 0.22 µm in the older group. Post-hoc comparisons also showed a significant difference between the Mid-30s and Over 38 group ($p<0.05$), going from 0.66 ± 0.18 µm to 0.76 ± 0.22 µm (see **Table 3.1**). This is in keeping with the observed increase in MI-derived aneuploidy in oocytes from women in their mid to late thirties.

To test whether the entire kinetochore structure comes apart with age, we also looked at the relationship between patient age and inter-kinetochore distances measured with CENP-E, an outer kinetochore marker. As with CREST, there is a gradual increase in inter-kinetochore distance (n = 24 oocytes; R = 0.645; **Figure 3.13b**). The difference in inter-kinetochore distance between the 'under 33' and 'over 38' age groups is also significant ($p<0.0001$), rising from 0.69 ± 0.23 µm in the under 33 group to 0.83 ± 0.22 µm in the over 38 group. The subset of oocytes from women with no known fertility issues (n = 5; marked in **Figure 3.13** and see also **Table 2.1**) also fit this trend suggesting that this effect does not arise as a result of clinical factors. There was weak correlation between the total FSH dose received by each woman and inter-kinetochore distance (R = 0.415; **Figure 2.1**), which may indicate that exogenous gonadotrophin exposure has a small contribution towards this effect. In mouse, FSH exposure affects chromosome alignment, with chromosomes in oocytes exposed to high FSH more scattered about the spindle (Roberts *et al.*, 2005). Because oocytes included in this study were fixed in varying stages of MI it was not possible to reliably ascertain the level of chromosomal scattering. Overall, this data shows that sister kinetochore separation increases with female age, which supports the idea that there is a decline in centromeric cohesin with age.

Table 3.1.

a. Inter-kinetochore distance measurements

	CREST		CENP-E	
Age group	**Mean ± SD (μm)**	**n**	**Mean ± SD (μm)**	**n**
Under 33	0.63 ± 0.18	267	0.69 ± 0.23	207
Mid-30s	0.66 ± 0.19	237	0.72 ± 0.21	213
Over 38	0.76 ± 0.22	314	0.83 ± 0.22	286
All	**0.69 ± 0.20**	**818**	**0.75 ± 0.23**	**706**

b. Tukey post-hoc HSD comparison

		CREST		CENP-E	
Comparison		**Abs difference in mean (μm)**	**>HSD**	**Abs difference in mean (μm)**	**>HSD**
Under 33	**Mid-30s**	0.038		0.042	
Mid-30s	**Over 38**	0.092	*	0.107	*
Over 38	**Under 33**	0.130	*	0.149	*

Table 3.1. Inter-kinetochore measurements using CREST and CENP-E to mark individual kinetochores. (a) Table shows mean ± SD inter-kinetochore distances for the two different kinetochore markers for each of the three age groups. A one-way analysis of variance (ANOVA) test yielded a significant difference between the age groups for both CREST ($p = 0.00265$) and CENP-E ($p = 0.00225$). (b) The ANOVA was followed up with a Tukey post-hoc HSD test to conduct a pairwise comparison between the age groups. If the absolute difference in means between two groups is greater than the HSD value (calculated using a significance level of 0.05) then the difference is considered to be significant. For CREST, the HSD was calculated to be 0.0506, and for CENP-E it was 0.0551. For both CREST and CENP-E, comparing the two younger age groups did not yield a significant difference. However, comparing the Over 38 age group with the two younger groups did. Abs: absolute. HSD: honestly significant difference. n: number of sister kinetochore pairs. SD: standard deviation. *represents a significant difference.

3.3.3. Univalents are the most common abnormality in metaphase I oocytes

Given that there was an apparent decline in cohesin with age, the next question I asked was whether there were any abnormalities in chromosome configuration (for instance, the presence of single chromatids or univalents) in the oocytes included in the analysis that could have arisen as a result of cohesin decline. As cohesin is involved in chiasmata maintenance, we would expect to see an increase in univalents (bivalents that have come apart) with cohesin loss. We would also expect to see single chromatids which can also arise as a result of cohesin loss. To identify whether the oocytes included in this research had any abnormalities in chromosome configuration that would make them prone to aneuploidy, I used Imaris and Fiji to identify individual bivalents within each oocyte and the kinetochores associated with each. In 17 oocytes, it was possible to account for the arrangement of all chromosomes. For the remaining oocytes in the population, the overlapping chromosomal staining made it impossible to identify all homologues definitively. Of the 17 oocytes, I identified 7/17 (41%) as having abnormal chromosome configurations (see **Figure 3.14** for examples). Six of the seven contained univalents (bivalents that have come apart) and one oocyte contained two trivalents (see **Table 3.2**). The remaining 10 had the normal arrangement of chromosomes that we would expect in an MI-stage oocyte, i.e. 23 bivalents each associated with two pairs of sister kinetochores. There was a mild relationship with age, as the oocytes with normal chromosomal arrangements had an average age of 32.4 ± 2.9 years (mean ± SD), whilst those with abnormal arrangements had an average age of 35.6 ± 3.6 years ($p = 0.09$, two-tailed *t*-test assuming unequal variance).

Because cohesin is thought to play a role in maintenance of chiasmata, I hypothesised that oocytes with univalents (which can form as a result of chiasmata loss) would have overall reduced cohesin compared to oocytes with normal chromosomal architecture. To test this, I compared inter-kinetochore distances between normal oocytes (ones that contained 23 bivalents, each associated with two pairs of sister kinetochores) and those with some abnormal configurations of chromosomes (**Figure 3.15a**). Although the overall average

for the abnormal oocytes was slighter higher, only in 3/7 oocytes was the measurement higher than the average over all oocytes (**Figure 3.15b**). The remaining four did not have increased sister separation, and were in fact below the overall average for all oocytes. It may therefore be a possibility that cohesin loss occurs in a more localised manner, i.e. occurring on only a few chromosomes, rather than over all chromosomes of the oocyte. I therefore examined kinetochore pairs on individual univalents (**Figure 3.15c**). Of the 15 univalents, 12 had kinetochore pairs that appeared to be bi-oriented. The inter-kinetochore distances between these bi-oriented kinetochores was generally significantly larger than the inter-kinetochore distance between all kinetochores, with a mean separation distance of 1.70 µm (n = 12 pairs, range: 1.25–2.82 µm), indicating that centromeric cohesin between these pairs had been depleted (**Figure 3.15d**).

3.4. Conclusion

Using high-resolution imaging in fixed intact human oocytes, I have demonstrated that the human meiotic kinetochore adopts a unique arrangement in which sister kinetochores in MI are routinely separated. We have shown that internal architecture of the kinetochore does not change from mitosis, and that each sister retains its ability to act as an independent attachment site. Importantly, we have shown that sister kinetochore separation increases with female age, which may reflect a decline in meiotic cohesin, and hence may contribute to the increased levels of aneuploidy we observe in oocytes from older women.

Table 3.2.

Oocyte code	Age	Mean inter-kinetochore distance (μm)	Abnormal chr config? (y/n)	Details
1291a1	26.2	0.441865095	n	23 bivalents
1257b1	28.1	0.839032386	y	22 bivalents, 2 univalents
1262a1	29.1	0.665095157	n	23 bivalents
1282a2	30.2	0.604780421	n	23 bivalents
1333a1	32.1	0.634653815	n	23 bivalents
1274a2	32.4	0.660308085	n	23 bivalents
1331a1	33.8	0.663418262	n	23 bivalents
1325a2	34.7	0.634320797	y	22 bivalents, 2 univalents
1280a1	34.9	0.763591841	n	23 bivalents
1285a3	35.1	0.658027761	n	23 bivalents
1285a4	35.1	0.687407925	n	23 bivalents
1285a1	35.1	0.64807879	y	20 bivalents, 6 univalents
1285a6	35.1	0.654302372	y	22 bivalents, 1 univalent
1317a1	35.3	0.591870489	n	23 bivalents
1277a1	38.3	0.961970221	y	20 bivalents, 2 trivalents
1251a1	39.0	0.957105968	y	22 bivalents, 2 univalents
1332a1	39.1	0.743011863	y	22 bivalents, 2 univalents

Table 3.2. Details of chromosome configuration in oocytes for which all kinetochores could be accounted for. Oocytes are ordered by patient age at the time of egg collection. Oocytes with abnormal chromosome configuration, as designated in column 4, are highlighted.

Figure 3.14

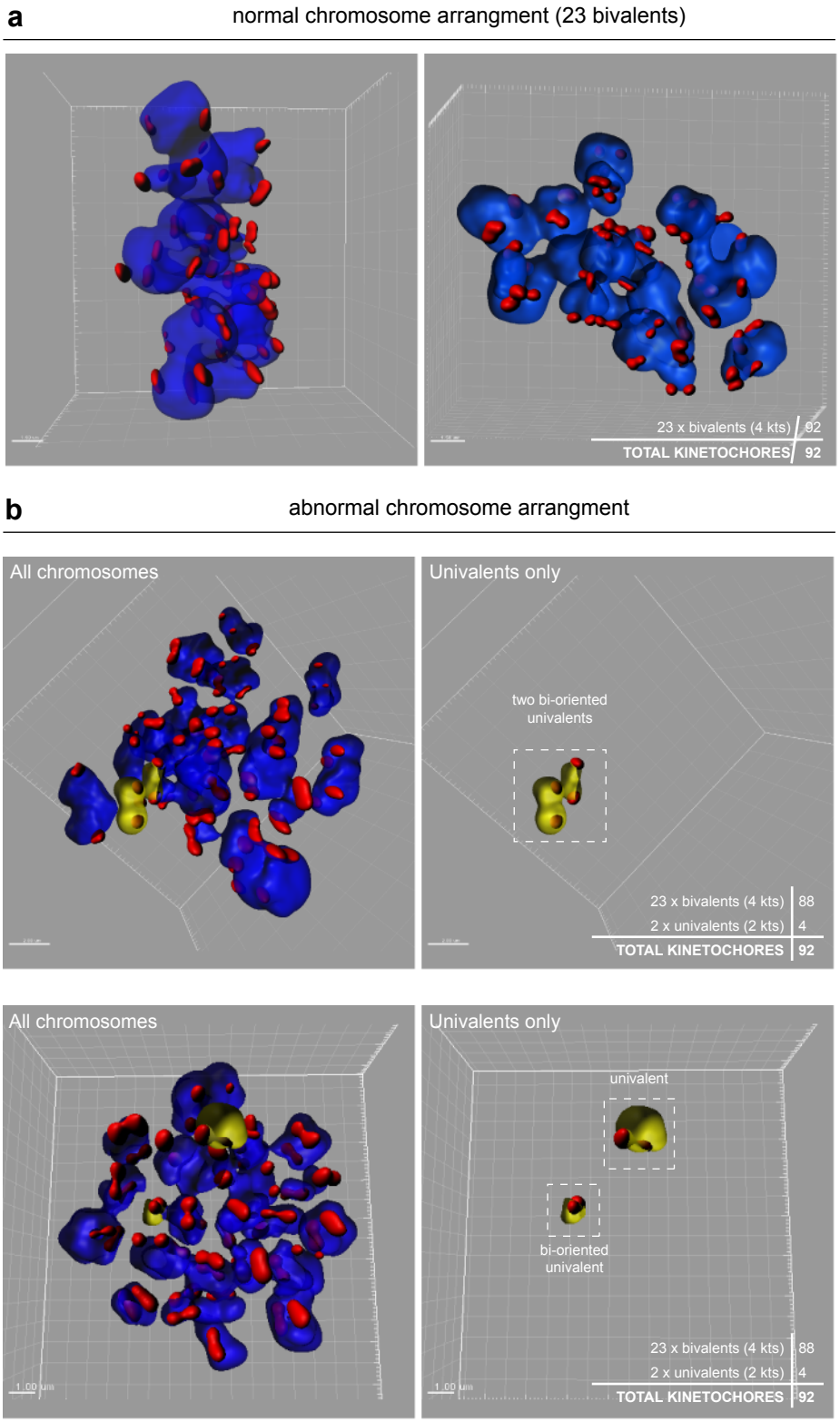

Figure 3.14. 3D reconstruction of chromosomal arrangement in metaphase I oocytes. (a) Chromosomes from two normal oocytes, each with 23 bivalents. (b) Chromosomes in two abnormal oocytes, each with 22 bivalents (blue) and 2 univalents (yellow).

Figure 3.15

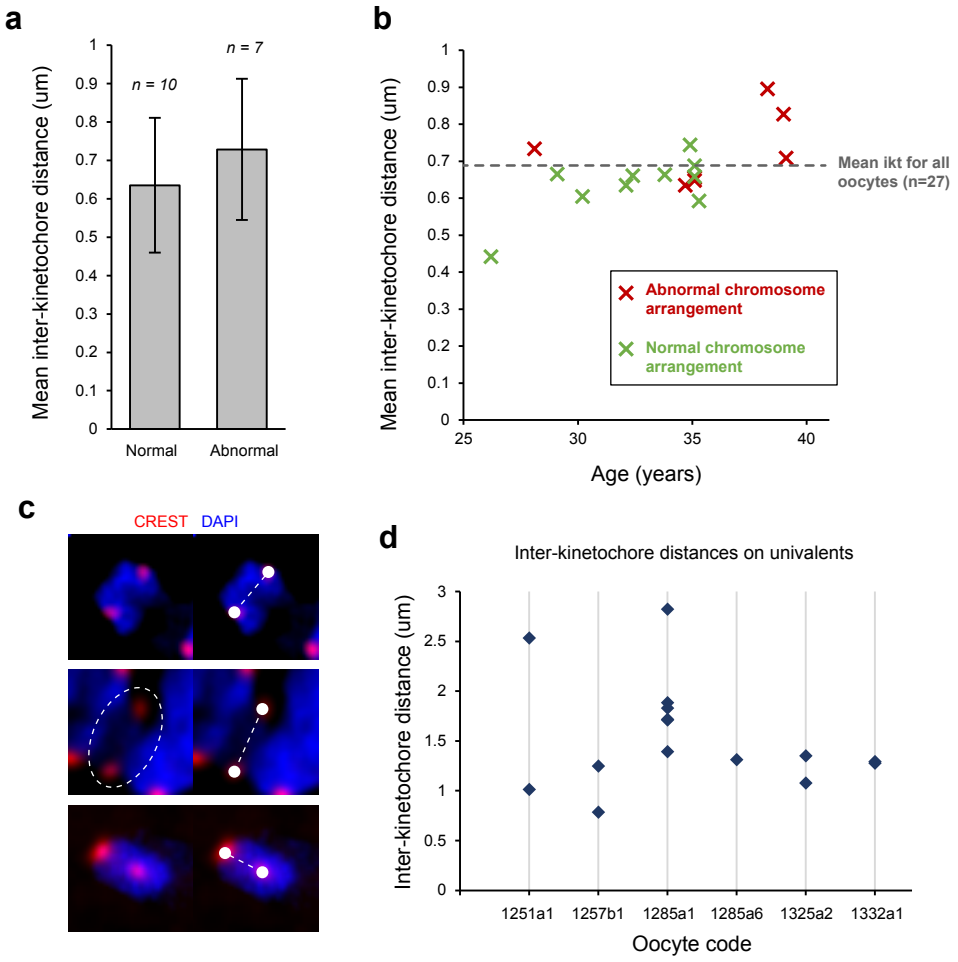

Figure 3.15. Inter-kinetochore distances in oocytes in which chromosomal status could be assessed. (a) Mean inter-kinetochore distance in oocytes that had normal (n = 10) and abnormal (n = 7) chromosome arrangement. (b) Oocyte-wide inter-kinetochore distances in normal (green) and abnormal (red) oocytes, in comparison to the mean over all oocytes (dotted grey line). (c) Maximal projection images of univalents. (d) Chart showing inter-kinetochore distances for all univalents, which are higher than the overall average.

Chapter 4: Discussion

In this study, I aimed to characterise the organisation of the meiotic kinetochore in intact human MI oocytes. I found that, unlike in previous organisms studied, sister kinetochores are generally separated in MI, and that the distance of separation increases with increasing female age.

4.1. Use of human oocytes

Study of human oocytes is challenging, given the invasive nature of oocyte collection, ethical considerations and scarcity of material. In addition to these impediments, the oocytes themselves are highly sensitive to variations in temperature and pH, requiring careful monitoring of external conditions (Pickering *et al.*, 1990, Dale *et al.*, 1998). The problem of access to material can be overcome to some extent by using oocytes from women undergoing fertility treatment. However, the oocytes available to research via this avenue are typically only those that are not suitable for use in the donating patient's treatment. This raises potential concerns about the quality of the oocytes available because (a) they come from sub-fertile women and (b) they are oocytes that have failed to mature *in vivo*, despite exposure of the woman to hormonal stimulation aimed at producing mature (MII) oocytes. There are also concerns that the stimulation itself can be a contributor to aneuploidy.

To provide some reassurance concerning these issues, I showed that women included in the study who have presumed normal fertility (i.e. they are undergoing IVF due to male-factor infertility or are in same-sex relationships) exhibit the same results as sub-fertile women. Furthermore, because the women in the study experience infertility for a range of different conditions, as presented in **Table 2.1**, it is highly unlikely that medical factors are responsible for the consistent results in kinetochore structure that were observed. To assess the effects of hormonal stimulation, I measured correlation between the total FSH dose received by patients and meiotic kinetochore features, and found that

it did not explain my observations (see **Figure 2.1**), although there was a mild correlation between total FSH dose and increased inter-kinetochore distance. Nonetheless, the results presented in this thesis are consistent with those of Zielinska *et al.*, who studied human oocytes obtained from ICSI cycles, which would also have been exposed to a regimen of gonadotrophin stimulation involving exogenous FSH (Zielinska *et al.*, 2015). In another human oocyte study, Holubcova *et al.* demonstrated that the majority of clinically discarded immature human oocytes are able to undergo anaphase and exhibit consistent patterns of spindle assembly and chromosome segregation (Holubcova *et al.*, 2015). Together, this shows that these oocytes can be valuable tools for studying human female meiosis.

In selecting MI oocytes for analysis, only those in which chromosomes were in bivalents were included; hence, although 119 immature (GV and MI) oocytes were fixed and stained, only a small fraction of these were analysed. Because patients often had both normal and abnormal appearing oocytes, both in terms of their appearance post-fixation and according to embryologists' records, these abnormalities are unlikely to be linked to the clinical condition of the patients and are likely to reflect natural variation.

4.2. Sister kinetochores in MI oocytes appear to be routinely separated in MI

Because distinct kinetochore pairs accounted for the majority of pairs in all oocytes from the women who donated to the study, this indicated that separated sister kinetochores are an intrinsic feature of human MI oocytes. This is different from yeast or mouse in which kinetochores are tightly held together during MI (Sarangapani *et al.*, 2014, Kim *et al.*, 2015), and plants in which only the outer plates of the kinetochores are fused (Li & Dawe, 2009). The human MI oocytes that I observed more closely resembled mouse Meikin-deficient oocytes, in which cohesin between sister kinetochores is no longer protected, resulting in sister kinetochore separation (Kim *et al.*, 2015). Although a Meikin homologue exists in humans and has been visualised at centromeres in pachytene spermatocytes by immunofluorescence (Kim *et al.*, 2015), it has yet to be

observed in human oocytes. Future studies will therefore need to investigate firstly whether Meikin localises to centromeres/kinetochores in human oocytes, and secondly if there are changes in Meikin levels at kinetochores in oocytes of different materal ages. An alternative explanation for my result is that the antibodies used to detect kinetochores are unable to bind to the region of overlap between sister kinetochores, possibly as a result of Meikin or another meiotic kinetochore regulator in this location. This could effectively 'mask' the region and prevent its detection with antibodies. However, given that I observed the presence of overlapping kinetochore pairs in addition to separated kinetochore pairs, this explanation seems unlikely.

Although distinct pairs accounted for the majority of sister kinetochores, 22.9% of kinetochore pairs appeared as single spots, termed 'overlapping' pairs. The proportions of distinct and overlapping kinetochore pairs varied among oocytes, and even among oocytes from the same patient (see **Figure 3.5**), which may indicate that there is centromeric stretching between sister kinetochores, as in mitosis (Jaqaman *et al.*, 2010). In mitosis, centromeric stretching occurs as a result of forces exerted on chromosomes by k-fibres attached to kinetochores, resulting in a push-and-pull motion that helps to align chromosomes at the metaphase plate (Skibbens *et al.*, 1993). As the oocytes were fixed during the dynamic process of meiotic spindle assembly we are only seeing a snapshot of kinetochore arrangement in MI. It has been shown through live-cell imaging that the process of spindle assembly is highly protracted and dynamic in human oocytes, with chromosomes moving around the spindle region for up to 13 hours after GVBD, and then oscillating about the spindle equator up to anaphase onset (Holubcova *et al.*, 2015). It is possible that during this period of assembly, stretching occurs between sister kinetochores, similar to what occurs in mitosis, although the side-by-side arrangement of sisters precludes the possibility of push-and-pull dynamics. Finally, the possibility also remains that if imaged at higher resolution overlapping pairs may be resolved into two distinct spots, because we are currently restricted by the diffraction limit of the light microscope. Using super-resolution microscopy, such as 3D structured illumination microscopy, may enable resolution of overlapping pairs.

It is also possible that the stage of MI at which the oocyte was fixed affects sister kinetochore separation. Because of the nature of human oocyte collection, it is not possible to precisely ascertain whether the oocytes in this study are in early or late stage MI; it is likely that they reflect varying stages of MI. It may be a possibility that in early stages of MI, kinetochores are separated, but closer to anaphase they become unified. However, as oocytes in this study that appear to be in late metaphase (see **Figure 3.2d,iv**) also have separated kinetochores this seems unlikely. High-resolution live-cell imaging is need to answer the question of whether sister kinetochore geometry changes during the transition from metaphase to anaphase I.

The mean inter-kinetochore distance for all oocytes was 0.69 ± 0.20 μm (mean ± SD; n = 818 pairs from 27 oocytes), which is greater than that in mice which is around 0.4 μm (Kim *et al.*, 2015). My measured value in MI oocytes was closer to the inter-kinetochore distances in human and mouse metaphase II-stage oocytes (Duncan *et al.*, 2012, Merriman *et al.*, 2013). The second meiotic division involves segregation of sister chromatids, so although cohesin remains between sister kinetochores, they are not as tightly fused together as they are in MI, routinely appearing (in both mouse and human) as two separate spots. This indicates that in human MI oocytes, the structures holding sister kinetochores together are intrinsically weaker than the fused sister kinetochores at MI in other organisms, and hence they more closely resemble sister kinetochores at the second meiotic division.

4.3. Internal kinetochore architecture in meiosis I resembles that of mitosis

By staining oocytes with markers of the inner plate, outer plate and fibrous corona, I was able to show that the entire kinetochore structure appears to be separated in MI, as the different markers (CREST, Bub1, Hec1, and CENPE) exhibit similar patterns of staining. This suggests that in addition to the inner kinetochore that interacts with chromosomes, the regions responsible for attachment are also separated, represented by Hec1 and Bub1, which may have implications for the ways in which attachments are formed.

By measuring the inter-kinetochore distance using CENP-E, the outermost kinetochore marker, I showed that the degree of separation was similar for the inner and outer kinetochore. The slightly increased overall measurement for CENP-E in comparison to CREST may reflect a degree of outer kinetochore 'swivel', which has been proposed as a mechanism for kinetochores to be able to attach to microtubule fibres at the periphery of the spindle (Smith *et al.*, 2016). This difference may also reflect pivoting within the kinetochore, which may be necessary for sisters to achieve side-by-side arrangement.

Using these different kinetochore markers, it was possible to measure intra-kinetochore distances and hence assess the nano-scale architecture of the kinetochore architecture. Between MI and MII oocytes, we found only a minimal change in kinetochore architecture in the distance from CENP-E to CREST (see **Figure 3.9**), indicating that the internal structure remains unaltered in MI despite the side-by-side arrangement of sisters. Further work is needed to determine whether the differences are important. The location of CENP-E and Bub1 was also consistent with measurements of the same proteins on human mitotic kinetochores (Wan *et al.*, 2009), indicating that the outer kinetochore is not altered between mitosis and meiosis. However, the distance from the outer kinetochore (represented by CENP-E) to the CREST signal was ~50 nm larger than that measured in mitotic kinetochores to CENP-A, suggesting that the inner kinetochore and/or centromere is either stretched or expanded compared to a mitotic kinetochore. Interestingly, such conformational changes have been also been reported for mitotic kinetochores when constitutive centromere-associated network (CCAN) linkers are depleted (Suzuki *et al.*, 2014). One caveat of this is that CREST antisera also recognise CENP-C and CENP-B, which are located further into the centromeric chromatin (Earnshaw, 2015). Although other antibodies targeted towards a single inner plate protein were tested, none of these worked reliably. However, the CREST signal in MI oocytes formed a single spot unlike mitotic cells where the signal spreads into the centromere. Moreover, CENP-C is positioned distal to CENP-A during mitosis (Suzuki *et al.*, 2014). Thus, there is support for differences in the organisation of the MI and mitotic inner kinetochore/centromere. As the kinetochore-tracking software is

currently configured for mitotic cells, in which sister pairs are back-to-back, future work will focus on optimising the system for MI. In particular it will be informative to compare internal architecture between sister kinetochore pairs to determine whether there is a relationship between intra- and inter-kinetochore distance.

4.4. Sister kinetochores in metaphase I form dual k-fibre attachments

The ability of sister kinetochore pairs on a homologous chromosome to form dual k-fibre attachments indicates that both sisters are functionally active and are each capable of acting as independent attachment sites. I speculate that the presence of a monotelic population (one sister attached) may represent either an immature attachment or the result of an error-correction event. Dual k-fibre attachments may pose a significant problem for achieving stable co-orientation (in which both pairs of sister kinetochores are attached to k-fibres from their respective spindle poles) as there are potentially twice the number of kinetochore-microtubule attachments for the cell to correct. Moreover, the method of sensing and correcting these attachments would differ from mitosis, because sisters are in a side-by-side arrangement, so there are likely to be different tensile forces acting between them in comparison to mitosis. It may be a possibility that inter-homologue tension plays a role in meiotic error correction rather than inter-kinetochore tension as in mitosis (**Figure 4.1**). Given that data from both mouse and human oocytes indicate that the oocyte's ability to correct unstable kinetochore-microtubule attachments is less efficient than in mitosis (Yoshida *et al.*, 2015), the larger number of possible connections along with the side-by-side arrangement of sisters may contribute to the increased spindle assembly time that is observed in human oocytes (Holubcova *et al.*, 2015). This situation is dramatically different to what is known about mouse oocyte MI, in which the majority of sister kinetochores are held together by Meikin (Kim *et al.*, 2015), thus forming a single k-fibre attachment (Kitajima *et al.*, 2011, FitzHarris, 2012, Touati *et al.*, 2015, Yoshida *et al.*, 2015).

It is also possible that lateral attachments play a role in meiosis. To visualise kinetochore-microtubule attachments I used cold-shock treatment which causes

Figure 4.1

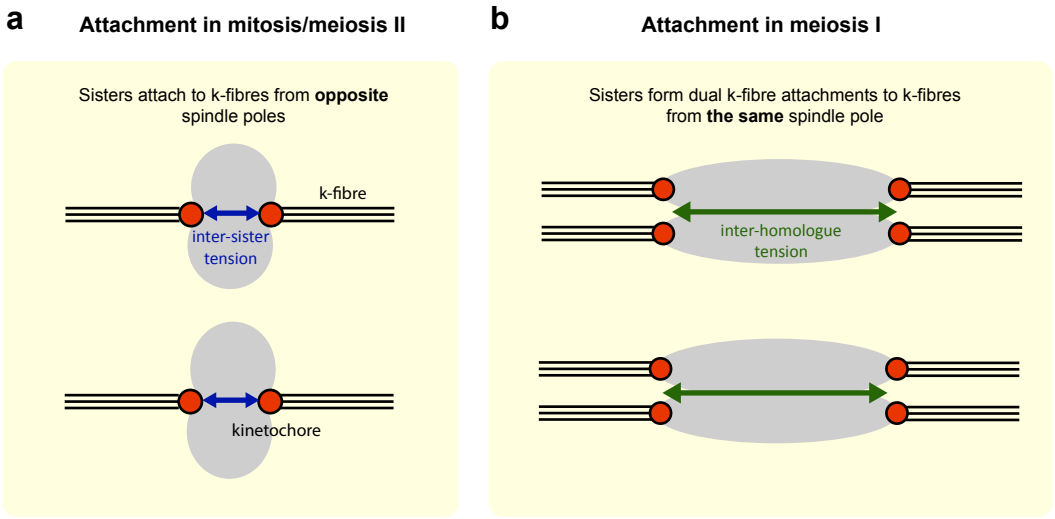

Figure 4.1. Model for sister kinetochore attachment in MI. (a) Attachment in mitosis/MII, in which sister kinetochores attach to k-fibres from opposite poles. Blue arrows represent tension between sisters. (b) Proposed model for attachment in MI, in which sister kinetochores attach to k-fibres from the same spindle pole. Green arrows represent inter-homologue tension.

microtubules that are not attached in an end-on fashion to depolymerize. In mouse, there is evidence that lateral attachments play a role in aligning chromosomes at the equator in MI, because end-on attachments are only observed at the end of MI, by which stage bivalents are already correctly oriented and kinetochores are stretched towards the poles (Brunet *et al.*, 1999). The identification of just a small number of end-on attachments in the human oocytes included in this study may reflect a possible contribution by lateral attachments to achieving bi-orientation.

4.5. Sister kinetochore separation increases with age

Having established that sister kinetochore pairs in MI are separated in human oocytes, I next set out to investigate whether there was a relationship between female age and kinetochore organisation. The absence of a correlation between age and the proportion of distinct sister kinetochore pairs in human MI was different to reports in mouse (Chiang *et al.*, 2010). This is likely to reflect the fact that in this study population, the vast majority of kinetochores were separated, even in the youngest patients. I did find, however, that in the two youngest patients (ages 26.2 and 27.7) a relatively high proportion of kinetochores were classified as ‘overlapping’. This might suggest that coming apart of sister kinetochores happens some years before aneuploidies first begin to arise, however without the ability to study oocytes from women at younger ages, this cannot be tested. It is unlikely that oocytes from a younger population will be readily obtained, because it is rare for younger patients (< 25 years) to have IVF. Other methods of deriving oocytes from younger patients involve growth and *in vitro* maturation of oocytes isolated from resected ovarian tissue; however, as these are occasional samples and usually donated by cancer patients, there is the possibility that oocytes may have undergone molecular damage. Nonetheless, given that the incidence of trisomic pregnancy is similar for women in their late teens/early 20s (2–3%) and their early 30s (~5%), we would not expect to see a dramatic difference in kinetochore geometry in women at earlier ages in comparison with those studied. In contrast, the incidence of trisomy for women in their late 30s/early 40s is around 15% (Hassold & Hunt, 2001).

Here, I show for the first time in intact human MI oocytes that the entire kinetochore structure, from the centromeric inner plate to the fibrous corona, comes apart with age (see **Figure 4.2**). The increase in sister kinetochore separation applied to measurements made using both CREST and CENP-E, and the increase in inter-kinetochore distance followed a similar trend for both, indicating that the entire kinetochore structure comes further apart over time. This result is in keeping with findings from monastrol-treated mouse MI oocytes (Chiang *et al.*, 2010) and metaphase spreads from mouse and human MII oocytes (Duncan *et al.*, 2012, Merriman *et al.*, 2013), which show that aged oocytes have sister kinetochores that are further apart. The data is also in agreement with that shown by Zielinska *et al.* in human MI oocytes obtained from women undergoing ICSI treatment (Zielinska *et al.*, 2015).

This increase in inter-kinetochore separation in human oocytes is likely to reflect a decline in centromeric cohesion with age. This is based on evidence that the connection between sister kinetochores in both mitosis and meiosis is at least partly dependent on cohesin levels (Eckert *et al.*, 2007, Chiang *et al.*, 2010). In mitosis, loss of pericentromeric cohesin causes increased stretching of centromeres, indicating that the connection between sisters is elastic (Eckert *et al.*, 2007). Support for an age-dependent decline in cohesin has also been hinted at in previous studies of human oocytes (Duncan *et al.*, 2012; Tsutsumi *et al.*, 2014). However, no studies have so far been able to visualise cohesin directly in mature human oocytes, which leaves open the possibility that other factors contribute to this effect. In mouse, Meikin loss has been shown to cause a similar effect (Kim *et al.*, 2015), so there is also the possibility that loss of a meiotic kinetochore regulator also contributes to this effect, however the precise identity of this regulator is unclear, particularly as Meikin has not been visualised in human oocytes. The precise mechanisms behind a potential decline in cohesin are unclear, however it may reflect natural ageing and protein degradation. An age-related decline in the meiotic cohesin protector, Sgo2, has also been observed in mouse (Lee *et al.*, 2008), so there is also the possibility that loss of cohesin protection by shugoshin precedes its decline in human

Figure 4.2

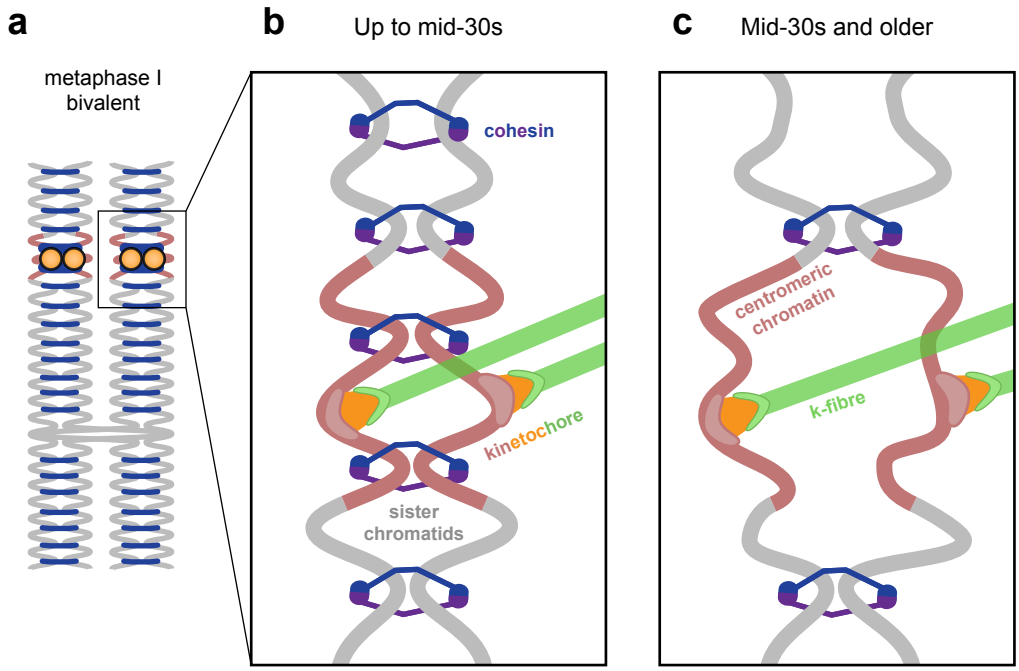

Figure 4.2. Sister kinetochores on bivalents come apart with female age in metaphase I stage human oocytes. (a) Schematic of a bivalent in meiosis I, showing sister kinetochores (orange) in a side-by-side arrangement and cohesin rings (blue) located along chromosome arms and enriched at centromeres. (b) Enlarged representation of meiotic sister kinetochores in oocytes from younger women. Kinetochores on sister chromatids form two distinctly separate units, each of which is able to form an attachment to a kinetochore-fibre (k-fibre, green). (c) In older women, we hypothesise that reduced cohesin, particularly at the centromeres, results in sister kinetochores moving apart. This may make it more difficult for them to co-ordinate their attachments to k-fibres emanating from the same spindle pole.

oocytes. Future work to directly visualise cohesin in human oocytes using immunofluorescence or live-cell protein markers will be valuable.

The maternal age-dependent change in centromeric chromatin may have implications for the formation of stable k-fibre attachments. One report in mouse has shown that separated sister kinetochores in aged oocytes do not form more unstable attachments than fused pairs, but they do have a slightly increased propensity to form merotelic attachments (Shomper *et al.*, 2014), indicating that cohesin loss and subsequent separation of sisters does not severely affect attachment. However, given that the degree of separation of kinetochores in human oocytes is greater than that in mice, it may be a possibility that kinetochore pairs with an inter-kinetochore distance beyond a certain threshold are prone to mis-attachment, particularly as individual kinetochores within a pair act as separate attachment sites. This could be investigated by live-cell imaging.

4.6. Presence of univalents is the most common abnormality in human metaphase I oocytes

One of the advantages of studying meiotic chromosomes *in situ* using high-resolution microscopy was that it was possible to study chromosome configuration in oocytes and to determine whether there were any abnormalities or features that predisposed the oocytes to aneuploidy. Given the relatively high inter-kinetochore distances that I had measured previously, particularly in older oocytes, I expected that single chromatids would be the most likely abnormality, particularly as premature separation of sisters has been cited as one of the most common causes of aneuploidy. Strikingly, however, of the 17 oocytes for which I was able to account for all chromosomes, the presence of univalents was the most common abnormality, and no oocytes with single chromatids were identified. Recently, two papers have described the phenomenon of bivalent conversion into univalents during MI in both mouse and human as a contributor to aneuploidy (Ottolini *et al.*, 2015, Sakakibara *et al.*, 2015). These univalents often separate their sisters at the first meiotic division (rather than the second), hence this type of division is referred to as ‘reverse segregation’. The majority

of the bivalents I identified had bi-oriented, and would likely go on to separate sister chromatids, which is in keeping with this data.

The average age of the oocytes with abnormal chromosome configurations was higher than that of normal oocytes, which is consistent with the known increase in aneuploidy with age. Importantly, the 'abnormal' oocytes that I identified are not aneuploid as they still had the correct numbers of chromosomes and kinetochores (hence they would not be picked up in a genetic screen); it is the arrangement of the chromosomes that was abnormal and may have made them more prone to aneuploidy. Although the abnormally organised oocytes were on average older, the average inter-kinetochore distance over the entire oocyte was not higher in these oocytes, suggesting that univalents do not arise as a result of generalised reduced cohesin. A caveat of this is that I was only able to identify 7 abnormal oocytes, therefore more data addressing this point is required. It is likely that cohesin had been lost on the univalents that had bi-oriented, because they had sister kinetochores with separation distances of >1.2 µm. However, it is not clear from the data whether this separation would precede bi-orientation or occur after it.

4.7. Conclusions and future directions

In summary, my results provide the first insight into MI kinetochore geometry in intact human oocytes. I show that the majority of sister kinetochores in MI oocytes are separated, which may indicate that the cohesin holding them together is inherently weaker than in other species. This raises the question of why meiosis in humans is apparently less secure. One possibility is the idea of meiotic drive, in which centromere strength (determined by the number of microtubule-binding elements) affects the positioning of chromosomes on the meiotic spindle and increases the chances of a chromosome being inherited in the egg (Henikoff *et al.*, 2001, Chmátal *et al.*, 2014). It is possible that both sister kinetochores retain their ability to bind for this reason, and the apparent absence of a regulator such as Meikin may facilitate the formation of stronger attachments.

The overall structure and architecture of individual kinetochores appears to resemble that of mitosis and meiosis II, in which sister kinetochores attach to spindle fibres from opposite poles, indicating that kinetochores do not undergo internal structural changes prior to meiosis I. I show that the degree of separation increases with age, consistent with the profile of maternal age-related aneuploidies in women. I also show that, as well as the chromatin-associated inner plate, the outer microtubule-interacting regions of the kinetochore are also separated, which enables sister kinetochores to act as individual attachment sites. This results in the formation of dual k-fibre attachments. Since both sister kinetochores are able to form k-fibre attachments, stable bi-orientation may be more difficult to achieve, which may be exacerbated by increasing inter-kinetochore distances with increasing maternal age. These features of kinetochores in MI oocytes may shed light on the particularly high incidence of chromosome segregation errors at first meiosis in human oocytes.

An important aspect of future research will be to study kinetochore dynamics during MI using high-resolution live-cell imaging (see **Appendix A**). This will enable us to answer many key questions about meiosis I that have been raised by these findings, including whether increased inter-kinetochore distance predisposes to erroneous kinetochore-microtubule attachments, how sister kinetochore dynamics differ from mitosis/MII, and whether lateral attachments play a role in MI. In the first human oocyte live-cell imaging paper, Holubcova *et al.* showed that human oocytes form many erroneous attachments during the spindle assembly process in MI, although the imaging was not of high enough resolution to resolve individual kinetochores within pairs (Holubcova *et al.*, 2015). Other studies have used kinetochore tracking to study the movement of kinetochore pairs in mouse MI oocytes (Kitajima *et al.*, 2011), an approach that would be valuable in human oocytes if individual sisters could be resolved, as this would enable us to study their behaviour during this highly error-prone division.

References

Adhikari D & Liu K (2013) Regulation of Quiescence and Activation of Oocyte Growth in Primordial Follicles. *Oogenesis,*(Coticchio G, Albertini DF & De Santis L, eds.), p.^pp. 49-62. Springer London, London.

Anderson DE, Losada A, Erickson HP & Hirano T (2002) Condensin and cohesin display different arm conformations with characteristic hinge angles. *The Journal of cell biology* **156**: 419-424.

Anderson E & Albertini DF (1976) Gap junctions between the oocyte and companion follicle cells in the mammalian ovary. *The Journal of cell biology* **71**: 680-686.

Angell R (1997) First-meiotic-division nondisjunction in human oocytes. *American journal of human genetics* **61**: 23-32.

Angell RR (1991) Predivision in human oocytes at meiosis I: a mechanism for trisomy formation in man. *Human genetics* **86**: 383-387.

Armond JW, Vladimirou E, McAinsh AD & Burroughs NJ (2016) KiT: a MATLAB package for kinetochore tracking. *Bioinformatics* **32**: 1917-1919.

Baart EB, Martini E, Eijkemans MJ, Van Opstal D, Beckers NG, Verhoeff A, Macklon NS & Fauser BC (2007) Milder ovarian stimulation for in-vitro fertilization reduces aneuploidy in the human preimplantation embryo: a randomized controlled trial. *Hum Reprod* **22**: 980-988.

Barton SE & Ginsburg ES (2012) Oocyte Retrieval and Embryo Transfer. *In Vitro Fertilization: A Comprehensive Guide,*(Ginsburg ES & Racowsky C, eds.), p.^pp. 55-74. Springer New York, New York, NY.

Battaglia DE, Goodwin P, Klein NA & Soules MR (1996) Influence of maternal age on meiotic spindle assembly in oocytes from naturally cycling women. *Hum Reprod* **11**: 2217-2222.

Bernard P, Maure JF, Partridge JF, Genier S, Javerzat JP & Allshire RC (2001) Requirement of heterochromatin for cohesion at centromeres. *Science* **294**: 2539-2542.

Bickel SE, Orr-Weaver TL & Balicky EM (2002) The sister-chromatid cohesion protein ORD is required for chiasma maintenance in Drosophila oocytes. *Curr Biol* **12**: 925-929.

Bleazard T, Ju YS, Sung J & Seo JS (2013) Fine-scale mapping of meiotic recombination in Asians. *BMC genetics* **14**: 19.

Bloom KS (2014) Centromeric Heterochromatin: The Primordial Segregation Machine. *Annual review of genetics* **48**: 457-484.

Brito IL, Monje-Casas F & Amon A (2010) The Lrs4-Csm1 monopolin complex associates with kinetochores during anaphase and is required for accurate chromosome segregation. *Cell Cycle* **9**: 3611-3618.

Brunet S, Maria AS, Guillaud P, Dujardin D, Kubiak JZ & Maro B (1999) Kinetochore Fibers Are Not Involved in the Formation of the First Meiotic Spindle in Mouse Oocytes, but Control the Exit from the First Meiotic M Phase. *The Journal of cell biology* **146**: 1-12.

Buonomo SB, Clyne RK, Fuchs J, Loidl J, Uhlmann F & Nasmyth K (2000) Disjunction of homologous chromosomes in meiosis I depends on proteolytic cleavage of the meiotic cohesin Rec8 by separin. *Cell* **103**: 387-398.

Burkhardt S, Borsos M, Szydlowska A, Godwin J, Williams SA, Cohen PE, Hirota T, Saitou M & Tachibana-Konwalski K (2016) Chromosome Cohesion Established by Rec8-Cohesin in Fetal Oocytes Is Maintained without Detectable Turnover in Oocytes Arrested for Months in Mice. *Curr Biol* **26**: 678-685.

Carabatsos MJ, Sellitto C, Goodenough DA & Albertini DF (2000) Oocyte-granulosa cell heterologous gap junctions are required for the coordination of nuclear and cytoplasmic meiotic competence. *Dev Biol* **226**: 167-179.

Carey AS & Murray PJ (2006) Chapter 30 - Puberty and Precocious Puberty A2 - Bieber, Eric J. *Clinical Gynecology,*(Sanfilippo JS & Horowitz IR, eds.), p.^pp. 443-467. Churchill Livingstone, Philadelphia.

Chan GK, Liu ST & Yen TJ (2005) Kinetochore structure and function. *Trends Cell Biol* **15**: 589-598.

Chang CR, Wu CS, Hom Y & Gartenberg MR (2005) Targeting of cohesin by transcriptionally silent chromatin. *Genes Dev* **19**: 3031-3042.

Cheeseman IM, Chappie JS, Wilson-Kubalek EM & Desai A (2006) The conserved KMN network constitutes the core microtubule-binding site of the kinetochore. *Cell* **127**: 983-997.

Cheong YC, Ginsburg ES & Macklon NS (2012) Ovulation Stimulation and Cycle Management in IVF. *In Vitro Fertilization: A Comprehensive Guide,*(Ginsburg ES & Racowsky C, eds.), p.^pp. 31-53. Springer New York, New York, NY.

Chiang T, Duncan FE, Schindler K, Schultz RM & Lampson MA (2010) Evidence that weakened centromere cohesion is a leading cause of age-related aneuploidy in oocytes. *Curr Biol* **20**: 1522-1528.

Chmátal L, Gabriel SI, Mitsainas GP, Martínez-Vargas J, Ventura J, Searle JB, Schultz RM & Lampson MA (2014) Centromere strength provides the cell biological basis for meiotic drive and karyotype evolution in mice. *Current biology : CB* **24**: 2295-2300.

Corbett KD, Yip CK, Ee LS, Walz T, Amon A & Harrison SC (2010) The monopolin complex crosslinks kinetochore components to regulate chromosome-microtubule attachments. *Cell* **142**: 556-567.

Dale B, Menezo Y, Cohen J, DiMatteo L & Wilding M (1998) Intracellular pH regulation in the human oocyte. *Hum Reprod* **13**: 964-970.

De Felici M (2013) Origin, Migration, and Proliferation of Human Primordial Germ Cells. *Oogenesis,*(Coticchio G, Albertini DF & De Santis L, eds.), p.^pp. 19-37. Springer London, London.

Duncan FE, Hornick JE, Lampson MA, Schultz RM, Shea LD & Woodruff TK (2012) Chromosome cohesion decreases in human eggs with advanced maternal age. *Aging Cell* **11**: 1121-1124.

Earnshaw WC (2015) Discovering centromere proteins: from cold white hands to the A, B, C of CENPs. *Nature reviews Molecular cell biology* **16**: 443-449.

Eckert CA, Gravdahl DJ & Megee PC (2007) The enhancement of pericentromeric cohesin association by conserved kinetochore components promotes high-fidelity chromosome segregation and is sensitive to microtubule-based tension. *Genes Dev* **21**: 278-291.

Edwards RG (1965) Maturation in vitro of mouse, sheep, cow, pig, rhesus monkey and human ovarian oocytes. *Nature* **208**: 349-351.

Edwards RG, Bavister BD & Steptoe PC (1969) Early stages of fertilization in vitro of human oocytes matured in vitro. *Nature* **221**: 632-635.

Eppig J (2001) Oocyte control of ovarian follicular development and function in mammals. *Reproduction* **122**: 829-838.

Eppig JJ (2001) Oocyte control of ovarian follicular development and function in mammals. *Reproduction* **122**: 829-838.

Fisher JM, Harvey JF, Morton NE & Jacobs PA (1995) Trisomy 18: studies of the parent and cell division of origin and the effect of aberrant recombination on nondisjunction. *American journal of human genetics* **56**: 669-675.

FitzHarris G (2012) Anaphase B precedes anaphase A in the mouse egg. *Curr Biol* **22**: 437-444.

Foley EA & Kapoor TM (2013) Microtubule attachment and spindle assembly checkpoint signalling at the kinetochore. *Nature reviews Molecular cell biology* **14**: 25-37.

Fragouli E, Lenzi M, Ross R, Katz-Jaffe M, Schoolcraft WB & Wells D (2008) Comprehensive molecular cytogenetic analysis of the human blastocyst stage. *Hum Reprod* **23**: 2596-2608.

Fragouli E, Alfarawati S, Goodall NN, Sanchez-Garcia JF, Colls P & Wells D (2011) The cytogenetics of polar bodies: insights into female meiosis and the diagnosis of aneuploidy. *Mol Hum Reprod* **17**: 286-295.

Fritzler MJ & Kinsella TD (1980) The CREST syndrome: a distinct serologic entity with anticentromere antibodies. *The American journal of medicine* **69**: 520-526.

Gabriel AS, Thornhill AR, Ottolini CS, Gordon A, Brown AP, Taylor J, Bennett K, Handyside A & Griffin DK (2011) Array comparative genomic hybridisation on first polar bodies suggests that non-disjunction is not the predominant mechanism leading to aneuploidy in humans. *J Med Genet* **48**: 433-437.

Gandhi R, Gillespie PJ & Hirano T (2006) Human Wapl is a cohesin-binding protein that promotes sister-chromatid resolution in mitotic prophase. *Curr Biol* **16**: 2406-2417.

Garcia-Cruz R, Brieno MA, Roig I, Grossmann M, Velilla E, Pujol A, Cabero L, Pessarrodona A, Barbero JL & Garcia Caldes M (2010) Dynamics of cohesin proteins REC8, STAG3, SMC1 beta and SMC3 are consistent with a role in sister chromatid cohesion during meiosis in human oocytes. *Hum Reprod* **25**: 2316-2327.

Gerton JL & Hawley RS (2005) Homologous chromosome interactions in meiosis: diversity amidst conservation. *Nature reviews Genetics* **6**: 477-487.

Gougeon A (2013) *The early stages of follicular growth. Biology and Pathology of the Oocyte*. Cambridge University Press.

Grewal SI & Jia S (2007) Heterochromatin revisited. *Nature reviews Genetics* **8**: 35-46.

Griesinger G, Diedrich K, Devroey P & Kolibianakis EM (2006) GnRH agonist for triggering final oocyte maturation in the GnRH antagonist ovarian hyperstimulation protocol: a systematic review and meta-analysis. *Hum Reprod Update* **12**: 159-168.

Gruber S, Haering CH & Nasmyth K (2003) Chromosomal cohesin forms a ring. *Cell* **112**: 765-777.

Gudimchuk N, Vitre B, Kim Y, Kiyatkin A, Cleveland DW, Ataullakhanov FI & Grishchuk EL (2013) Kinetochore kinesin CENP-E is a processive bi-directional tracker of dynamic microtubule tips. *Nat Cell Biol* **15**: 1079-1088.

Haering CH, Lowe J, Hochwagen A & Nasmyth K (2002) Molecular architecture of SMC proteins and the yeast cohesin complex. *Mol Cell* **9**: 773-788.

Hall HE, Surti U, Hoffner L, Shirley S, Feingold E & Hassold T (2007) The origin of trisomy 22: evidence for acrocentric chromosome-specific patterns of nondisjunction. *Am J Med Genet A* **143a**: 2249-2255.

Hall HE, Chan ER, Collins A, Judis L, Shirley S, Surti U, Hoffner L, Cockwell AE, Jacobs PA & Hassold TJ (2007) The origin of trisomy 13. *Am J Med Genet A* **143a**: 2242-2248.

Handel MA & Schimenti JC (2010) Genetics of mammalian meiosis: regulation, dynamics and impact on fertility. *Nature reviews Genetics* **11**: 124-136.

Handyside AH (1996) Moisaicism in the human preimplantation embryo. *Reproduction, nutrition, development* **36**: 643-649.

Hassold T & Chiu D (1985) Maternal age-specific rates of numerical chromosome abnormalities with special reference to trisomy. *Human genetics* **70**: 11-17.

Hassold T & Hunt P (2001) To err (meiotically) is human: the genesis of human aneuploidy. *Nature reviews Genetics* **2**: 280-291.

Hassold T, Hall H & Hunt P (2007) The origin of human aneuploidy: where we have been, where we are going. *Human molecular genetics* **16 Spec No. 2**: R203-208.

Hassold T, Merrill M, Adkins K, Freeman S & Sherman S (1995) Recombination and maternal age-dependent nondisjunction: molecular studies of trisomy 16. *American journal of human genetics* **57**: 867-874.

Hassold T, Abruzzo M, Adkins K, Griffin D, Merrill M, Millie E, Saker D, Shen J & Zaragoza M (1996) Human aneuploidy: incidence, origin, and etiology. *Environ Mol Mutagen* **28**: 167-175.

Hauf S, Waizenegger IC & Peters JM (2001) Cohesin cleavage by separase required for anaphase and cytokinesis in human cells. *Science* **293**: 1320-1323.

Henderson SA & Edwards RG (1968) Chiasma frequency and maternal age in mammals. *Nature* **218**: 22-28.

Henikoff S, Ahmad K & Malik HS (2001) The centromere paradox: stable inheritance with rapidly evolving DNA. *Science* **293**: 1098-1102.

Herbert AD, Carr AM & Hoffmann E (2014) FindFoci: a focus detection algorithm with automated parameter training that closely matches human assignments, reduces human inconsistencies and increases speed of analysis. *PLoS One* **9**: e114749.

Hirano T (2006) At the heart of the chromosome: SMC proteins in action. *Nature reviews Molecular cell biology* **7**: 311-322.

Hirano T (2012) Condensins: universal organizers of chromosomes with diverse functions. *Genes Dev* **26**: 1659-1678.

Hirshfield AN (1992) Heterogeneity of cell populations that contribute to the formation of primordial follicles in rats. *Biol Reprod* **47**: 466-472.

Hodges CA, Revenkova E, Jessberger R, Hassold TJ & Hunt PA (2005) SMC1beta-deficient female mice provide evidence that cohesins are a missing link in age-related nondisjunction. *Nature genetics* **37**: 1351-1355.

Hodges CA, Ilagan A, Jennings D, Keri R, Nilson J & Hunt PA (2002) Experimental evidence that changes in oocyte growth influence meiotic chromosome segregation. *Hum Reprod* **17**: 1171-1180.

Holubcova Z, Blayney M, Elder K & Schuh M (2015) Human oocytes. Error-prone chromosome-mediated spindle assembly favors chromosome segregation defects in human oocytes. *Science* **348**: 1143-1147.

Hoque MT & Ishikawa F (2001) Human chromatid cohesin component hRad21 is phosphorylated in M phase and associated with metaphase centromeres. *J Biol Chem* **276**: 5059-5067.

Hsueh AJW & Kawamura K (2013) Follicle and oocyte developmental dynamics. *Biology and Pathology of the Oocyte: Role in Fertility, Medicine and Nuclear Reprograming,*(Trounson A, Gosden R & Eichenlaub-Ritter U, eds.), p.^pp. 62-72. Cambridge University Press.

Human Fertilisation and Embryology Authority, 2016. Fertility Treatment in 2014: Trends and Figures. *http://www.hfea.gov.uk/*

Hunt PA & Hassold TJ (2008) Human female meiosis: what makes a good egg go bad? *Trends Genet* **24**: 86-93.

Hunter N & Kleckner N (2001) The single-end invasion: an asymmetric intermediate at the double-strand break to double-holliday junction transition of meiotic recombination. *Cell* **106**: 59-70.

Hussin J, Roy-Gagnon MH, Gendron R, Andelfinger G & Awadalla P (2011) Age-dependent recombination rates in human pedigrees. *PLoS Genet* **7**: e1002251.

Jacobs PA, Baikie AG, Court Brown WM & Strong JA (1959) The somatic chromosomes in mongolism. *Lancet (London, England)* **1**: 710.

Jaqaman K, King EM, Amaro AC*, et al.* (2010) Kinetochore alignment within the metaphase plate is regulated by centromere stiffness and microtubule depolymerases. *The Journal of cell biology* **188**: 665-679.

Jessberger R (2012) Age-related aneuploidy through cohesion exhaustion. *EMBO Rep* **13**: 539-546.

Jones KT, Lane SIR & Holt JE (2013) Start and Stop Signals of Oocyte Meiotic Maturation. *Oogenesis,*(Coticchio G, Albertini DF & De Santis L, eds.), p.^pp. 183-193. Springer London, London.

Kapoor TM, Lampson MA, Hergert P, Cameron L, Cimini D, Salmon ED, McEwen BF & Khodjakov A (2006) Chromosomes can congress to the metaphase plate before biorientation. *Science* **311**: 388-391.

Keeney S, Giroux CN & Kleckner N (1997) Meiosis-specific DNA double-strand breaks are catalyzed by Spo11, a member of a widely conserved protein family. *Cell* **88**: 375-384.

Kim J, Ishiguro K, Nambu A*, et al.* (2015) Meikin is a conserved regulator of meiosis-I-specific kinetochore function. *Nature* **517**: 466-471.

Kitajima TS, Ohsugi M & Ellenberg J (2011) Complete kinetochore tracking reveals error-prone homologous chromosome biorientation in mammalian oocytes. *Cell* **146**: 568-581.

Kitajima TS, Miyazaki Y, Yamamoto M & Watanabe Y (2003) Rec8 cleavage by separase is required for meiotic nuclear divisions in fission yeast. *The EMBO Journal* **22**: 5643-5653.

Kitajima TS, Sakuno T, Ishiguro K, Iemura S, Natsume T, Kawashima SA & Watanabe Y (2006) Shugoshin collaborates with protein phosphatase 2A to protect cohesin. *Nature* **441**: 46-52.

Klein NA, Battaglia DE, Fujimoto VY, Davis GS, Bremner WJ & Soules MR (1996) Reproductive aging: accelerated ovarian follicular development associated with a monotropic follicle-stimulating hormone rise in normal older women. *J Clin Endocrinol Metab* **81**: 1038-1045.

Kong A, Barnard J, Gudbjartsson DF*, et al.* (2004) Recombination rate and reproductive success in humans. *Nature genetics* **36**: 1203-1206.

Kueng S, Hegemann B, Peters BH, Lipp JJ, Schleiffer A, Mechtler K & Peters JM (2006) Wapl controls the dynamic association of cohesin with chromatin. *Cell* **127**: 955-967.

Kuleszewicz K, Fu X & Kudo NR (2013) Cohesin loading factor Nipbl localizes to chromosome axes during mammalian meiotic prophase. *Cell Div* **8**: 12.

Kuliev A, Zlatopolsky Z, Kirillova I, Spivakova J & Cieslak Janzen J (2011) Meiosis errors in over 20,000 oocytes studied in the practice of preimplantation aneuploidy testing. *Reproductive biomedicine online* **22**: 2-8.

Labarta E, Bosch E, Alama P, Rubio C, Rodrigo L & Pellicer A (2012) Moderate ovarian stimulation does not increase the incidence of human embryo chromosomal abnormalities in in vitro fertilization cycles. *J Clin Endocrinol Metab* **97**: E1987-1994.

Lamb NE, Sherman SL & Hassold TJ (2005) Effect of meiotic recombination on the production of aneuploid gametes in humans. *Cytogenet Genome Res* **111**: 250-255.

Lamb NE, Yu K, Shaffer J, Feingold E & Sherman SL (2005) Association between maternal age and meiotic recombination for trisomy 21. *American journal of human genetics* **76**: 91-99.

Lamb NE, Freeman SB, Savage-Austin A*, et al.* (1996) Susceptible chiasmate configurations of chromosome 21 predispose to non-disjunction in both maternal meiosis I and meiosis II. *Nature genetics* **14**: 400-405.

Lampson MA & Cheeseman IM (2011) Sensing centromere tension: Aurora B and the regulation of kinetochore function. *Trends Cell Biol* **21**: 133-140.

Larionov VL, Karpova TS, Kouprina NY & Jouravleva GA (1985) A mutant of Saccharomyces cerevisiae with impaired maintenance of centromeric plasmids. *Current genetics* **10**: 15-20.

Lee J, Kitajima TS, Tanno Y, Yoshida K, Morita T, Miyano T, Miyake M & Watanabe Y (2008) Unified mode of centromeric protection by shugoshin in mammalian oocytes and somatic cells. *Nat Cell Biol* **10**: 42-52.

Lei L & Spradling AC (2013) Mouse primordial germ cells produce cysts that partially fragment prior to meiosis. *Development (Cambridge, England)* **140**: 2075-2081.

Lengronne A, Katou Y, Mori S, Yokobayashi S, Kelly GP, Itoh T, Watanabe Y, Shirahige K & Uhlmann F (2004) Cohesin relocation from sites of chromosomal loading to places of convergent transcription. *Nature* **430**: 573-578.

Lenzi ML, Smith J, Snowden T, Kim M, Fishel R, Poulos BK & Cohen PE (2005) Extreme heterogeneity in the molecular events leading to the establishment of chiasmata during meiosis i in human oocytes. *American journal of human genetics* **76**: 112-127.

Li G & Zhu P (2015) Structure and organization of chromatin fiber in the nucleus. *FEBS letters* **589**: 2893-2904.

Li X & Dawe RK (2009) Fused sister kinetochores initiate the reductional division in meiosis I. *Nat Cell Biol* **11**: 1103-1108.

Lipkin SM, Moens PB, Wang V*, et al.* (2002) Meiotic arrest and aneuploidy in MLH3-deficient mice. *Nature genetics* **31**: 385-390.

Lister LM, Kouznetsova A, Hyslop LA*, et al.* (2010) Age-related meiotic segregation errors in mammalian oocytes are preceded by depletion of cohesin and Sgo2. *Curr Biol* **20**: 1511-1521.

Liu L & Keefe DL (2008) Defective cohesin is associated with age-dependent misaligned chromosomes in oocytes. *Reproductive biomedicine online* **16**: 103-112.

Llano E, Gomez R, Gutierrez-Caballero C*, et al.* (2008) Shugoshin-2 is essential for the completion of meiosis but not for mitotic cell division in mice. *Genes Dev* **22**: 2400-2413.

MacDonald M, Hassold T, Harvey J, Wang LH, Morton NE & Jacobs P (1994) The origin of 47,XXY and 47,XXX aneuploidy: heterogeneous mechanisms and role of aberrant recombination. *Human molecular genetics* **3**: 1365-1371.

Macklon NS & Fauser BC (1999) Aspects of ovarian follicle development throughout life. *Horm Res* **52**: 161-170.

Macklon NS, Stouffer RL, Giudice LC & Fauser BC (2006) The science behind 25 years of ovarian stimulation for in vitro fertilization. *Endocr Rev* **27**: 170-207.

Maggiulli R, Ubaldi F & Rienzi LF (2012) Oocyte Insemination and Culture. *In Vitro Fertilization: A Comprehensive Guide,*(Ginsburg ES & Racowsky C, eds.), p.^pp. 83-98. Springer New York, New York, NY.

Maresca TJ & Salmon ED (2009) Intrakinetochore stretch is associated with changes in kinetochore phosphorylation and spindle assembly checkpoint activity. *The Journal of cell biology* **184**: 373-381.

Mayer TU, Kapoor TM, Haggarty SJ, King RW, Schreiber SL & Mitchison TJ (1999) Small molecule inhibitor of mitotic spindle bipolarity identified in a phenotype-based screen. *Science* **286**: 971-974.

Mazaud S, Guigon CJ, Lozach A, Coudouel N, Forest MG, Coffigny H & Magre S (2002) Establishment of the reproductive function and transient fertility of female rats lacking primordial follicle stock after fetal gamma-irradiation. *Endocrinology* **143**: 4775-4787.

McKinley KL & Cheeseman IM (2016) The molecular basis for centromere identity and function. *Nature reviews Molecular cell biology* **17**: 16-29.

Melby TE, Ciampaglio CN, Briscoe G & Erickson HP (1998) The symmetrical structure of structural maintenance of chromosomes (SMC) and MukB proteins: long, antiparallel coiled coils, folded at a flexible hinge. *The Journal of cell biology* **142**: 1595-1604.

Merriman JA, Lane SI, Holt JE, Jennings PC, Garcia-Higuera I, Moreno S, McLaughlin EA & Jones KT (2013) Reduced chromosome cohesion measured by interkinetochore distance is associated with aneuploidy even in oocytes from young mice. *Biol Reprod* **88**: 31.

Michaelis C, Ciosk R & Nasmyth K (1997) Cohesins: chromosomal proteins that prevent premature separation of sister chromatids. *Cell* **91**: 35-45.

Miller SA, Johnson ML & Stukenberg PT (2008) Kinetochore attachments require an interaction between unstructured tails on microtubules and Ndc80(Hec1). *Current biology : CB* **18**: 1785-1791.

Monje-Casas F, Prabhu VR, Lee BH, Boselli M & Amon A (2007) Kinetochore orientation during meiosis is controlled by Aurora B and the monopolin complex. *Cell* **128**: 477-490.

Munne S & Wells D (2017) Detection of mosaicism at blastocyst stage with the use of high-resolution next-generation sequencing. *Fertil Steril* **107**: 1085-1091.

Munne S, Sandalinas M, Escudero T, Marquez C & Cohen J (2002) Chromosome mosaicism in cleavage-stage human embryos: evidence of a maternal age effect. *Reproductive biomedicine online* **4**: 223-232.

Munne S, Magli C, Adler A, Wright G, de Boer K, Mortimer D, Tucker M, Cohen J & Gianaroli L (1997) Treatment-related chromosome abnormalities in human embryos. *Hum Reprod* **12**: 780-784.

Musacchio A & Salmon ED (2007) The spindle-assembly checkpoint in space and time. *Nature reviews Molecular cell biology* **8**: 379-393.

Nagaoka SI, Hassold TJ & Hunt PA (2012) Human aneuploidy: mechanisms and new insights into an age-old problem. *Nature reviews Genetics* **13**: 493-504.

Nasmyth K (2002) Segregating sister genomes: the molecular biology of chromosome separation. *Science* **297**: 559-565.

Nasmyth K & Haering CH (2005) The structure and function of SMC and kleisin complexes. *Annual review of biochemistry* **74**: 595-648.

Nasmyth K & Haering CH (2009) Cohesin: its roles and mechanisms. *Annu Rev Genet* **43**: 525-558.

O'Shaughnessy PJ, Dudley K & Rajapaksha WR (1996) Expression of follicle stimulating hormone-receptor mRNA during gonadal development. *Molecular and cellular endocrinology* **125**: 169-175.

Oliveira RA, Coelho PA & Sunkel CE (2005) The condensin I subunit Barren/CAP-H is essential for the structural integrity of centromeric heterochromatin during mitosis. *Mol Cell Biol* **25**: 8971-8984.

Ono T, Fang Y, Spector DL & Hirano T (2004) Spatial and temporal regulation of Condensins I and II in mitotic chromosome assembly in human cells. *Mol Biol Cell* **15**: 3296-3308.

Ottolini CS, Newnham LJ, Capalbo A*, et al.* (2015) Genome-wide maps of recombination and chromosome segregation in human oocytes and embryos show selection for maternal recombination rates. *Nature genetics* **47**: 727-735.

Page SL & Hawley RS (2004) The genetics and molecular biology of the synaptonemal complex. *Annu Rev Cell Dev Biol* **20**: 525-558.

Palermo GD, Neri QV, Monahan D & Rosenwaks Z (2012) Micromanipulation: Intracytoplasmic Sperm Injection and Assisted Hatching. *In Vitro Fertilization: A Comprehensive Guide,*(Ginsburg ES & Racowsky C, eds.), p.^pp. 99-114. Springer New York, New York, NY.

Papavassiliou P, Charalsawadi C, Rafferty K & Jackson-Cook C (2015) Mosaicism for trisomy 21: a review. *Am J Med Genet A* **167a**: 26-39.

Parelho V, Hadjur S, Spivakov M*, et al.* (2008) Cohesins functionally associate with CTCF on mammalian chromosome arms. *Cell* **132**: 422-433.

Parra MT, Viera A, Gomez R, Page J, Benavente R, Santos JL, Rufas JS & Suja JA (2004) Involvement of the cohesin Rad21 and SCP3 in monopolar attachment of sister kinetochores during mouse meiosis I. *J Cell Sci* **117**: 1221-1234.

Pellestor F, Anahory T & Hamamah S (2005) The chromosomal analysis of human oocytes. An overview of established procedures. *Hum Reprod Update* **11**: 15-32.

Pellestor F, Andreo B, Arnal F, Humeau C & Demaille J (2002) Mechanisms of non-disjunction in human female meiosis: the co-existence of two modes of malsegregation evidenced by the karyotyping of 1397 in-vitro unfertilized oocytes. *Hum Reprod* **17**: 2134-2145.

Pepling ME (2006) From primordial germ cell to primordial follicle: mammalian female germ cell development. *Genesis (New York, NY : 2000)* **44**: 622-632.

Pepling ME (2013) Follicle formation and oocyte death. *Biology and Pathology of the Oocyte: Role in Fertility, Medicine and Nuclear Reprograming,*(Trounson A, Gosden R & Eichenlaub-Ritter U, eds.), p.^pp. 38-49. Cambridge University Press, Cambridge.

Pepling ME & Spradling AC (2001) Mouse ovarian germ cell cysts undergo programmed breakdown to form primordial follicles. *Dev Biol* **234**: 339-351.

Petronczki M, Matos J, Mori S, Gregan J, Bogdanova A, Schwickart M, Mechtler K, Shirahige K, Zachariae W & Nasmyth K (2006) Monopolar attachment of sister kinetochores at meiosis I requires casein kinase 1. *Cell* **126**: 1049-1064.

Pezzi N, Prieto I, Kremer L, Perez Jurado LA, Valero C, Del Mazo J, Martinez AC & Barbero JL (2000) STAG3, a novel gene encoding a protein involved in meiotic chromosome pairing and location of STAG3-related genes flanking the Williams-Beuren syndrome deletion. *Faseb j* **14**: 581-592.

Pickering SJ, Braude PR, Johnson MH, Cant A & Currie J (1990) Transient cooling to room temperature can cause irreversible disruption of the meiotic spindle in the human oocyte. *Fertil Steril* **54**: 102-108.

Polani PE & Crolla JA (1991) A test of the production line hypothesis of mammalian oogenesis. *Human genetics* **88**: 64-70.

Prieto I, Suja JA, Pezzi N, Kremer L, Martinez AC, Rufas JS & Barbero JL (2001) Mammalian STAG3 is a cohesin specific to sister chromatid arms in meiosis I. *Nat Cell Biol* **3**: 761-766.

Prieto I, Tease C, Pezzi N, Buesa JM, Ortega S, Kremer L, Martinez A, Martinez AC, Hulten MA & Barbero JL (2004) Cohesin component dynamics during meiotic prophase I in mammalian oocytes. *Chromosome Res* **12**: 197-213.

Rabitsch KP, Petronczki M, Javerzat JP, Genier S, Chwalla B, Schleiffer A, Tanaka TU & Nasmyth K (2003) Kinetochore recruitment of two nucleolar proteins is required for homolog segregation in meiosis I. *Developmental cell* **4**: 535-548.

Revenkova E & Jessberger R (2005) Keeping sister chromatids together: cohesins in meiosis. *Reproduction* **130**: 783-790.

Revenkova E, Herrmann K, Adelfalk C & Jessberger R (2010) Oocyte cohesin expression restricted to predictyate stages provides full fertility and prevents aneuploidy. *Curr Biol* **20**: 1529-1533.

Revenkova E, Eijpe M, Heyting C, Hodges CA, Hunt PA, Liebe B, Scherthan H & Jessberger R (2004) Cohesin SMC1 beta is required for meiotic chromosome dynamics, sister chromatid cohesion and DNA recombination. *Nat Cell Biol* **6**: 555-562.

Riris S, Cawood S, Gui L, Serhal P & Homer HA (2013) Immunofluorescence staining of spindles, chromosomes, and kinetochores in human oocytes. *Methods Mol Biol* **957**: 179-187.

Roberts R, Iatropoulou A, Ciantar D, Stark J, Becker DL, Franks S & Hardy K (2005) Follicle-stimulating hormone affects metaphase I chromosome alignment and increases aneuploidy in mouse oocytes matured in vitro. *Biol Reprod* **72**: 107-118.

Rowsey R, Gruhn J, Broman KW, Hunt PA & Hassold T (2014) Examining variation in recombination levels in the human female: a test of the production-line hypothesis. *American journal of human genetics* **95**: 108-112.

Sakakibara Y, Hashimoto S, Nakaoka Y, Kouznetsova A, Hoog C & Kitajima TS (2015) Bivalent separation into univalents precedes age-related meiosis I errors in oocytes. *Nature communications* **6**: 7550.

Santos MA, Kuijk EW & Macklon NS (2010) The impact of ovarian stimulation for IVF on the developing embryo. *Reproduction* **139**: 23-34.

Sarangapani KK, Duro E, Deng Y*, et al.* (2014) Sister kinetochores are mechanically fused during meiosis I in yeast. *Science* **346**: 248-251.

Schalch T & Steiner FA (2017) Structure of centromere chromatin: from nucleosome to chromosomal architecture. *Chromosoma* **126**: 443-455.

Schuh M & Ellenberg J (2007) Self-organization of MTOCs replaces centrosome function during acentrosomal spindle assembly in live mouse oocytes. *Cell* **130**: 484-498.

Schwacha A & Kleckner N (1995) Identification of double Holliday junctions as intermediates in meiotic recombination. *Cell* **83**: 783-791.

Shintomi K & Hirano T (2007) How are cohesin rings opened and closed? *Trends in biochemical sciences* **32**: 154-157.

Shomper M, Lappa C & FitzHarris G (2014) Kinetochore microtubule establishment is defective in oocytes from aged mice. *Cell Cycle* **13**: 1171-1179.

Skibbens RV, Skeen VP & Salmon ED (1993) Directional instability of kinetochore motility during chromosome congression and segregation in mitotic newt lung cells: a push-pull mechanism. *The Journal of cell biology* **122**: 859-875.

Smith CA, McAinsh AD & Burroughs NJ (2016) Human kinetochores are swivel joints that mediate microtubule attachments. *Elife* **5**.

Steptoe PC & Edwards RG (1978) Birth after the reimplantation of a human embryo. *Lancet (London, England)* **2**: 366.

Strunnikov AV, Larionov VL & Koshland D (1993) SMC1: an essential yeast gene encoding a putative head-rod-tail protein is required for nuclear division and defines a new ubiquitous protein family. *The Journal of cell biology* **123**: 1635-1648.

Sullivan BA & Karpen GH (2004) Centromeric chromatin exhibits a histone modification pattern that is distinct from both euchromatin and heterochromatin. *Nature structural & molecular biology* **11**: 1076-1083.

Suzuki A, Badger BL, Wan X, DeLuca JG & Salmon ED (2014) The architecture of CCAN proteins creates a structural integrity to resist spindle forces and achieve proper Intrakinetochore stretch. *Developmental cell* **30**: 717-730.

Suzuki H, Kanai-Azuma M & Kanai Y (2015) From Sex Determination to Initial Folliculogenesis in Mammalian Ovaries: Morphogenetic Waves along the Anteroposterior and Dorsoventral Axes. *Sexual development : genetics, molecular biology, evolution, endocrinology, embryology, and pathology of sex determination and differentiation* **9**: 190-204.

Tachibana-Konwalski K, Godwin J, Borsos M, Rattani A, Adams DJ & Nasmyth K (2013) Spindle assembly checkpoint of oocytes depends on a kinetochore structure determined by cohesin in meiosis I. *Curr Biol* **23**: 2534-2539.

Tachibana-Konwalski K, Godwin J, van der Weyden L, Champion L, Kudo NR, Adams DJ & Nasmyth K (2010) Rec8-containing cohesin maintains bivalents without turnover during the growing phase of mouse oocytes. *Genes Dev* **24**: 2505-2516.

Tanaka K, Chang HL, Kagami A & Watanabe Y (2009) CENP-C functions as a scaffold for effectors with essential kinetochore functions in mitosis and meiosis. *Developmental cell* **17**: 334-343.

Tarlatzis BC, Fauser BC, Kolibianakis EM, Diedrich K, Rombauts L & Devroey P (2006) GnRH antagonists in ovarian stimulation for IVF. *Hum Reprod Update* **12**: 333-340.

Tease C, Hartshorne GM & Hulten MA (2002) Patterns of meiotic recombination in human fetal oocytes. *American journal of human genetics* **70**: 1469-1479.

Toth A, Ciosk R, Uhlmann F, Galova M, Schleiffer A & Nasmyth K (1999) Yeast cohesin complex requires a conserved protein, Eco1p(Ctf7), to establish cohesion between sister chromatids during DNA replication. *Genes Dev* **13**: 320-333.

Toth A, Rabitsch KP, Galova M, Schleiffer A, Buonomo SB & Nasmyth K (2000) Functional genomics identifies monopolin: a kinetochore protein required for segregation of homologs during meiosis i. *Cell* **103**: 1155-1168.

Touati SA, Buffin E, Cladiere D, Hached K, Rachez C, van Deursen JM & Wassmann K (2015) Mouse oocytes depend on BubR1 for proper chromosome segregation but not for prophase I arrest. *Nature communications* **6**: 6946.

Treff NR, Northrop LE, Kasabwala K, Su J, Levy B & Scott RT, Jr. (2011) Single nucleotide polymorphism microarray-based concurrent screening of 24-chromosome aneuploidy and unbalanced translocations in preimplantation human embryos. *Fertil Steril* **95**: 1606-1612.e1601-1602.

Tsutsumi M, Fujiwara R, Nishizawa H, Ito M, Kogo H, Inagaki H, Ohye T, Kato T, Fujii T & Kurahashi H (2014) Age-related decrease of meiotic cohesins in human oocytes. *PLoS One* **9**: e96710.

Uhlmann F (2016) SMC complexes: from DNA to chromosomes. *Nature reviews Molecular cell biology* **17**: 399-412.

Verdaasdonk JS & Bloom K (2011) Centromeres: unique chromatin structures that drive chromosome segregation. *Nature reviews Molecular cell biology* **12**: 320-332.

Verlinsky Y, Cieslak J, Ivakhnenko V*, et al.* (2001) Chromosomal abnormalities in the first and second polar body. *Molecular and cellular endocrinology* **183 Suppl 1**: S47-49.

Voullaire L, Slater H, Williamson R & Wilton L (2000) Chromosome analysis of blastomeres from human embryos by using comparative genomic hybridization. *Human genetics* **106**: 210-217.

Wan X, O'Quinn RP, Pierce HL*, et al.* (2009) Protein architecture of the human kinetochore microtubule attachment site. *Cell* **137**: 672-684.

Wang C, Zhou B & Xia G (2017) Mechanisms controlling germline cyst breakdown and primordial follicle formation. *Cellular and molecular life sciences : CMLS* **74**: 2547-2566.

Watanabe Y & Nurse P (1999) Cohesin Rec8 is required for reductional chromosome segregation at meiosis. *Nature* **400**: 461-464.

Watanabe Y & Kitajima TS (2005) Shugoshin protects cohesin complexes at centromeres. *Philos Trans R Soc Lond B Biol Sci* **360**: 515-521, discussion 521.

Weber SA, Gerton JL, Polancic JE, DeRisi JL, Koshland D & Megee PC (2004) The kinetochore is an enhancer of pericentric cohesin binding. *PLoS Biol* **2**: E260.

Wells D, Escudero T, Levy B, Hirschhorn K, Delhanty JD & Munne S (2002) First clinical application of comparative genomic hybridization and polar body testing for preimplantation genetic diagnosis of aneuploidy. *Fertil Steril* **78**: 543-549.

Wilton L, Voullaire L, Sargeant P, Williamson R & McBain J (2003) Preimplantation aneuploidy screening using comparative genomic hybridization or fluorescence in situ hybridization of embryos from patients with recurrent implantation failure. *Fertil Steril* **80**: 860-868.

Winey M, Morgan GP, Straight PD, Giddings TH, Jr. & Mastronarde DN (2005) Three-dimensional ultrastructure of Saccharomyces cerevisiae meiotic spindles. *Mol Biol Cell* **16**: 1178-1188.

Winters T, McNicoll F & Jessberger R (2014) Meiotic cohesin STAG3 is required for chromosome axis formation and sister chromatid cohesion. *EMBO J* **33**: 1256-1270.

Wood AJ, Severson AF & Meyer BJ (2010) Condensin and cohesin complexity: the expanding repertoire of functions. *Nature reviews Genetics* **11**: 391-404.

Yokobayashi S & Watanabe Y (2005) The kinetochore protein Moa1 enables cohesion-mediated monopolar attachment at meiosis I. *Cell* **123**: 803-817.

Yoon PW, Freeman SB, Sherman SL, Taft LF, Gu Y, Pettay D, Flanders WD, Khoury MJ & Hassold TJ (1996) Advanced maternal age and the risk of Down syndrome characterized by the meiotic stage of chromosomal error: a population-based study. *American journal of human genetics* **58**: 628-633.

Yoshida S, Kaido M & Kitajima TS (2015) Inherent Instability of Correct Kinetochore-Microtubule Attachments during Meiosis I in Oocytes. *Developmental cell* **33**: 589-602.

Zaragoza MV, Jacobs PA, James RS, Rogan P, Sherman S & Hassold T (1994) Nondisjunction of human acrocentric chromosomes: studies of 432 trisomic fetuses and liveborns. *Human genetics* **94**: 411-417.

Zielinska AP, Holubcova Z, Blayney M, Elder K & Schuh M (2015) Sister kinetochore splitting and precocious disintegration of bivalents could explain the maternal age effect. *Elife* **4**: e11389.

Appendix A. Establishing a live-cell imaging platform for studying human oocytes

A1. Introduction

In addition to fixed-cell data, I aimed to acquire information from live oocytes by imaging them as they progressed through the first and second meiotic divisions. Through live-cell imaging, it would be possible to answer many questions that fixed cell analysis cannot. In particular, I wanted to investigate whether oocytes with separated sister kinetochores were able to divide normally and whether an increased separation distance made oocytes more prone to errors at cytokinesis. Described here are initial attempts to establish a live cell imaging platform for human eggs.

Live-cell imaging in human oocytes presents several technical challenges. Firstly, there is the limited availability of the material and its acquisition which is highly dependent on clinical variables. Secondly, human oocytes are highly sensitive to small changes in temperature and pH (Pickering *et al.*, 1990, Dale *et al.*, 1998). Nonetheless, Holubcova et al. were able to establish the first platform for live-cell imaging in human oocytes using mRNA microinjection to visualise chromosomes and microtubules (Holubcova *et al.*, 2015). I aimed to use a similar approach to further study kinetochore organisation and behaviour during meiosis. A particular goal was to establish a method of studying oocytes that would enable high-resolution visualisation of the kinetochores during MI, so that we could study their behaviour during this error-prone division.

A2. Methods

A2.1. Molecular Biology

A.2.1.1. Plasmids

The following plasmids were used in in this project:

Table A2.1. Plasmids

Plasmid name	Encoded protein	Resistance marker	Source	Use
pGEMHE-H2B-mRGFP	Histone 2B	Ampicillin	Schuh & Ellenberg, 2007	Microinjection
pGEMHE-Mad2-mEGFP	Mad2	Ampicillin	Kitajima et al., 2007	Plasmid production
Ndc80-mCherry	Ndc80	Kanamycin	Smith et al., 2016	Plasmid production
Ndc80-mEGFP	Ndc80	Ampicillin	This work	Microinjection

A2.1.2. Production of Ndc80-EGFP construct

An Ndc80-EGFP construct was prepared using PCR-based molecular cloning. A Mad2-EGFP plasmid construct was used as the vector plasmid and an Ndc80-tagRFP plasmid (McAinsh lab) for the Ndc80 insert. Mad2-EGFP was digested using NcoI and NheI. The Ndc80 sequence was isolated using PCR (conditions in **Table A2.2**) with forward and reverse primers incorporating the restriction enzyme sites and targeted to the start of Ndc80 and the end of the linker region respectively (see **Table A2.3**). The final product was purified using a gel extraction kit (Qiagen). For ligation, the concentration of the insert and vector were estimated in Nanodrop. A 3:1 ratio of vector to insert was used. Ligation was undertaken for 45 min at room temperature. Following ligation, the total volume of the ligation mix was added to DH5-α competent cells. These were plated onto ampicillin plates and left overnight at 37ºC. A miniprep

procedure was used to isolate plasmids. The final plasmid construct was confirmed by sequencing (SourceBioscience; see **Table A2.4**).

Table A2.2. PCR conditions (30 cycles)

	Temp (°C)	Time
Initial denaturation	98	30 s
Denaturation	98	10 s
Annealing	65	30 s
Extension	72	1 min
Final extension	72	5 min
Hold	4	

Table A2.3. Primers used for PCR of Ndc80 insert

Primer	**Sequence**
Forward	gatccgctagcatgaagcgcagttcagtttc NheI site
Reverse	cagacccatggatcccgggtggaacagaa NcoI site

Table A2.4. Primers for sequencing

Primer	**Sequence (5' to 3')**	**Source**
EGFP Nrev	cgtcgccgtccagctcgaccag	SourceBioscience (stock)
T7 promoter	taatacgactcactataggg	SourceBioscience (stock)
Ndc80 forward	atccgctagcatgaagcgcagttcagt	Smith et al., 2016
Ndc80 reverse	ggatcccgggtggaacagaacttccag	Smith et al., 2016

A2.1.3. Production of messenger RNA

A T7 MMESSAGE kit (Ambion) was used to transcribe mRNA from plasmids. The resulting mRNA was purified using a RNA elution kit (Qiagen) which excludes unincorporated nucleotides. Electrophoresis was used to determine the size and purity of the final product. For RNA electrophoresis, a 1% gel was

prepared using RNase-free agarose (Seakem). Approximately 0.5 µg of mRNA was mixed with 2X loading buffer containing foramide (Ambion). Prior to running on the gel, the mRNA and loading buffer were incubated for 10 min at 70ºC. The mRNA was then run at 120 mV for 20 min alongside an 0.5–10 kb RNA ladder (Invitrogen) which had undergone the same pre-treatment steps as the mRNA. The concentration of mRNA was estimated in Nanodrop 2000.

A2.2. Human oocytes

A2.2.1. Microinjection of human oocytes

Following collection (as described in main Methods section), oocytes were transferred into pre-equilibriated G-MOPS (Vitrolife) media with 5% human serum albumin (Vitrolife). They were transported from the IVF clinic at University Hospitals Coventry & Warwickshire to the Centre for Mechanochemical Cell Biology, University of Warwick, in a 37ºC transport incubator, where they were moved into fresh media and placed in a 37ºC incubator with 5% CO_2. Oocytes were microinjected on a heated stage using a clinical standard microinjector equipped with injection and holding pipettes (The Pipette Company, Australia). Between 15–20 pl of 1 µg/µl mRNA was injected into each oocyte. Following mRNA injection, oocytes were incubated for at least 4 hours following micro-injection. For imaging, oocytes were placed in a ~50 µl drop of media overlaid with sterile mineral oil. In total, 11 GV oocytes (acquired on the day of collection from the patient) and 36 MII oocytes (acquired on the day following collection) were used.

A2.2.2. SiR-DNA treatment

Following microinjection and prior to imaging, oocytes were moved into G-MOPS containing 2 µg/µl SiR-DNA (Spirochrome), a cell-permeable DNA probe, and the efflux pump inhibitor verapamil (1 µg/µl). Incubation times of 30 min, 1 hour and 2 hours were tested. As there were no differences between the

oocytes treated for 30 min compared to those treated for longer periods, an incubation time of 30 min was used for subsequent treatments.

A2.2.3. Imaging

Initial imaging was performed on a Zeiss LSM 510 fluorescent confocal microscope using a 63x oil immersion objective. Live-cell imaging was performed on a Deltavision microscope (Applied Precision, LLC) with a 60x 1.4 NA oil immersion objective. For overnight time-lapse, 11 z-sections spaced 2 µm apart were taken every 15 min over 11 hours.

A3. Preliminary Results

Initial imaging of oocytes micro-injected with mRNA encoding H2B-mRFP and Ndc80-EGFP revealed fluorescent patches in all oocytes, including ones that had not been injected with mRNA. These were visible when imaging at 488 and 561 wavelengths, suggesting that the patches were auto-fluorescent (**Figure A1**). These patches are likely to correspond to lipofuscin bodies. Lipofuscin bodies (>5 μm) have been observed previously in live oocytes and embryos of all stages and do not appear to be associated with cell death or maternal age, however larger lipofuscin bodies (>5 μm) have been associated with reduced IVF fertilisation rates (Otsuki *et al.*, 2007).

In one micro-injected GV-stage oocyte we observed fluorescent structures in the 561 (red) channel, but not under the 488 wavelength, indicating that these were not lipofuscin bodies, and that mRNA encoding H2B-mRFP had been translated and incorporated (**Figure A2**). During overnight time-lapse imaging, the fluorescent structure did not move, which may indicate oocyte cell death.

SiR (silicon–rhodamine) DNA, a cell-permeable marker of DNA that displays minimal toxicity and is compatible with high-resolution live-cell imaging (Lukinavicius *et al.*, 2015), was also used to stain oocytes The SiR-DNA was tested by incubating oocytes for 30 minutes, or 1, 2 or 3 hours in media containing SiR-DNA prior to imaging and after mRNA microinjection. In one GV oocyte, it was possible to see fluorescent structures that may have corresponded to DNA (**Figure A3**). However, as before, these structures did not move or display any dynamic behaviour during overnight imaging of this oocyte. In all cases in which the SiR-DNA was utilised in oocytes donated from IVF cycles, it was possible to see chromatin from the sperm with which the oocytes had been previously incubated, indicating that the SiR-DNA treatment was working, however oocyte chromosomes were not visible. To visualise the stain, we also incubated oocytes with verapamil, an efflux pump inhibitor that can improve the SiR-DNA signal, however this did not enable visualisation of oocyte chromosomes.

Figure A1

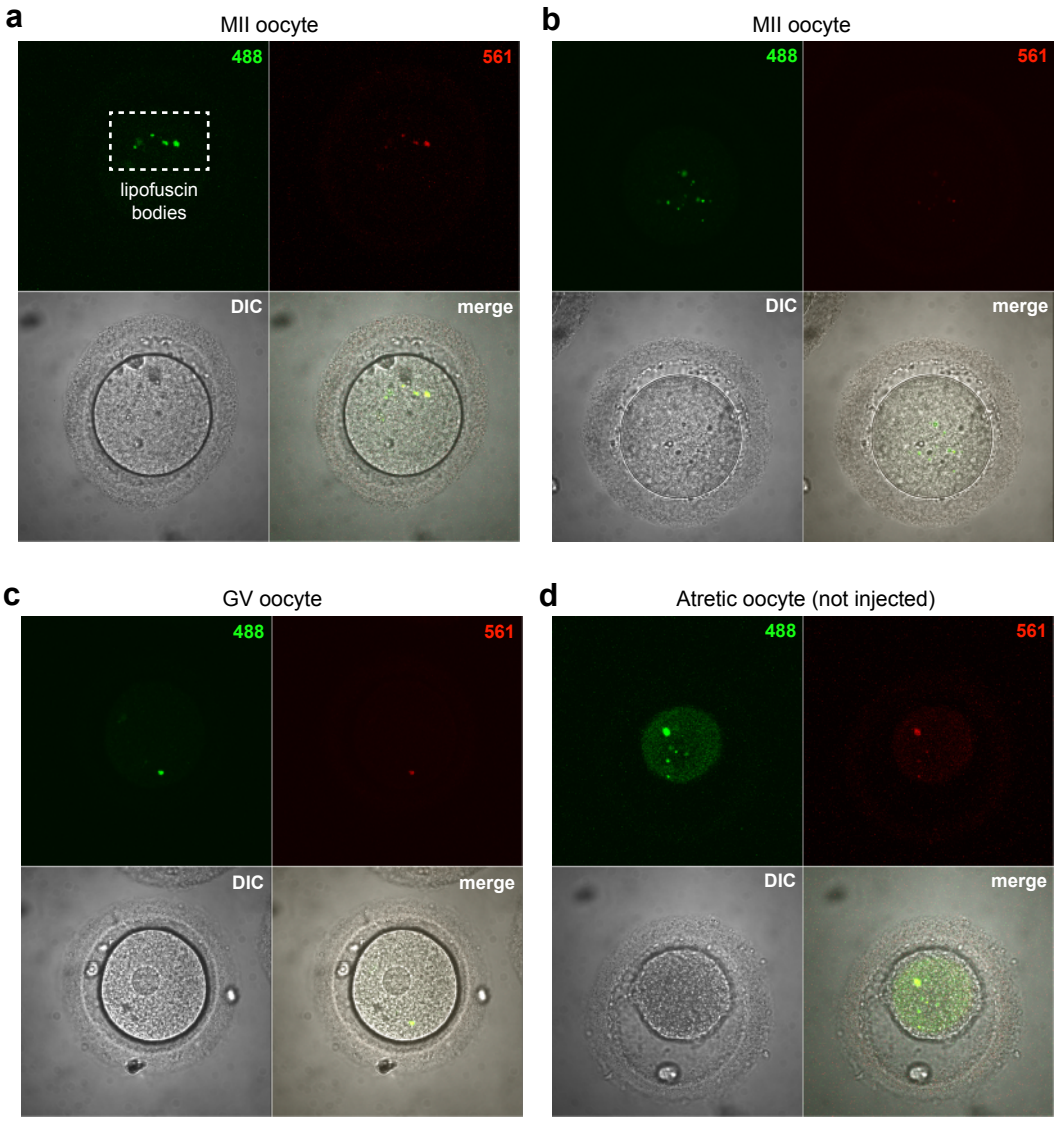

Figure A1. Auto-fluorescent lipofuscin bodies in oocytes. Oocytes imaged on a Zeiss LSM 510. (a–c) Oocytes injected with mRNA encoding H2B-mRFP and Ndc80-EGFP. (d) Atretic oocyte which was not injected, also showing the presence of lipofuscin bodies.

Figure A2

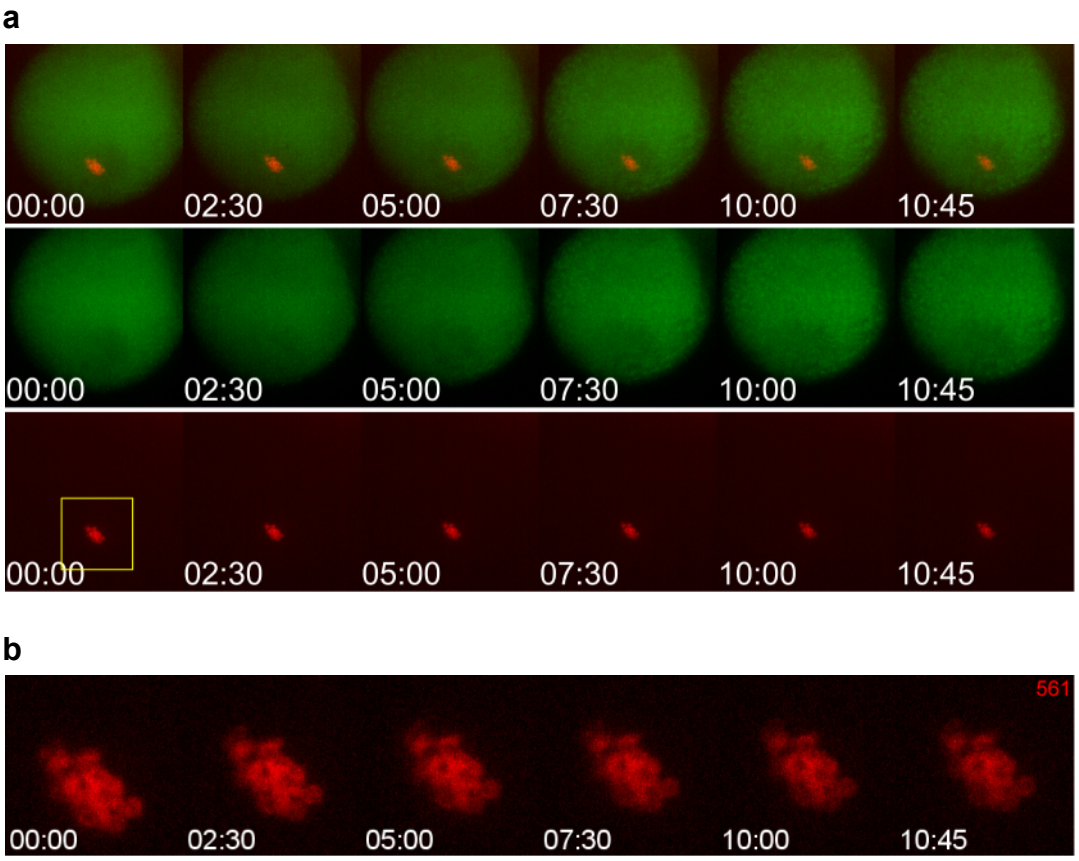

Figure A2. Timelapse of a germinal vesicle (GV) stage oocyte microinjected with messenger RNA encoding H2B-mRFP and Ndc80-EGFP. (a) The presence of fluorescence in the 561 channel indicates that the mRNA encoding H2B-mRFP was translated. There is no fluorescence in the 488 channel, indicating that this is unlikely to be auto-fluorescence. (b) Enlarged view of the fluorescent structure in the 561 channel. Time is given in hours and minutes. Images were acquired every 15 min over a period of 11 hours.

Figure A3

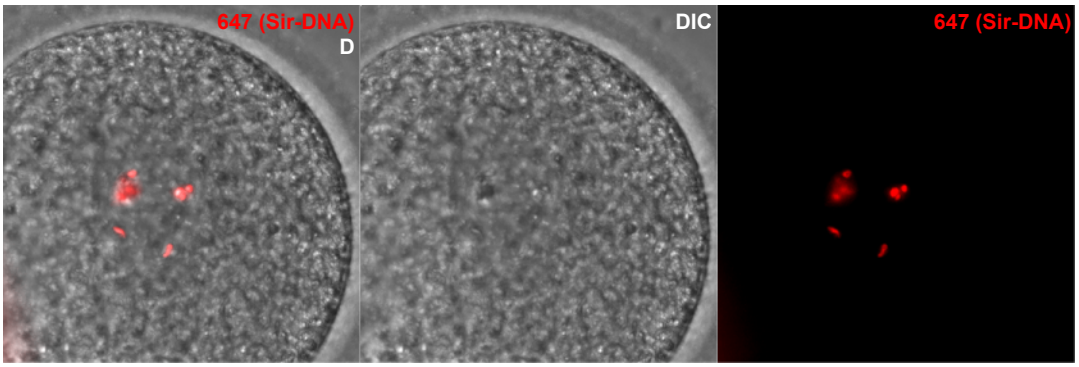

Figure A3. Oocyte stained with SiR-DNA, a cell-permeable live-cell DNA stain that contains a far-red fluorogenic marker. This germinal vesicle (GV) stage oocyte was incubated with SiR-DNA for 30 mins, after which far-red fluorescent structures could be seen within the GV that are likely to correspond to oocyte DNA. The structures did not move after overnight imaging, indicating possible cell death.

A4. Discussion

The experiments described here detail efforts to establish high-resolution imaging in oocytes. In the majority of cases, it was not possible to visualise chromosomes in the oocytes. The nature of the experiments required oocytes to be briefly in environments in which temperature and CO_2 levels could not be strictly controlled, e.g. during microinjection and during oocyte transfer into different solutions. As numerous studies have reported, exposure of oocytes to room temperature for short periods of time (between 10–30 minutes) can cause meiotic spindle disruption and chromosome scattering from which few oocytes can recover (Pickering *et al.*, 1990, Wang *et al.*, 2001). It is therefore possible that oocytes had undergone spindle disruption which may have disturbed the chromosomes and prevented incorporation of proteins translated from mRNA.

Another factor that is likely to have impacted the methods is the quality and availability of the material. For live-cell imaging, GV oocytes that can be donated to research on the day of collection from the patient are the optimal material, however these samples are limited and just account for approximately one fifth of the oocytes used for this work (see Methods for details). The remainder were MII oocytes that became available to research on the day following collection, after overnight incubation.

Although use of the SiR-DNA stain enabled visualisation of sperm chromosomes, in no oocytes could we see oocyte chromosomes. It is possible that oocyte chromosomes were not visible when using SiR-DNA due to inability of the stain to reach the chromosomes. Unlike in spermatozoa, in oocytes the stain must penetrate through the zona pellucida and a vast amount of cytoplasmic material to reach the chromosomes. It is likely that further optimisation when using this stain in human oocytes is required.

References

Dale B, Menezo Y, Cohen J, DiMatteo L & Wilding M (1998) Intracellular pH regulation in the human oocyte. *Hum Reprod* **13**: 964-970.

Holubcova Z, Blayney M, Elder K & Schuh M (2015) Human oocytes. Error-prone chromosome-mediated spindle assembly favors chromosome segregation defects in human oocytes. *Science* **348**: 1143-1147.

Lukinavicius G, Blaukopf C, Pershagen E*, et al.* (2015) SiR-Hoechst is a far-red DNA stain for live-cell nanoscopy. *Nature communications* **6**: 8497.

Otsuki J, Nagai Y & Chiba K (2007) Lipofuscin bodies in human oocytes as an indicator of oocyte quality. *J Assist Reprod Genet* **24**: 263-270.

Pickering SJ, Braude PR, Johnson MH, Cant A & Currie J (1990) Transient cooling to room temperature can cause irreversible disruption of the meiotic spindle in the human oocyte. *Fertil Steril* **54**: 102-108.

Wang WH, Meng L, Hackett RJ, Odenbourg R & Keefe DL (2001) Limited recovery of meiotic spindles in living human oocytes after cooling-rewarming observed using polarized light microscopy. *Hum Reprod* **16**: 2374-2378.

Appendix B. Publication in Biology Open

Patel J, Tan SL, Hartshorne GM, McAinsh AD. Unique geometry of sister kinetochores in human oocytes during meiosis I may explain maternal age-associated increases in chromosomal abnormalities. Biol Open. 2015; 5(2): 178-84. doi: 10.1242/bio.016394.

© 2016. Published by The Company of Biologists Ltd | Biology Open (2016) 5, 178-184 doi:10.1242/bio.016394

RESEARCH ARTICLE

Unique geometry of sister kinetochores in human oocytes during meiosis I may explain maternal age-associated increases in chromosomal abnormalities

Jessica Patel[1], Seang Lin Tan[2], Geraldine M. Hartshorne[1,3] and Andrew D. McAinsh[4,*]

ABSTRACT

The first meiotic division in human oocytes is highly error-prone and contributes to the uniquely high incidence of aneuploidy observed in human pregnancies. A successful meiosis I (MI) division entails separation of homologous chromosome pairs and co-segregation of sister chromatids. For this to happen, sister kinetochores must form attachments to spindle kinetochore-fibres emanating from the same pole. In mouse and budding yeast, sister kinetochores remain closely associated with each other during MI, enabling them to act as a single unified structure. However, whether this arrangement also applies in human meiosis I oocytes was unclear. In this study, we perform high-resolution imaging of over 1900 kinetochores in human oocytes, to examine the geometry and architecture of the human meiotic kinetochore. We reveal that sister kinetochores in MI are not physically fused, and instead individual kinetochores within a pair are capable of forming independent attachments to spindle k-fibres. Notably, with increasing female age, the separation between kinetochores increases, suggesting a degradation of centromeric cohesion and/or changes in kinetochore architecture. Our data suggest that the differential arrangement of sister kinetochores and dual k-fibre attachments may explain the high proportion of unstable attachments that form in MI and thus indicate why human oocytes are prone to aneuploidy, particularly with increasing maternal age.

KEY WORDS: Aneuploidy, Chromosome segregation, Human, Kinetochore, Meiosis, Oocyte

INTRODUCTION

The chances of a chromosomally abnormal pregnancy increase dramatically in humans with advancing maternal age (Nagaoka et al., 2012). Most meiosis-derived aneuploidies in early embryos originate from the first meiotic division of the oocyte, which is particularly error-prone (Hassold and Hunt, 2001). During the first meiotic division, sister chromatids segregate together, which requires kinetochores on sister chromatids to form attachments to spindle kinetochore-fibres (k-fibres) from the same pole of the spindle. This is in contrast to mitosis and meiosis II (MII), in which sisters form attachments to opposite spindle poles. In meiosis I (MI), therefore, it follows that the arrangement of sister kinetochores will be different; a side-by-side rather than the usual 'back-to-back' arrangement is likely (Watanabe, 2012). Of the meiotic sister kinetochores that have been studied so far, in maize, yeast and mouse, all appear to be in close association with each other, appearing as a single coherent unit. In maize and yeast, there is evidence that sisters are physically tethered: in maize, a Mis12-Ndc80 bridge links sisters (Li and Dawe, 2009); and in budding yeast, the monopolin complex performs a similar cross-linking role (Corbett et al., 2010; Sarangapani et al., 2014). In mouse oocytes, the meiotic regulator protein Meikin is important for keeping sister kinetochores together; loss of Meikin results in separation of sister kinetochores from a single unit into two distinct foci (Kim et al., 2015). A similar effect occurs in oocytes of aged mice, which is likely to reflect a loss of centromeric cohesin (Chiang et al., 2010). In human oocytes, the structure of the meiotic kinetochore is largely unknown with an initial study suggesting that inter-sister distances may increase in aged human oocytes (Sakakibara et al., 2015). It possible that an altered kinetochore geometry contributes to the features of human MI that differ from other species including the much higher incidence of aneuploidy and the protracted spindle assembly period (Holubcova et al., 2015).

RESULTS

To investigate the geometry of sister kinetochores in MI, we examined sister kinetochore pairs in MI oocytes from women undergoing assisted reproduction following ovarian stimulation (Table S1). Our knowledge of mammalian meiosis is mostly based on mouse oocytes, because immature human oocytes available for research are typically only those that are not suitable for use in the donating patient's fertility treatment. However, it has been shown that the majority of clinically discarded immature human oocytes are able to undergo anaphase and exhibit consistent patterns of spindle assembly and chromosome segregation (Holubcova et al., 2015), highlighting their usefulness as tools for understanding human female meiosis. We therefore used human oocytes that had not yet completed the first meiotic division, confirmed by the absence of a polar body (Fig. 1A). Oocytes were fixed in paraformaldehyde and immunofluorescence was performed with CREST antisera to mark the centromere/inner kinetochore and DAPI to visualise chromosomes. High-resolution 3D image stacks (250×50 nm *z*-sections) of the meiotic chromosomes and kinetochores were collected using spinning-disk confocal microscopy. The number of CREST foci within these oocytes was considerably higher than 46, the number of kinetochores expected in a euploid MI oocyte in which all sister kinetochores are fused. This therefore raised the possibility that sister kinetochores are not fused. To investigate this, we marked sister kinetochore pairs in 3D

[1]Warwick Medical School, University of Warwick, Coventry CV4 7AL, UK. [2]Department of Obstetrics and Gynecology, McGill University, Montreal, Quebec H3A 1A1, Canada. [3]University Hospitals Coventry and Warwickshire NHS Trust, Coventry CV2 2DX, UK. [4]Centre for Mechanochemical Cell Biology, Warwick Medical School, University of Warwick, Coventry CV4 7AL, UK.

*Author for correspondence (a.d.mcainsh@warwick.ac.uk)

Received 3 December 2015; Accepted 22 December 2015

Biology Open (2016) 5, 178-184 doi:10.1242/bio.016394

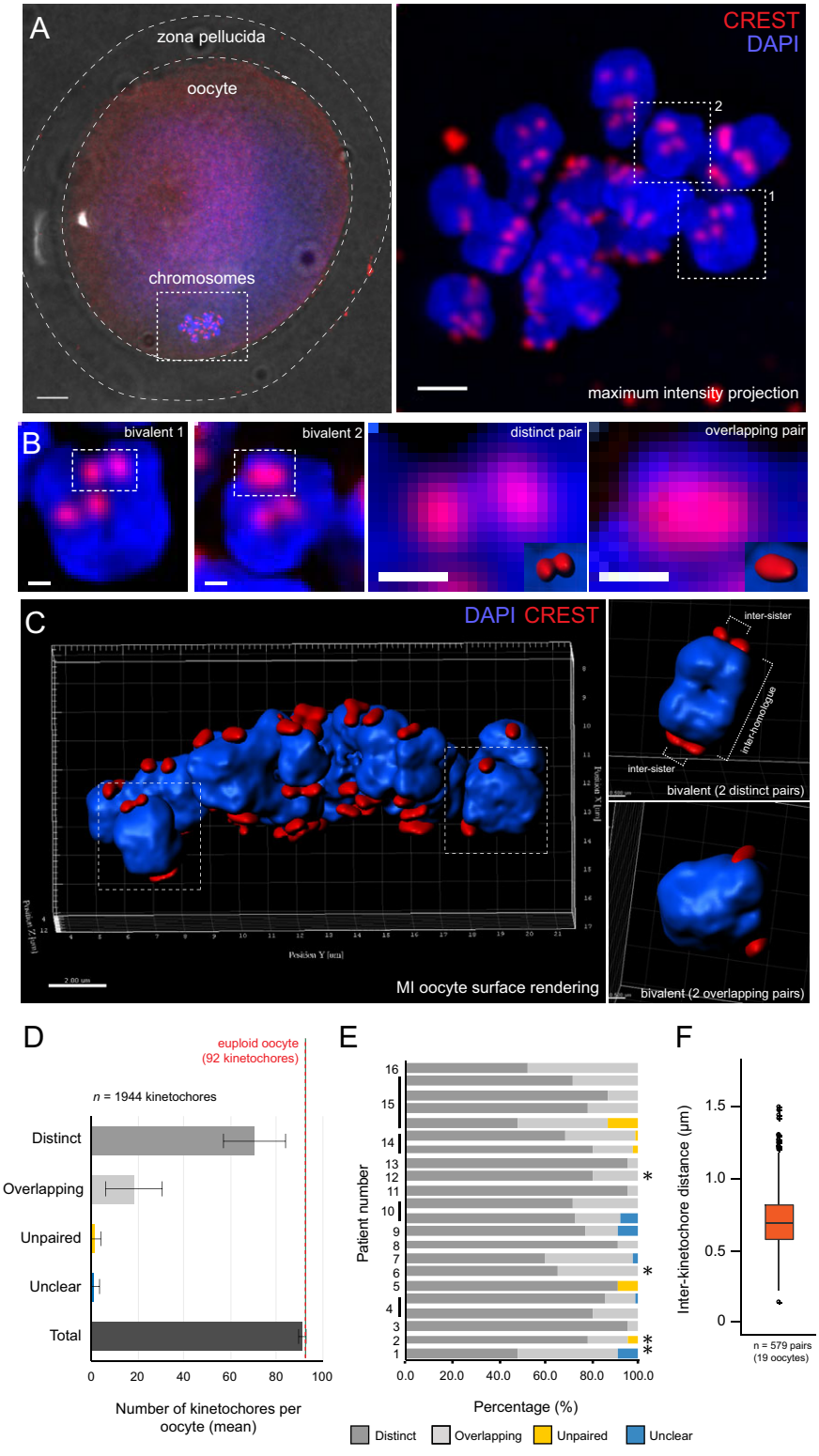

Fig. 1. Sister kinetochores in meiosis I (MI) human oocytes are not fused. (A) Left panel: fixed human oocyte in MI. Dotted lines mark zona pellucida, oocyte and chromosomes (60× objective; scale bar=5 µm). Right panel: maximum intensity projection of the meiotic chromosomes within this same oocyte (100× objective; scale bar=2 µm). (B) Enlarged bivalents outlined in A, right panel, in which two kinetochore pairs per bivalent can be seen. Further enlargements of representative examples of distinct and overlapping sister kinetochore pairs are shown. Scale bars=0.5 µm. (C) 3D reconstruction of the kinetochores and chromosomes in an MI oocyte by surface rendering. To the right are two examples of individual bivalents showing the two categories of kinetochore pairs. (D) Mean±s.d. number of kinetochores within each oocyte, classified according to whether kinetochores were within distinct or overlapping pairs (*n*=1944 kinetochores from 22 oocytes). For a small number of kinetochores, sister kinetochores were so far apart (>1.5 µm) that they were classified as 'unpaired'. A small number of foci could not be reliably identified as being either single kinetochores or overlapping pairs and these were classified as 'unclear'. (E) Proportion of distinct and overlapping pairs for each individual oocyte. Asterisks indicate oocytes from women with no known fertility issues. (F) Inter-kinetochore distance as measured from the CREST signal (*n*=579 sister kinetochore pairs from 19 oocytes). Box plot represents interquartile range (IQR); whiskers extend to most extreme value within 1.5×IQR.

image stacks, then classified these pairs on the basis of whether they appeared as 'distinct' pairs (two distinct spots) or 'overlapping' pairs (a single spot) (Fig. 1B). To confirm identity of pairs, we used surface rendering in three dimensions, which made it possible to identify individual bivalents associated with two sister kinetochore pairs (Fig. 1C). Classification was performed using *z*-projection images incorporating 20 *z*-sections (1.0 µm) centred about marked pairs (Fig. S1).

The majority (78%) of sister kinetochore pairs were identified as being distinct, with an average of 35 (range: 22–44) distinct pairs per oocyte (*n*=22 oocytes, Fig. 1D). A euploid oocyte has 46 kinetochore pairs in total, so distinct pairs account for the majority of kinetochore pairs in the population of oocytes we studied. The remaining 22% of sister kinetochore pairs were classified as overlapping, with an average of 10 (range: 0–22) overlapping pairs per oocyte. There were no differences in oocytes from women

Biology Open (2016) 5, 178-184 doi:10.1242/bio.016394

with no known fertility issues, i.e. couples with male factor infertility (marked with asterisks in Fig. 1E; see also Table S1), indicating that these observations are unlikely to result from infertility issues. To quantify the degree of separation, we used CREST signals to measure the inter-kinetochore distance between distinct sister pairs (see Fig. 1C, upper right panel). Distances were measured in 3D using the peak intensity of the kinetochore signal to mark individual kinetochore positions. The median inter-kinetochore distance was 0.69±0.21 µm (median±s.d.; n=579 pairs from 19 oocytes; Fig. 1F).

The kinetochore is a large multi-subunit structure, consisting of an inner plate, outer plate and fibrous corona (Chan et al., 2005). A possible arrangement for human meiotic sister kinetochores may involve distinct inner plates (as we observed through CREST staining) but fused outer plates, an architecture observed in maize MI (Li and Dawe, 2009). As the outer plate is involved in formation of stable k-fibre attachments (Sundin et al., 2011), this model would enable sisters to form a single k-fibre attachment between them to ensure co-segregation. To test whether this model applies in humans, we used immunofluorescence to label the inner plate/centromere (CREST), outer plate (Bub1) and the fibrous corona (CENP-E) in oocytes (Wan et al., 2009; Earnshaw, 2015). Strikingly, the outer kinetochore markers also appeared separated in MI sister kinetochore pairs (Fig. 2A), demonstrating that the entire kinetochore structure is distinct. By fixing whole intact oocytes, it was also possible visualise the side-by-side arrangement of sister kinetochores, and show that the inner kinetochore (CREST) is located towards the centromeric chromatin, with the outer kinetochore (CENP-E) facing outwards (Fig. 2B,C). This indicates that the overall kinetochore architecture appears to be similar to that found in mitosis. Together, this data indicates that human MI sister kinetochores do not appear to be fused.

One possibility is that in human MI, only one sister kinetochore is active and the other is shut off. To test this, we examined kinetochore-microtubule attachments in oocytes subjected to cold-shock treatment, which destabilises microtubules that are not attached to kinetochores in an end-on configuration. In a small number of cases (n=5 sister kinetochore pairs from three oocytes), we observed pairs in which one kinetochore was attached to a k-fibre but its sister was not. However, more frequently, we noted the presence of kinetochore pairs with dual k-fibre attachments (n=20), in which each sister within the pair was attached to a distinct k-fibre (Fig. 3). These attachments were observed in both distinct (18/20) and overlapping (2/20) kinetochore pairs, thereby providing evidence that homologous chromosomes can connect to the meiotic spindle via two independent attachment sites.

During the first meiotic division, unlike in mitosis, cohesin is protected between sister kinetochores to ensure co-segregation (Kitajima et al., 2004). Cohesin loss over time has been the focus of many studies investigating maternal age-related aneuploidy (Jessberger, 2012). Therefore, we tested whether the high proportion of distinct pairs that we observed was associated with patient age. We found that there was no significant correlation between age and proportion of distinct pairs in our sample (Fig. 4A), although in the two youngest patients (26 and 27 years) just over 50% were separated, suggesting there may be a mild age-related effect.

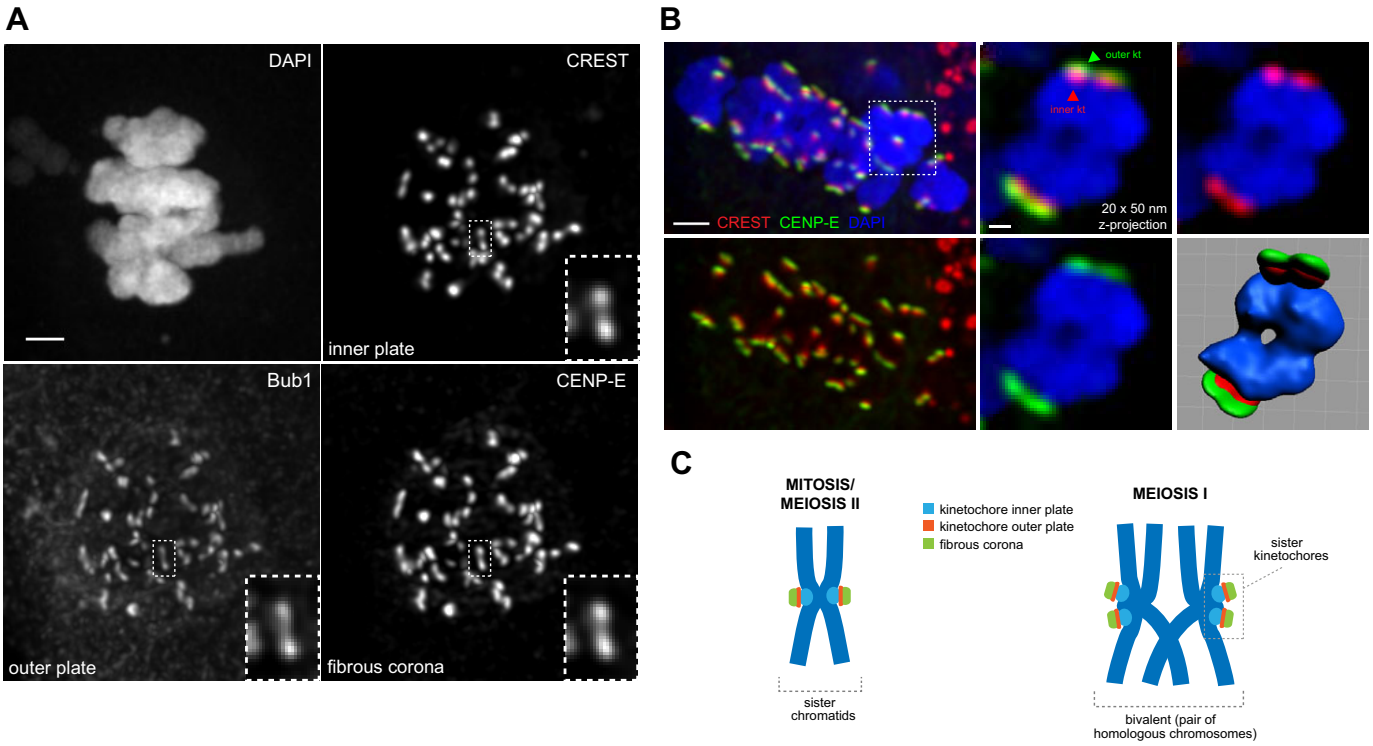

Fig. 2. Inner/outer/corona regions of each sister kinetochore are distinct. (A) Chromosomes in a meiosis I (MI) oocyte stained with CREST antisera (kinetochore inner plate/centromere), anti-Bub1 antibodies (kinetochore outer plate) and anti-CENP-E antibodies (fibrous corona). Image is a maximum intensity projection incorporating 100×50 nm z-sections (5.0 µm). Inset shows a distinct sister kinetochore pair. Scale bar=2 µm. (B) Left upper and lower panels show a maximum intensity projection (100 × 50 nm z-sections) of chromosomes in an MI oocyte stained for CREST, CENP-E and DAPI. Lower-left panel shows the kinetochores only, in which CREST is clearly located towards the centromeric chromatin, with CENP-E on the outside. A projection (20 × 50 nm z-sections) of the outlined bivalent chromosome is shown in the middle and right panels, in which the arrangement of the inner (CREST, red) and outer (CENP-E, green) kinetochore can be seen more clearly. The bottom right panel depicts the surface rendered bivalent. Scale bars=2 µm (left panel), 0.5 µm (right panel). (C) Schematic showing the arrangement of sister kinetochores in mitosis (back-to-back) and the proposed arrangement in meiosis I (side-by-side).

Biology Open (2016) 5, 178-184 doi:10.1242/bio.016394

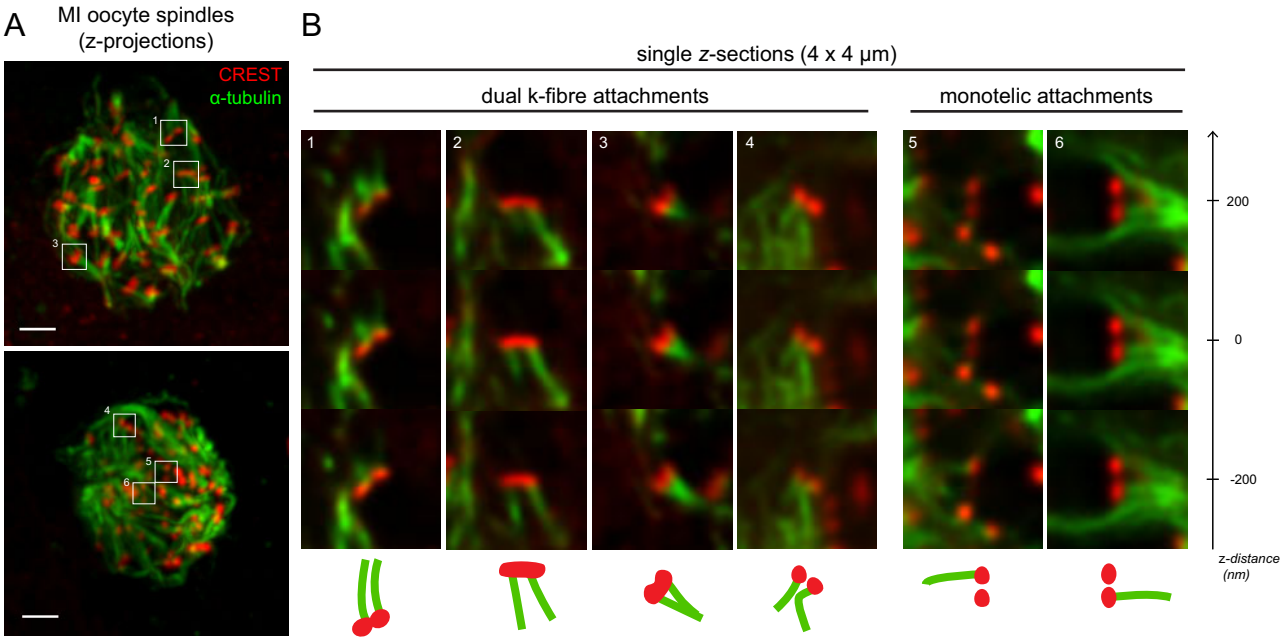

Fig. 3. Sister kinetochore pairs in meiosis I (MI) engage with independent kinetochore-fibres. (A) Two MI human oocyte spindles stained for microtubules (anti-α-tubulin) and kinetochores (CREST antisera) after cold-shock treatment. (B) Enlarged *z*-sections of the six different kinetochore pairs outlined by white boxes in A, with dual and monotelic attachments as indicated. Three *z*-sections from the stack are shown for each pair, at –200 nm, 0 nm and +200 nm. Scale bar=2 μm.

However, we noticed that in oocytes from older women, sister kinetochore pairs appeared to be further apart than in oocytes from younger patients (Fig. 4B). We therefore revisited our inter-kinetochore distance measurements and examined them in the context of age. Using both CREST and CENP-E as kinetochore markers, we found that there was a gradual increase in inter-kinetochore distance over the entire kinetochore structure with age (Fig. 4C). The subset of oocytes from women with no known fertility issues (n=4; labelled in Fig. 4C and see Table S1) also fit this trend suggesting this is part of the normal ageing process. As the majority of aneuploidies in human embryos arise when a woman is in her mid to late thirties (Hassold and Hunt, 2001), we compared oocytes from women under 33 years of age (age range: 26.2–32.4 years) with oocytes from women over 38 years of age (age range: 38.4–40.7 years). We found a significant increase in inter-kinetochore distance from a mean of 0.65±0.20 μm (n=214 pairs from seven oocytes) in women under 33 to 0.79±0.21 μm (n=216 pairs from seven oocytes) in those over 38 (P<0.0001, unpaired t-test) (Fig. 4D). We also compared these oocytes (under 33 years) with oocytes from women in their mid-thirties, for which the mean inter-kinetochore distance was 0.69±0.19 (n=149 pairs from five oocytes; age range: 34.9–35.1). We found that the difference in inter-kinetochore distance was not significant between the two younger groups of patients, but it was significant when comparing women in their mid-thirties with those over 38 years of age (P<0.0001). This is in keeping with the observed increase in MI-derived aneuploidy in oocytes from women in their mid to late thirties.

DISCUSSION

In this study, we aimed to characterise the geometry of the meiotic kinetochore in human MI oocytes. Because distinct kinetochore pairs accounted for the majority of pairs in all oocytes from all women who donated to the study, this indicated to us that separated sister kinetochores are an intrinsic feature of human MI oocytes. This is different from yeast or mouse in which kinetochores are tightly held together during MI (Sarangapani et al., 2014; Kim et al., 2015), and plants in which only the outer plates of the kinetochores are fused (Li and Dawe, 2009). The human MI oocytes that we observed more closely resembled mouse Meikin-deficient oocytes, in which cohesin between sister kinetochores is no longer protected resulting in sister kinetochore separation (Kim et al., 2015). The variation in proportions of distinct and overlapping kinetochore pairs, even among oocytes from the same patient, may indicate a degree of compliance between sister kinetochores, as in mitosis (Jaqaman et al., 2010).

The ability of sister kinetochore pairs on a homologous chromosome to form dual k-fibre attachments indicates that both sisters are functionally active and are each capable of acting as independent attachment sites. We speculate that the presence of a monotelic population (one sister attached) may represent either an immature attachment or the result of an error-correction event. Clearly, the presence of four independent attachment sites could pose a significant problem for achieving stable co-orientation (both pairs of sister kinetochores attached to k-fibres from their respective spindle poles), particularly as the sister kinetochores move further apart. Furthermore, it means that there are potentially twice the number of kinetochore-microtubule attachments for the cell to correct. Given that data from both mouse and human oocytes indicate that the oocyte's ability to correct unstable kinetochore-microtubule attachments is less efficient than in mitosis (Yoshida et al., 2015), the larger number of possible connections may contribute to the increased spindle assembly time that is observed in human oocytes (Holubcova et al., 2015). This situation is dramatically different to what is known about mouse oocyte MI, in which the majority of sister kinetochores are held together by Meikin (Kim et al., 2015), thus forming a single k-fibre attachment (Kitajima et al., 2011; FitzHarris, 2012; Touati et al., 2015; Yoshida et al., 2015).

The absence of a correlation between age and the proportion of separated sister kinetochore pairs in human MI is different to what has been reported in mouse MI (Chiang et al., 2010). This is likely to reflect the fact that in our study population, the vast majority of

Biology Open (2016) 5, 178-184 doi:10.1242/bio.016394

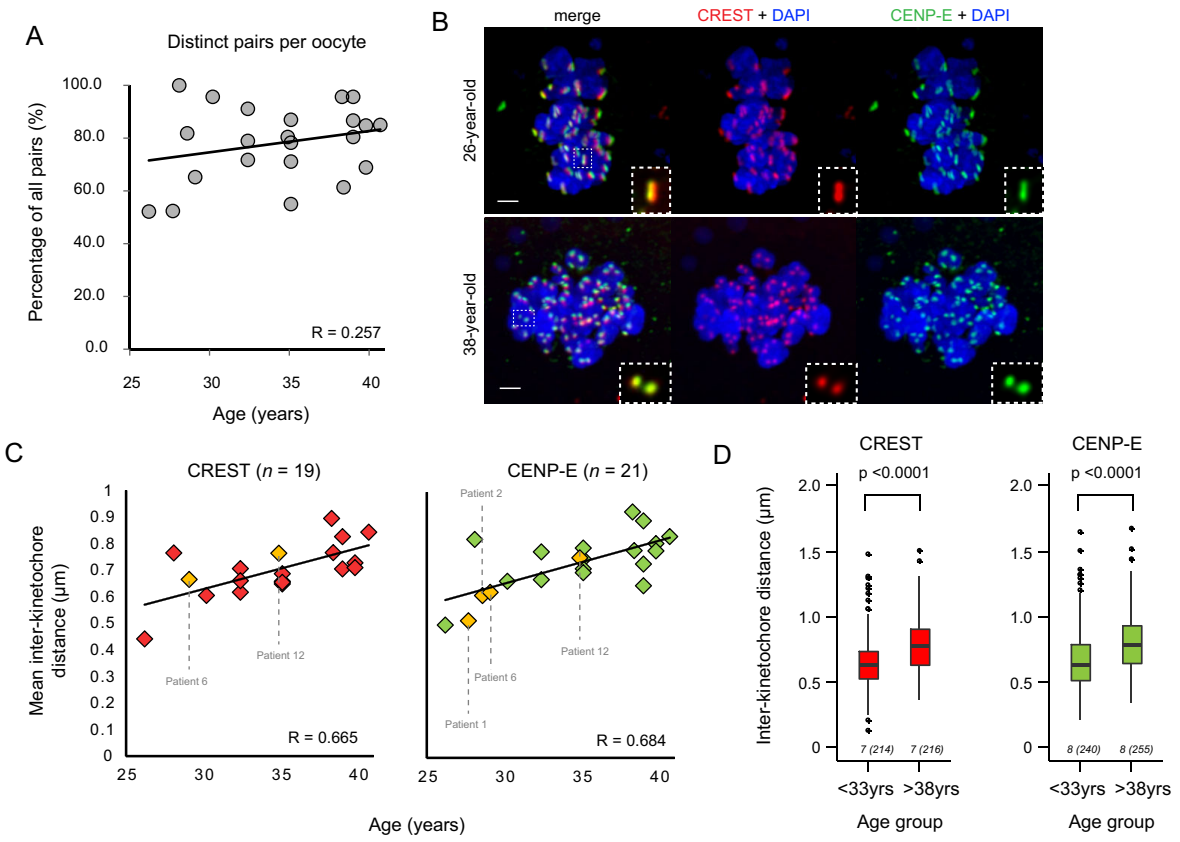

Fig. 4. Inter-kinetochore distance between sister kinetochores in meiosis I increases with maternal age. (A) Relationship between proportion of distinct pairs per oocyte and female age (n=22 oocytes). (B) Comparison of oocyte chromosomes from a 26-year-old patient and a 38-year-old patient, showing increased inter-kinetochore distance with kinetochores marked with CREST antisera (red) and anti-CENP-E antibodies (green). Inset: representative example of a distinct kinetochore pair from each oocyte. Scale bars=2 µm. (C) Increasing inter-kinetochore distance with female age. Distance was measured in 3D from image stacks of kinetochore pairs, using CREST antisera (left plot) and anti-CENP-E antibodies (right plot) to mark the inner and outer regions of the kinetochores respectively. Patients with no known fertility problems (n=4) are marked in yellow. Patient numbers correspond to those shown in Table S1. R=linear correlation coefficient. (D) Comparison of inter-kinetochore distance between women under 33 years of age with women over 38 (P<0.0001, unpaired t-test) for CREST and CENP-E. Box plots represent interquartile range (IQR); whiskers extend to most extreme value within 1.5×IQR. The number of oocytes in each group is shown beneath each plot, with the total number of measurements in brackets.

kinetochores are separated, even in the youngest patients. No samples below 26 years of age were available because it is extremely rare for younger patients to have IVF. Nevertheless, the incidence of trisomic pregnancy is similar for women in their late teens/early twenties (2–3%) and their early thirties (~5%), so we would not expect to see a dramatic difference in kinetochore geometry in women at earlier ages than those studied. In comparison, the incidence of trisomy for women in their late thirties/early forties is around 15% (Hassold and Hunt, 2001).

We show here that in intact human MI oocytes the entire kinetochore inner-to-outer-to-corona structure comes apart with age. This is in keeping with findings from monastrol-treated mouse MI oocytes (Chiang et al., 2010) and metaphase spreads from mouse and human MII oocytes (Merriman et al., 2013; Duncan et al., 2012). The maternal age-dependent change in centromeric chromatin may have implications for the formation of stable k-fibre attachments. One report in mouse has shown that separated sister kinetochores in aged oocytes do not form more unstable attachments than fused pairs, but they do have a slightly increased propensity to form merotelic attachments (Shomper et al., 2014), indicating that cohesin loss and subsequent separation of sisters does not severely affect attachment. However, given that the degree of separation of kinetochores in human oocytes is greater than that in mice, it may be a possibility that kinetochore pairs with an inter-kinetochore distance beyond a certain threshold are prone to mis-attachment, particularly as individual kinetochores within a pair act as separate attachment sites. It is also important to bear in mind that our results are only indicative of cohesin loss, and without direct study of cohesin there is the possibility that these changes in kinetochore geometry could be caused by other factors, such as changes in kinetochore or chromatin structure or microtubule-pulling forces.

In summary, our results provide a detailed insight into MI kinetochore geometry in intact human oocytes. We show that the majority of sister kinetochores in MI oocytes are separate, and that the degree of separation increases with age, consistent with the profile of maternal age-related aneuploidies in women. We also show that, as well as the chromatin-associated inner plate, the outer microtubule-interacting regions of the kinetochore are also separate, which facilitates the sister kinetochores acting as individual attachment sites. Since both sister kinetochores are able to form k-fibre attachments, stable bi-orientation may be more difficult to achieve, which may be exacerbated by increasing inter-kinetochore distances with increasing maternal age. These features of kinetochores in MI oocytes may shed light on the particularly high incidence of chromosome segregation errors at first meiosis in human oocytes.

Biology Open (2016) 5, 178-184 doi:10.1242/bio.016394

MATERIALS AND METHODS

Donation of human oocytes to research

Approval for the project was granted by the NHS Research Ethics Committee (04/Q2802/26) and the Human Fertilisation and Embryology Authority (HFEA; Research Licence RO155). Informed consent for donation of oocytes to research was provided by patients undergoing *in vitro* fertilisation (IVF) or intracytoplasmic sperm injection (ICSI) at the Centre for Reproductive Medicine, University Hospitals Coventry and Warwickshire NHS Trust. All oocytes used for research were unsuitable for the patient's treatment and would otherwise have been discarded. For purposes of selection for research use, oocytes were presumed to be in MI if neither a germinal vesicle nucleus nor polar bodies were visible by light microscopy. This initial clinical assessment was further informed by detailed analysis of chromosomes in the course of the research.

Whole oocyte fixation

Whole oocytes were fixed and stained using a method previously described (Riris et al., 2013). Briefly, oocytes were washed in PHEM buffer (60 mM PIPES, 25 mM HEPES, 10 mM EGTA, 4 mM $MgSO_4.7H_2O$; pH 6.9) with 0.25% Triton X-100, then fixed in 3.7% paraformaldehyde in PHEM for 30 min. Following fixation, they were washed in PBB (0.5% BSA in PBS), permeabilised with 0.25% Triton X-100 in PBS for 15 min, then transferred to a blocking solution (3% BSA in PBS with 0.05% Tween-20) where they were stored at 4°C overnight. For cold shock treatment, oocytes were placed in ice-cold media for 1 min immediately upon receipt, then fixation and immunofluorescence were performed as described.

Immunofluorescence

Immunofluorescence was performed using a method previously described (Riris et al., 2013). Oocytes were incubated at 37°C for 1 h with primary antibodies diluted in blocking solution, followed by a 15 min wash in PBB with 0.05% Tween-20, then incubation with secondary antibodies for 1 h, followed by a final wash step. Primary antibodies included: anti-centromere antibody derived from human CREST serum (1:50; Antibodies Incorporated, Davis, CA, USA), rabbit anti-CENP-E (1:200; Meraldi et al., 2004) mouse monoclonal antibody against α-tubulin (1:200; T6074 Sigma-Aldrich, St Louis, MO, USA), mouse monoclonal antibody to Hec1 9G3 (1:50; ab3613 Abcam, Cambridge, UK) and mouse monoclonal antibody to Bub1 (1:50; Meraldi et al., 2004). Secondary tagged antibodies were diluted 1:200 and included anti-mouse Alexa Fluor 488®, anti-rabbit Alexa 594® and anti-human Alexa 647® (Stratech, Suffolk, UK). Oocytes were mounted in ProLong® Gold Antifade Mountant with DAPI (Invitrogen, Carlsbad, CA, USA) for detection of chromosomes.

Imaging

All imaging was performed on an UltraView spinning-disk confocal microscope (Perkin Elmer, Waltham, MA, USA). 3D image stacks were collected using a 60× NA1.4 (100×1 µm *z*-sections) and 100× NA1.4 (250×50 nm *z*-sections) oil objective. Images were acquired using Volocity software.

Image and data analysis

Images were deconvolved using Huygens X11 (Scientific Volume Imaging B. V., Hilversum, Netherlands). Kinetochores were classified on the basis of their appearance in maximal projection images incorporating 10×50 nm *z*-sections above and below a manually marked point where the kinetochore/kinetochore pair appeared (covering a *z*-distance of 1.0 µm). To distinguish overlapping kinetochore pairs from single kinetochores, we used 3D reconstructions in Imaris (Bitplane, Zurich, Switzerland) to examine them in their chromosomal context. If foci could not be reliably classified, for instance due to overlapping chromosomes or kinetochore signal, they were classified as unclear. Inter-kinetochore distance was measured using the FindFoci plugin in ImageJ, which identifies regions of peak intensity in 3D image stacks (Herbert et al., 2014). For kinetochores in different *z*-sections, the Pythagorean formula was used to calculate inter-kinetochore distance. Statistical analysis of inter-kinetochore measurements was performed in Excel (Microsoft) or R (http://www.r-project.org/).

Acknowledgements

We thank all patients for donating oocytes and are grateful to the clinical embryologists at the Centre for Reproductive Medicine, University Hospitals Coventry & Warwickshire for their assistance with oocyte identification and collection, in particular Debbie Taylor and Hannah Williams for their technical assistance. We thank Jan Brosens for helpful discussions and Patrick Meraldi for anti-Bub1/CENP-E antibodies.

Competing interests

The authors declare no competing or financial interests.

Author contributions

Project was conceived and supervised by A.D.M. and G.M.H. G.M.H. was Person Responsible to the Human Fertilisation and Embryology Authority and consented the patients donating oocytes. J.P. carried out all experiments and analysis. J.P., A.D.M., G.M.H. and S.L.T. prepared the manuscript.

Funding

This work was supported by the Montreal Reproductive and Regenerative Medicine Foundation and a Warwick Collaborative Postgraduate Research Scholarship (J.P.). A.D.M. is supported by a Wellcome Trust Senior Investigator Award [grant number: 106151/Z/14/Z].

Supplementary information

Supplementary information available online at
http://bio.biologists.org/lookup/suppl/doi:10.1242/bio.016394/-/DC1

References

Chan, G. K., Liu, S.-T. and Yen, T. J. (2005). Kinetochore structure and function. *Trends Cell Biol.* **15**, 589-598.

Chiang, T., Duncan, F. E., Schindler, K., Schultz, R. M. and Lampson, M. A. (2010). Evidence that weakened centromere cohesion is a leading cause of age-related aneuploidy in oocytes. *Curr. Biol.* **20**, 1522-1528.

Corbett, K. D., Yip, C. K., Ee, L.-S., Walz, T., Amon, A. and Harrison, S. C. (2010). The monopolin complex crosslinks kinetochore components to regulate chromosome-microtubule attachments. *Cell* **142**, 556-567.

Duncan, F. E., Hornick, J. E., Lampson, M. A., Schultz, R. M., Shea, L. D. and Woodruff, T. K. (2012). Chromosome cohesion decreases in human eggs with advanced maternal age. *Aging Cell* **11**, 1121-1124.

Earnshaw, W. C. (2015). Discovering centromere proteins: from cold white hands to the A, B, C of CENPs. *Nat. Rev. Mol. Cell Biol.* **16**, 443-449.

Fitzharris, G. (2012). Anaphase B precedes anaphase A in the mouse egg. *Curr. Biol.* **22**, 437-444.

Hassold, T. and Hunt, P. (2001). To err (meiotically) is human: the genesis of human aneuploidy. *Nat. Rev. Genet.* **2**, 280-291.

Herbert, A. D., Carr, A. M. and Hoffmann, E. (2014). FindFoci: a focus detection algorithm with automated parameter training that closely matches human assignments, reduces human inconsistencies and increases speed of analysis. *PLoS ONE* **9**, e114749.

Holubcova, Z., Blayney, M., Elder, K. and Schuh, M. (2015). Error-prone chromosome-mediated spindle assembly favors chromosome segregation defects in human oocytes. *Science* **348**, 1143-1147.

Jaqaman, K., King, E. M., Amaro, A. C., Winter, J. R., Dorn, J. F., Elliott, H. L., Mchedlishvili, N., McClelland, S. E., Porter, I. M., Posch, M. et al. (2010). Kinetochore alignment within the metaphase plate is regulated by centromere stiffness and microtubule depolymerases. *J. Cell Biol.* **188**, 665-679.

Jessberger, R. (2012). Age-related aneuploidy through cohesion exhaustion. *EMBO Rep.* **13**, 539-546.

Kim, J., Ishiguro, K.-I., Nambu, A., Akiyoshi, B., Yokobayashi, S., Kagami, A., Ishiguro, T., Pendas, A. M., Takeda, N., Sakakibara, Y. et al. (2015). Meikin is a conserved regulator of meiosis-I-specific kinetochore function. *Nature* **517**, 466-471.

Kitajima, T. S., Kawashima, S. A. and Watanabe, Y. (2004). The conserved kinetochore protein shugoshin protects centromeric cohesion during meiosis. *Nature* **427**, 510-517.

Kitajima, T. S., Ohsugi, M. and Ellenberg, J. (2011). Complete kinetochore tracking reveals error-prone homologous chromosome biorientation in mammalian oocytes. *Cell* **146**, 568-581.

Li, X. and Dawe, R. K. (2009). Fused sister kinetochores initiate the reductional division in meiosis I. *Nat. Cell Biol.* **11**, 1103-1108.

Meraldi, P., Draviam, V. M. and Sorger, P. K. (2004). Timing and checkpoints in the regulation of mitotic progression. *Dev. Cell* **7**, 45-60.

Merriman, J. A., Lane, S. I. R., Holt, J. E., Jennings, P. C., Garcia-Higuera, I., Moreno, S., McLaughlin, E. A. and Jones, K. T. (2013). Reduced chromosome cohesion measured by interkinetochore distance is associated with aneuploidy even in oocytes from young mice. *Biol. Reprod.* **88**, 31.

Biology Open (2016) 5, 178-184 doi:10.1242/bio.016394

Nagaoka, S. I., Hassold, T. J. and Hunt, P. A. (2012). Human aneuploidy: mechanisms and new insights into an age-old problem. *Nat. Rev. Genet.* **13**, 493-504.

Riris, S., Cawood, S., Gui, L., Serhal, P. and Homer, H. A. (2013). Immunofluorescence staining of spindles, chromosomes, and kinetochores in human oocytes. *Methods Mol. Biol.* **957**, 179-187.

Sakakibara, Y., Hashimoto, S., Nakaoka, Y., Kouznetsova, A., Hoog, C. and Kitajima, T. S. (2015). Bivalent separation into univalents precedes age-related meiosis I errors in oocytes. *Nat. Commun.* **6**, 7550.

Sarangapani, K. K., Duro, E., Deng, Y., Alves, F. d. L., Ye, Q., Opoku, K. N., Ceto, S., Rappsilber, J., Corbett, K. D., Biggins, S. et al. (2014). Sister kinetochores are mechanically fused during meiosis I in yeast. *Science* **346**, 248-251.

Shomper, M., Lappa, C. and Fitzharris, G. (2014). Kinetochore microtubule establishment is defective in oocytes from aged mice. *Cell Cycle* **13**, 1171-1179.

Sundin, L. J. R., Guimaraes, G. J. and DeLuca, J. G. (2011). The NDC80 complex proteins Nuf2 and Hec1 make distinct contributions to kinetochore-microtubule attachment in mitosis. *Mol. Biol. Cell* **22**, 759-768.

Touati, S. A., Buffin, E., Cladiere, D., Hached, K., Rachez, C., Van Deursen, J. M. and Wassmann, K. (2015). Mouse oocytes depend on BubR1 for proper chromosome segregation but not for prophase I arrest. *Nat. Commun.* **6**, 6946.

Wan, X., O'Quinn, R. P., Pierce, H. L., Joglekar, A. P., Gall, W. E., DeLuca, J. G., Carroll, C. W., Liu, S.-T., Yen, T. J., McEwen, B. F. et al. (2009). Protein architecture of the human kinetochore microtubule attachment site. *Cell* **137**, 672-684.

Watanabe, Y. (2012). Geometry and force behind kinetochore orientation: lessons from meiosis. *Nat. Rev. Mol. Cell Biol.* **13**, 370-382.

Yoshida, S., Kaido, M. and Kitajima, T. S. (2015). Inherent instability of correct kinetochore-microtubule attachments during meiosis I in oocytes. *Dev. Cell* **33**, 589-602.

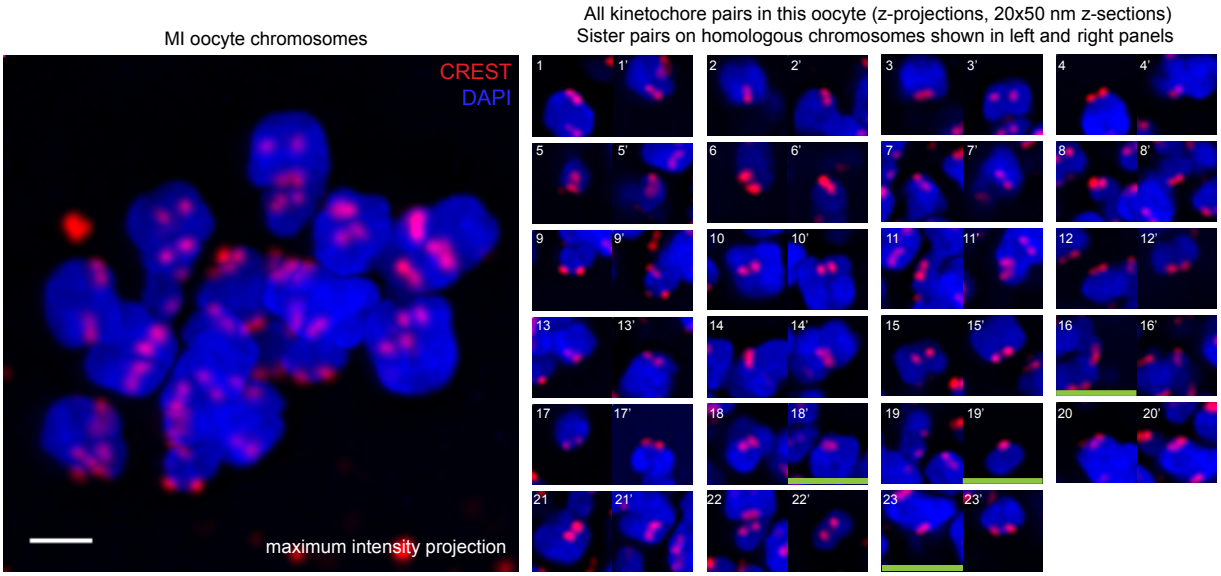

Fig. S1. Left: maximal projection of MI oocyte chromosomes. Right: z-projection images incorporating 20x50 nm z-sections centred about a manually marked kinetochore pair (centre of panel). Green bar marks 'overlapping' kinetochore pairs. Sister kinetochore pairs on homologous chromosomes are shown in right and left panels. Panels are 4x4 μm.

Table S1. Reasons for treatment in the women donating oocytes to this study

Patient number	Woman's age at egg collection	Pre-treatment parity of female partner	Reason for treatment	Outcome of treatment cycle
1	27.7	0+0	Same-sex female couple	Neg
2	28.6	0+0	Male factor infertility	1FH
3	39.0	0+0	Unexplained infertility	Neg
4	39.0	0+0	Unexplained infertility	Neg
5	28.1	0+0	Polycystic ovarian disease	1FH
6	29.1	0+1	Azoospermia	1FH
7	38.4	0+0	Unexplained infertility	1FH
8	32.4	0+0	Tubal factor	Neg
9	40.7	0+3	Recurrent miscarriage plus unexplained subfertility	2FH
10	32.4	0+0	Uterine factor	1FH
11	38.3	0+0	Unexplained infertility	1FH
12	34.9	0+0	Male factor infertility	1FH
13	30.2	0+0	Polycystic ovarian syndrome	Neg
14	39.8	1+1	Endometriosis, bicornate uterus	Neg
15	35.1	0+0	Polycystic ovarian syndrome	Neg
16	26.2	0+0	Endometriosis	1FH

Women with no known fertility issues, whose partner's infertility or absence of a male partner may explain the couple's infertility, are highlighted in grey. Patients 2, 5, 6, 7, 9, 10, 11, 12, 14 and 16 have demonstrated fertility by becoming pregnant either as a result of treatment or previously. Parity data is shown as parity (number of births >24 weeks) + gravidity (number of pregnancies). FH = fetal heart visible on ultrasound scan. Neg = no pregnancy.

Appendix C. Documentation

i. **HFEA Licence Centre 0013**
ii. **HFEA Licence Centre 0320**
iii. **HFEA Licence Centre 0340**
iv. **Patient information sheet**
v. **Patient consent form**

Human Fertilisation and Embryology Authority

Licensed Centre

Licence Reference:	R0155-5-a
Licence for:	Research
Project Reference:	R0155
Project Title:	Indicators of Oocyte and Embryo Development
Centre Reference:	0013
Centre Name:	Centre for Reproductive Medicine, Coventry
Licensed Premises:	University Hospitals Coventry & Warwickshire NHS Trust Clifford Bridge Road Coventry CV2 2DX
Person Responsible:	Dr Geraldine Hartshorne
Licence Holder:	Dr Geraldine Hartshorne

Signed

Peter Thompson
Chief Executive

Signed

Sally Cheshire
Chair

This Licence is granted Under Section 11 of the Human Fertilisation and Embryology Act 1990 ('the Act') and is subject to conditions set out in the

Valid from: 01/11/2014

Expires on: 31/10/2017

Human Fertilisation and Embryology Authority

Licensed Centre

Licence Reference:	R0155-2-a
Licence for:	Research
Project Reference:	R0155
Project Title:	Indicators of Oocyte and Embryo Development
Centre Reference:	0320
Centre Name:	Hartshorne and Genesis Group
Licensed Premises:	Clinical Sciences Research Institute Warwick Medical School Clifford Bridge Road Coventry CV2 2DX
Person Responsible:	Dr Geraldine Hartshorne
Licence Holder:	Professor John Davey

Signed

Peter Thompson
Chief Executive

Signed

Sally Cheshire
Chair

This Licence is granted Under Section 11 of the Human Fertilisation and Embryology Act 1990 ('the Act') and is subject to conditions set out in the accompanying annexes. This Licence authorises the activities to be carried out (listed below), at the premises (named on page 1), under the supervision

Valid from: 01/11/2014

Expires on: 31/10/2017

Human Fertilisation and Embryology Authority

Licensed Centre

Licence Reference:	R0155-1-a
Licence for:	Research
Project Reference:	R0155
Project Title:	Indicators of Oocyte and Embryo Development
Centre Reference:	0340
Centre Name:	Mechanochemical Cell Biology
Licensed Premises:	University of Warwick Warwick Medical School Gibbet Hill Coventry CV4 7AL
Person Responsible:	Dr Geraldine Hartshorne
Licence Holder:	Professor John Davey

Signed

Peter Thompson
Chief Executive

Signed

Sally Cheshire
Chair

This Licence is granted Under Section 11 of the Human Fertilisation and Embryology Act 1990 ('the Act') and is subject to conditions set out in the accompanying annexes. This Licence authorises the activities to be carried

Valid from: 01/11/2014

Expires on: 31/10/2017

University Hospital
Clifford Bridge Road
Coventry
CV2 2DX
Tel: 024 76964000

Version 6. 13 March 2014

PATIENT INFORMATION SHEET

Indicators of oocyte and embryo development

Dear Patient

You are being invited to take part in a research study.

Before you decide, it is important for you to understand why the research is being done and what it will involve. Please take time to read the following information carefully and discuss it with others if you wish. Ask us if there is anything that is not clear or if you would like more information. Take time to decide whether or not you wish to take part. Your decision in this respect will not affect your treatment at all.

If you do choose to participate in the research, you still remain free to withdraw your consent at any time before your material has been used in the research. Such withdrawal of consent will have no effect on your treatment or care.

Thank you for reading this.

Yours faithfully

Geraldine Hartshorne
Scientific Director
Centre for Reproductive Medicine

WHAT IS THE PURPOSE OF THE STUDY?

We are doing research to understand better how eggs and embryos are formed and grow. This is an ongoing study that has been in progress since 1996 and will continue until at least 2017.
At present, it is very difficult to identify the embryos that are most likely to implant when placed into the womb during fertility treatments. There are few markers that show clearly whether an egg or embryo is growing well. Moreover, it is possible that development could be affected by the laboratory environment because it is different to the environment in the body. For the future, we want to be able to tell whether eggs and embryos in our laboratory are growing well and whether any problems have arisen for any reason. To do this, we need to study eggs and embryos in great detail and using a variety of different scientific methods. This will tell us, for example, whether certain specialised molecules produced by the embryos or attached to the chromosomes, are behaving normally. We hope that in future, it may be possible to test embryos for these features to monitor normal development, and to check the risks of any new methods of fertility treatment that might be invented. We shall also collect digital images of embryos in order to construct virtual reality models for use in further research to develop new educational resources.

Why have I been chosen?

We would like to ask if you would be willing to let us use some of your eggs or embryos for our research. This would not affect your treatment at all as we would only use any 'left-overs' for research. These would normally be discarded. We would only use them in research if you agree and sign your consent on the form.
If you agree, we would like to use immature eggs (that cannot be used for treatment), eggs that do not fertilise normally, and poorly developing embryos that would not be stored frozen. Once you have finished your treatment, we would also like to use any embryos that you may have left over in the freezer.
None of the eggs or embryos would ever be used to treat anyone else or to make a pregnancy. Please note that eggs or embryos in a non-viable state may be taken to other research centres for study, such as the Universities of Warwick, Sussex, London or Paris, as the specialised equipment that we need to use is based there. Please be assured that any samples moved to other centres would be treated there with the same respect as if they remained here. All the samples will be anonymised so that your personal details would only be accessible under strictly controlled conditions and then only to Trust personnel who are already authorised to access your medical records. Also, please note that any immature eggs that become mature in the laboratory under specialised conditions may be injected with sperm from a donor to see if they will fertilise. Any embryos formed in this way could only develop for a day or two at most because the eggs would have already deteriorated. They would be incapable of normal development and would not be available to you or anyone else for treatment since they would be created using research methods.

Do I have to take part?

Participation is entirely voluntary and your decision in this respect will not affect any aspect of your treatment or its outcome.

What will happen to me if I take part?

Your treatment will proceed exactly the same way, whether or not you choose to take part. However, if you choose to participate, the embryologists in the laboratory will identify any of your eggs and embryos that cannot be used for your treatment and would otherwise be discarded. These would then be made available to researchers working on this project.
Only some patients will have any eggs or embryos left over, so not everyone is suitable to participate. This depends upon the type of treatment that you are having and what happens during your treatment.

What do I have to do?

Please take time to read the information and discuss with a member of staff any questions that you may have. If you wish to take part, please complete and sign the consent form. For use of eggs, only the woman needs to sign, but for use of embryos, both of the couple need to sign.

What are the possible benefits and risks of taking part?

There are no benefits to you personally of taking part. In future we hope that this research may bring benefits to other people going through fertility treatment.
There are no risks of this study over and above those of the treatment itself.

What happens when the research study stops?

At the end of this study, any eggs and embryos that have been used for research are normally disposed of. However, if you agree, it is possible that they can be kept in case they could be useful for other research projects in future. We would like to keep them for this purpose, however, you are under no obligation to agree to this, regardless of whether you agree to participate in the present study. Please would you indicate on the consent form whether you agree for this to be done. Rest assured that any such future research would be approved in advance by the Local Research Ethics Committee.

What if something goes wrong?

We do not envisage any problems arising during the course of this research. However, if an untoward event were to occur, please be assured that we will do everything we can to put matters right. You have a right to complain to the hospital through the normal NHS complaints procedure. If you wish to complain, please write to the hospital complaints

officer at the address above. In addition, you are also welcome to contact the Human Fertilisation and Embryology Authority which regulates research such as this. Their address is: 10 Spring Gardens, London, SW1A 2BU.

Will my taking part in this study be kept confidential?

Yes, your participation will be confidential. Any samples you provide and non-identifying information from your medical history will be stored in an anonymous form. Please note that such anonymised information may be stored on a computer database.

What will happen to the results of the research study?

The results will be published in a medical journal and presented to learned societies at conferences, but you would not be identified in any publication. The information that we gain will be of no use to you personally so we do not plan to tell you about it. But if you would like a copy of the final publication, please write to the principal investigator at the address above. Please note, it usually takes several years for results to be fully analysed and published.

It is possible that some of the results could be used to develop a virtual reality tool which might result in intellectual property rights, and possible financial benefit in the future, for some of the researchers.

Who is organising and funding the research?

This study is currently not receiving any specially allocated financial support or sponsorship.A small amount of general research funding is available through the Centre for Reproductive Medicine, allowing us to make some progress. No inducement or financial reward will be given to any of the staff involved in recruiting patients for this study.

If you would like to take part, please complete the consent form. You will be given the information sheet and a copy of the signed consent form to keep.

If you have any questions or queries, or decide to change your mind, please ask one of the staff, or contact:

Dr Geraldine Hartshorne
Scientific Director
Centre for Reproductive Medicine
UHCW NHS Trust, Coventry, CV2 2DX
Tel: 02476 968879.

You are also very welcome to contact the centre's independent counsellor for any reason. Making decisions about the use, donation or disposal of eggs or embryos can

be difficult. The counsellor is experienced in helping people with various queries and personal questions. She can be contacted directly on telephone number 02476968886.

Thank you for your help.

The Trust has access to interpreting and translation services. If you need this information in another language, please contact the Quality Manager on (024) 76968864, and we will do our best to accommodate your needs. The Trust operates a smoke free policy.

Document History

Author:	G Hartshorne
Department:	CRM
Contact Tel No:	(024) 76968976
Doc. Location:	QM computer, I drive (patient information / research), website
Version:	EMB-PI-000033V6
Reference No:	Quality/information sheets/donate research
Review Date:	June 2017

University Hospital
Clifford Bridge Road
Coventry CV2 2DX
Tel: 024 76 965000

Indicators of Oocyte and Embryo Development

Centre Number: 0013
Study Number: 04/Q2802/26
Name of Researcher: Dr Geraldine Hartshorne

Please initial box

1. I confirm that I have read and understand the Information sheet dated 13 March 2014 (version 6) for the above study and have had the opportunity to ask questions…….. ☐☐

2. I understand that my participation is voluntary and that I am free to withdraw (by written confirmation to the principal investigator) at any time until any samples are used, without giving any reason. My medical care or legal rights will not be affected…….. ☐☐

3. I understand that responsible individuals at the Centre for Reproductive Medicine may look at my medical notes. I give permission for them to collect anonymised medical history data…… ☐☐

4. I agree to take part in the above study…… ☐☐

5. I wish to offer the following material to research

   - Eggs (immature or unfertilised)…… ☐☐
   - Fresh embryos (unsuitable for cryopreservation)…... ☐☐
   - Frozen embryos (no longer required)……. ☐☐

6. At the end of the study, I agree that my anonymised material can be kept for future research…… ☐☐

Name of Female Patient	Date	Signature
Name of Male Patient	Date	Signature
Name of Person taking consent (if different from researcher)	Date	Signature
Researcher	Date	Signature

1 for patient 1 for researcher 1 to be kept with hospital notes

consent form version 6, 13 March 2014